Pre-normative research for safety of hydrogen driven vehicles and transport through tunnels and similar confined spaces

Clean Hydrogen Joint Undertaking (FCH JU)
Grant Agreement Number 826193

Deliverable D6.9
Recommendations for inherently safer use of hydrogen vehicles in underground traffic systems

Lead author: HSE (Ju Lynne Saw, Wayne Rattigan, Keith Moodie, Sarah Bergin, Jill Wilday, Mark Pursell)

Contributing authors: UU (Dmitriy Makarov, Sergii Kashkarov, Volodymyr Shentsov, Donatella Cirrone, Vladimir Molkov)
NCSRD (Stella Giannissi, Alexandros Venetsanos, Nektarios Koutsourakis, Ilias Tolias)
DTU (Luisa Giulani, Frank Markert, Lars Schiøtt Sørensen)
KIT (Zhanjie Xu, Mikhail Kuznetsov)
PS (Joachim Grune)
USN (André Gaathaug, Knut Vågsæther, Joachim Lundberg)
URS (Paola Russo)
CEA (Gilles Bernard-Michel, Didier Bouix, Etienne Studer)
NEN (Janwillem van den Berg)

Version: 220730
Delivery date for internal review: 28 July 2022
Due date: 30 April 2022
Dissemination level: Public

Clean Hydrogen Partnership

Co-funded by the European Union

Deliverable administration					
Work Package	WP6. Synthesis, Outreach and Dissemination (Task 6.3)				
N. and title	D6.9. Recommendations for inherently safer use of hydrogen vehicles in underground traffic systems				
Type	Report				
Status	~~Draft/Working/~~**Released**	Due	M38	Date	Original: 30-04-2022 Resubmission: 31-07-2022
Comments					

Development and revision			
Version No.	Date	Authors	Description
1	19 July 2021		Draft v1
2	25 November 2021		Incorporated input from partners, but a number are still outstanding
3	3 December 2021		Incorporated input from CEA, KIT/PS, DTU- For QA by UU
4	3-25 December 2021	Vladimir Molkov	Text review and comments
5	25 January 2022	Ju Lynne Saw	Further input from partners
6	11 February 2022	Ju Lynne Saw	Further input from partners
7	14 February 2022	Ju Lynne Saw	Further input from partners
8	16 February 2022	Ju Lynne Saw	Further input from partners prior to Project Meeting
9	21 March 2022	Ju Lynne Saw	Further input from partners
10	11 April 2022	Ju Lynne Saw	Draft for Consortium and SAB review, HSE internal QA
11	29 April 2022	Ju Lynne Saw	Incorporated Final Comments- Partners, EU, SAB, HSE Review
12	29 July 2022	Ju Lynne Saw	Partner modifications post-dissemination conference

Disclaimer

Acknowledgments

This project has received funding from the Fuel Cells and Hydrogen 2 Joint Undertaking (now Clean Hydrogen Partnership) under Grant Agreement No 826193. This Joint Undertaking receives support from the European Union's Horizon 2020 Research and Innovation program, Hydrogen Europe and Hydrogen Europe Research.

Co-funded by the European Union

Executive Summary

The main ambition of the HyTunnel-CS project is to allow hydrogen-powered vehicles to travel through or occupy underground traffic infrastructure more safely. The aim is to conduct internationally leading pre-normative research (PNR) to close knowledge gaps and technological bottlenecks in the provision of safety in the use of hydrogen-powered vehicles in underground transportation systems. These recommendations are the synthesis of the HyTunnel-CS outputs on understanding, prevention and mitigation strategies, and engineering solutions addressing hydrogen release and dispersion, thermal and pressure effects of unignited and ignited (fire) jets, deflagrations, detonations and hydrogen storage tank rupture in a fire in tunnels, underground parking, garages and similar confined spaces. The research approach that has underpinned the success of the project is considering hydrogen vehicle and underground traffic structure as a single system with an integrated safety approach using the synergies of theoretical, numerical and experimental studies. The project has developed a holistic understanding of interaction of hydrogen vehicles with tunnel equipment and structures using unique experimental facilities, including real tunnels, contemporary theoretical and numerical models, and simulations using high-performance computing. These recommendations for inherently safer use of hydrogen vehicles in enclosed transport systems for use by stakeholders is one of the main outcomes of HyTunnel-CS.

The recommendations include description of developed and validated models and tools to perform hydrogen safety engineering for confined spaces like tunnels, underground and multi-storey parking, garages and maintenance shops, hydrogen storage enclosures on board of trains, ships, aeroplanes, *etc*. The novel safety engineering solutions and breakthrough safety strategies for incident prevention and mitigation have been developed and validated. The recommendations are applicable, to different extents, for road and rail hydrogen systems and infrastructure, and maritime and aviation applications. The recommendations aim to provide easy reference to stakeholders from the underground traffic/ similar structures and hydrogen-powered transport sectors but could be useful to a wider range of stakeholders.

The recommendations seek to give guidance on the evaluation of appropriateness and effectiveness of conventional and innovative safety measures, in the event of incidents involving hydrogen-powered vehicles or hydrogen delivery transport in underground transportation systems and similar confined spaces. They also define the applicability range of recommended hazard and risk assessment models, tools and methodologies. In other words, the recommendations define the requirements for safety design and inherently safer use of hydrogen systems in tunnels and other enclosed spaces, i.e. for reduction of hazards and associated risk to acceptable level, improvement of life safety, property and environmental protection. A deeper knowledge and understanding of the underlying physical phenomena enable beyond the-state-of-the-art models, tools, engineering solutions and safety strategies is to be developed, to carry out hydrogen safety engineering with consistent performance-based assessment of hazards and associated risks of hydrogen vehicles in confined spaces. The findings of the HyTunnel-CS project will hopefully pave the way for the development of novel prevention and mitigation strategies by stakeholders following the “safety by design” approach, i.e. inherent safety.

Table of contents

Nomenclature and abbreviations

ACH	Air changes per hour
ADN	European Agreement concerning the International Carriage of Dangerous Goods by Inland Waterways
ADR	European Agreement Concerning the International Carriage of Dangerous Goods by Road
ALARP	As Low as Reasonably Practicable
ASET	Available Safe Egress Time
BLEVE	Boiling Liquid Expanding Vapour Explosion
BR	Blockage Ratio
CBG	Compressed Bio Gas
CcH2	Cryo-compressed hydrogen
CEA	"*Commissariat à l'énergie atomique et aux énergies alternatives*" French Atomic Energy Commission
CEN	*Comité Européen de Normalisation* (European Standardisation Organisation)
CFD	Computational Fluid Dynamics
CGH2	Compressed gaseous hydrogen
CHSS	Compressed Hydrogen Storage System
CNG	Compressed Natural Gas
DDT	Deflagration-to-Detonation Transition
DoA	Description of Actions
DTU	Technical University of Denmark
EC	European Commission
EHSP	European Hydrogen Safety Panel
EIHP2	European Integrated Hydrogen Project Phase II
EN	European Standard
EN Eurocode	Version of Eurocode approved by CEN as a European Standard
ENSOSP	*L'Ecole nationale supérieure des officiers de sapeurs-pompiers*
EoS	Equation of State
ETA	Event Tree Analysis
FA	Flame acceleration
FCEV	Fuel Cell Electric Vehicle
FCH JU	Fuel Cells and Hydrogen/ Clean Hydrogen Joint Undertaking
FED	Fractional Effective Dose
FEM	Finite Element Modelling
FHa	*Fundacion Para El Desarrollo De Las Nuevas Tecnologias Del Hidrogeno En Aragon*, Spain
FLIC	Flame with Implicit Convection model
FRP	Fibre Reinforced Polymer
FRR	Fire Resistance Rating
H_2	Hydrogen
HCM	Hydrocarbon modified
He	Helium
HSE	The Health & Safety Executive, United Kingdom
HGV	Heavy Goods Vehicle
HPV	Hydrogen-Powered Vehicles

HRR	Heat release rate
HRR/A	Specific heat release rate (HRR divided by fire source area, A)
IA HySafe	International Association for Hydrogen Safety
ICE	Internal Combustion Engine
ISO	International Standardization Organization
KIT	Karlsruhe Institute of Technology, Germany
LBG	Liquefied Bio Gas
LBT	Load-bearing thickness
LES	Large Eddy Simulation
LFL	Lower flammability limit
LH2	Liquid hydrogen
LNB	Leak-no-burst or microleak-no-burst
LNG	Liquefied natural gas
M	Milestone
MWP	Maximum working pressure
NCSRD	National Centre for Scientific Research Demokritos (Greece)
NEN	*Nederlands Normalisatie-instituut* (Netherlands Standardization Institute)
NWP	Nominal Working Pressure
OECD	Organisation for Economic Co-Operation and Development
PIARC	Permanent International Association of Road Congresses
PNR	Pre-normative research
PP	Polypropylene
PPP	Pressure Peaking Phenomenon
PRESLHY	Pre-normative Research for Safe Use of Liquid Hydrogen
PS	Pro-Science, GmbH
QRA	Quantitative Risk Assessment
QRAM	Quantitative Risk Assessment Model by PIARC & OECD to evaluate the risks of dangerous goods transport through road tunnels
RCS	Regulations, Codes and Standards
RID	Regulation concerning the International Carriage of Dangerous Goods by Rail
RSET	Required Safe Egress Time
RWS	*Rijkswaterstaat*
OEM	Original Equipment Manufacturer
SAB	Stakeholders Advisory Board
SDO	Standards Developing Organisations
SoC	State of Charge
SOP	Standard Operation Procedures
TNT	Trinitrotoluene
TPL	Thermal Protection Layer
TPRD	Thermally-activated Pressure Relief Device
TVD	Total Variation Diminishing
URS	University of Rome, *Università degli Studi di Roma "La Sapienza"*, Italy
USN	University of South-Eastern Norway
UU	Ulster University, legally known as University of Ulster, United Kingdom
VCE	Vapour Cloud Explosion
WP	Work Package

List of figures

List of tables

1. Introduction

1.1 Safety objectives for hydrogen vehicles in underground traffic systems

Tunnels are an increasingly important part of the traffic infrastructure. However, they create challenges for the prevention and management of incidents, fire and explosion protection and security risks against attacks or sabotage. Additionally, most vehicles will at some point during their operational cycle, operate within a confined area such as an enclosed car park, underground bus station, low-level railway station etc, with many of the characteristics similar to those of a tunnel. The use of alternative fuels, including compressed gaseous hydrogen (CGH_2), cryo-compressed hydrogen (CcH_2) and liquid hydrogen (LH_2), in tunnels and similar confined spaces, introduces new challenges in terms of life, property and environment protection.

Before the HyTunnel-CS project, knowledge gaps in understanding amongst stakeholders existed, on whether current safety provisions in tunnels, underground parking and similar confined spaces would be sufficient to manage the hazards and associated risks from incidents involving hydrogen-powered vehicles and trailers transporting hydrogen with their current safety design. In the absence of sufficient knowledge, it was hard to formulate new Regulations, Codes and Standards (RCS), or to determine the improvements required in existing ones. This was the main motivation of this pre-normative research (PNR) project.

The work started from the consolidation of existing knowledge and experience of partners, including the study “Internal project on investigating the use of hydrogen vehicles in road tunnels, Deliverable D111, 15 April 2009” by European Network of Excellence HySafe (NoE HySafe). This 2009 project of NoE HySafe, in which three partners (UU, KIT and HSE) of this consortium participated, identified the strong need for the development of validated hazards and risk assessment tools for the behaviour of hydrogen in tunnels and confined spaces after an accidental release.

The focus has been on conventional safety provisions for transport in tunnels and other confined spaces, such as underground and multi-storey parking to analyse their effectiveness and applicability to incidents involving hydrogen-powered vehicles and large-scale hydrogen transport. The consortium has undertaken a critical analysis of existing incidents and accidents with vehicle fires and explosions in confined spaces, available prevention and mitigation measures, and the state-of-the-art in hazards and risk assessment methodologies for road and railway tunnels and other confined spaces. The applicability of currently used safety systems and procedures was investigated, whilst also exploiting the knowledge and experience of hydrogen safety experts in the consortium, many of them members of the European Hydrogen Safety Panel (EHSP) and International Association for Hydrogen Safety (IA HySafe). The HyTunnel-CS project created a unique gathering of professional expertise that was enforced by members of Stakeholders Advisory Board (SAB) and the National Networks.

The HyTunnel-CS partners have reviewed the current knowledge surrounding safety in underground transportation systems and similar confined spaces: tunnels, underpasses, underground and multi-storey parking structures, garages, maintenance shops, *etc*. Unique large-scale experiments were carried out in leading European research facilities, including real tunnels. These experiments were used to close knowledge gaps and underpin the development, review

and validation of existing and new CFD models and engineering tools for assessment of hazards and associated risk in tunnels and similar confined spaces.

Only models and tools that have been successfully validated against experiments of hydrogen release, dispersion, combustion, storage tank reaction to fire, blast wave and fireball dynamics after tank rupture in a fire, can be applied to the design of hydrogen vehicles for inherently safe use in tunnels and other confined spaces.

In-depth safety considerations have been given to vehicles with various inventories of hydrogen onboard, including cars, buses, trucks, trains, *etc*.

Hydrogen-specific hazards, such as the pressure peaking phenomenon (PPP), and its main safety asset, buoyancy, were analysed to identify any changes necessary to the current design of hydrogen-powered vehicles, as well as current requirements regarding safety provisions in tunnels, underground parking, *etc*. This was based on the experience and knowledge accumulated by the project partners in hydrogen safety, specifically 8 of 13 partners who are current members of the International Association for Hydrogen Safety (UU, KIT, NCSRD, USN, HSE, DTU, CEA, PS) and 4 partners sitting on the European Hydrogen Safety Panel (UU, KIT, HSE, CEA).

Although hydrogen (H_2) typically behaves in a very benign manner, in the open atmosphere, any confinement or congestion can promote severe consequences. The outcomes of the HyIndoor project “Pre-normative research on safe indoor use of fuel cells and hydrogen systems”, in which 6 HyTunnel-CS partners (UU, KIT, NCSRD, HSE, CEA, PS) were either WP leaders or the suppliers of unique experiments, employed novel numerical models and innovative engineering correlations, to build on and exploit previously-generated knowledge. The main differences of HyTunnel-CS compared to HyIndoor include the high pressures releases of hydrogen of up to 70 MPa through realistic nozzle diameters, real onboard storage tanks, high hydrogen release flow rates and large-scale experimental facilities, including real tunnels. A review of the state-of-the-art in engineering tools for assessment of hydrogen hazards and associated risks was undertaken by partners UU, URS and DTU. These three partners developed an example Quantitative Risk Assessment (QRA) methodology, incorporating models and tools for assessment of incident consequences. The review assisted in the formulation of requirements for engineering tools and models to be developed in the HyTunnel-CS pre-normative research project, applicable to incident scenarios in road and railway tunnels underground and multi-storey car parking, garages, *etc*.

Following the requirements of Directive 2004/54/EC, the risk analysis methodology employed considers incidents that may affect the safety of other occupants of tunnels and confined spaces, not just the vehicle occupants, taking into account the nature and magnitude of possible consequences. The alternative hazards and associated risks prevention and reduction measures for hydrogen vehicles must ensure at least an equivalent level of safety as for fossil-fuel transport and traffic infrastructure.

The quantification of the harm criteria (Appendix 1), considering the interaction of hydrogen unignited and ignited releases (fire, deflagration, detonation, blast wave and fireball after tank rupture in fire) with existing safety installations in underground infrastructure, road and rail tunnels, is essential. For evacuation and emergency strategies as well as other mitigation technologies such as sprinklers, the time to reach harm or tenability criteria is important to evaluate safe egress conditions (ASET/RSET approach). Tenability in this context is the ability

of humans to perform cognitive and motor-skill functions at an acceptable level when exposed to a fire environment. Therefore, a tenability limit is the limit at which a human being is rendered physically incapacitated to escape from an incident; or is killed as a consequence of exposure to one or more factors such as temperature, toxicity, heat flux or smoke obscuration generated by say, a fire.

In a performance-based risk assessment, the primary objective is the safe egress of people and then sufficient structural integrity to allow for a safe emergency response. These criteria include the temperature of a hot layer, the humidity, the visibility, the quantity of toxic gases, *etc*. Such parameters are affected by hydrogen jet fires, deflagrations, and hence mitigation via water sprinklers, for example water sprays or mist may reduce the visibility and provide high humidity. These considerations are important to evaluate the efficiency of these mitigation measures, as well as the effectiveness of evacuation and rescue procedures.

Directive 2004/54/EC states that the main structure of all tunnels where a local collapse of the structure could have catastrophic consequences, for example, immersed tunnels or tunnels which can cause the collapse of important neighbouring structures, shall incorporate a sufficient level of fire resistance to prevent such a local collapse.

HyTunnel-CS addresses the whole range of hydrogen hazards associated with hydrogen-powered vehicles in confined spaces along with relevant incident prevention and mitigation techniques. These include:

- Hydrogen releases and its dispersion leading to the creation of flammable envelopes/clouds that could deflagrate or even transition to detonation. The size of the flammable envelope can be reduced by a reduction of the release orifice size, including that of any thermally-activated pressure relief devices (TPRD), provided that the fire resistance rating is still sufficient to exclude catastrophic rupture of high-pressure equipment. The main strategy is the prevention of flammable cloud formation under the ceiling of an underground structure and thus prevention of deflagration/detonation of a flammable layer under the ceiling if ignited.

- Hydrogen jet flame size and the related three hazard distances (fatality, injury and no-harm) can be assessed for free jets by the dimensional correlation for jet fires. They can be decreased by reduction of hydrogen release diameter and mass flow rate. Hazard distances of impinging jets, for example from TPRD downward orientation, can be assessed by using validated CFD models. The assessment of the interaction of large hydrogen jet fires with underground structures may require Finite Element Modelling (FEM) and simulations.

- Delayed ignition of hydrogen turbulent jets generates both thermal and pressure hazards. These can now be estimated based on HyTunnel-CS research. As expected, hazards due to the turbulent jet deflagration are reduced with the reduction of release diameter, for example, TPRD orifice size.

- Delayed ignition of a flammable layer formed under the ceiling of a structure is the event that should be prevented by all means, as the pressure effects from resultant blast waves and thermal effects from combustion products formed are especially harmful to people and destructive of vehicles and structures. These hazards result from the one-dimensional (tunnel) or two-dimensional (underground parking) space arrangement for blast wave decay and propagation of combustion products as compared to the open space incident scenarios (three-dimensional). The main deflagration prevention technique is the prevention of the flammable layer under the ceiling. The design of a vehicle should prevent the formation of a flammable

cloud under the ceiling of a confined space (it is worth mentioning that underground parking facilities have lower ceiling height compared to most of tunnels) that could result in a deflagration to detonation transition (DDT) event, this being the worst-case scenario for hydrogen incidents. HyTunnel-CS has developed an engineering correlation for DDT prevention. The validated CFD models are now available for assessment of consequences of deflagration and/or detonation in tunnels and other confined spaces.

- Pressure peaking phenomenon (PPP) is a characteristic unique to hydrogen, not seen in other fuels. CFD models, validated against large-scale experiments, are now available. The understanding of PPP is extremely important for the proper design of hydrogen vehicles for inherently safer use in garage-like enclosures with a limited area of vents. The phenomenon must also be accounted for in the design of hydrogen storage tanks and/or enclosures onboard of trains, ships, planes, *etc*.

- High-pressure hydrogen storage tank rupture in a fire must be prevented by all means necessary, to prevent devastating blast waves from propagating throughout the whole length of a tunnel with little decay. A fireball may also propagate along the tunnel behind the blast shock wave with a velocity up to 25 m/s. HyTunnel-CS has developed, for the first time, a storage tank-TPRD system model that permits the calculation of the 'safe' TPRD diameter for a compressed hydrogen storage system (CHSS) of arbitrary volume and pressure, as well as the required TPRD response time, that will exclude tank-TPRD system rupture in engulfing fire. OEMs are welcome to use this to minimise TPRD diameters for their vehicles' CHSS, improving the safety of HPVs parked underground or in private garages. However, there are limits to the ability of TPRDs to protect against tank rupture; examples of situations where this protection may fail are localised fires not affecting TPRD, isolation of the TPRD from a fire due to debris, *etc*., in an incident, long response time in the case of a 'small' fire, failure to open in fire or false opening due to a 'cycling issue', *etc*. HyTunnel-CS has addressed concerns regarding tank rupture through further testing of breakthrough safety technology invented at Ulster University (UU), this being the explosion-free-in-a-fire self-venting (TPRD-less) tanks. Vehicle designers can now use the TPRD-less self-venting storage tanks to eliminate blast waves, fireballs, projectiles, long flames, PPP and ultimately to reduce the risk associated with hydrogen-powered vehicles.

HyTunnel-CS's key message to stakeholders is that, to allow the inherently safer use of hydrogen vehicles in existing tunnels and underground parking, vehicle design is of paramount importance and should take account of the recommendations made by this document.

1.2 Incident scenarios with hydrogen transport in underground infrastructure

An assessment has been undertaken to identify the factors that contribute to the extent (hazard range) and severity (how badly it impacts humans/ environment) of an accident involving a hydrogen-powered vehicle in a tunnel or a similar confined space. The objective was to identify representative incident scenarios that will be used as the basis of researching how the potential consequence of an accident in a tunnel or confined space may be different to that of a comparable incident in an open environment; what safety strategies and engineering solutions are necessary to mitigate these differences. Members of SAB and representatives of National Networks were engaged in this exercise. The work included the definition, characterisation and categorisation of European tunnels and similar confined spaces. Relevant characteristics include tunnel length, cross-section area, width-to-height ratio, ventilation rate, *etc*.

In addition to parameters that should be considered following the requirements of Annex 1 of Directive 2004/54/EC, special attention was paid to the following aspects in the selection of scenarios for experimental, theoretical and numerical analysis and studies:

- Hydrogen releases and dispersion in tunnels with slope, where not only ventilation velocity determines the movement of smoke and gases and also their buoyancy. It should be noted that longitudinal gradients above 5% are not permitted by the Directive for new tunnels. In tunnels with gradients higher than 3%, additional and/or reinforced measures must be taken to enhance safety, based on risk analysis.
- Relation between concrete spalling and the way structural elements and linings are fixed.
- Tunnel operator's actions as the first responder, consequences of TPRD cooling by firefighters (note that TPRD-less tanks do not change existing intervention strategies and tactics of first responders).
- Inapplicability of Eurocodes to explosions produced by hydrogen tank rupture in a tunnel.
- Consequences of PPP for the intended functioning of doors and thus smoke propagation in cross-connections, shelters leading to escape routes to the open, *etc*. The Directive requires that "*appropriate means, such as doors, shall be used to prevent smoke and heat from reaching the escape routes behind the emergency exit, so that the tunnel users can safely reach the outside and the emergency services can have access to the tunnel*".
- Use of jet fans to transfer momentum to the main flow and the possibility of DDT.
- Permitting procedure for dangerous goods transportation through tunnels.
- Preservation of self-evacuation principle for hydrogen vehicles.
- Coupling fire dynamics and evacuation simulations.
- Coupling blast wave pressure loads and structural FEM simulations.
- Effect of hydrogen on back-layering.
- Worst-credible design scenarios, event frequencies, limits of leak rates and flammable cloud sizes, ventilation protocols, emergency preparedness, firefighting, rescue and evacuation.
- Effect of decreased ventilation rate in a fire, and innovative ventilation systems.
- Use of cheaper water spray systems in place of more expensive water mist systems.
- Explosion safety engineering for deflagrations and hydrogen tank rupture in a fire, *etc*.

The identification of typical potential accident scenarios was achieved in two ways. Firstly, through review of the HyTunnel-CS Description of Actions (DoA) of the Grant Agreement and HyTunnel-CS D1.1 (2019) and HyTunnel-CS D1.2 (2019), which reviewed underground safety provisions and hydrogen hazards, respectively. The second approach was to use the accident factors identified in HyTunnel-CS D1.3 (2019) to design scenarios based on the logical options and permutations of the accident factors. As an output from the work, ten accident scenarios were identified and formed a representative set of scenarios for the experiments. The HyTunnel-CS research proposal is aligned with the representative set of scenarios, which are:

1. Unignited hydrogen release and dispersion in a confined space with mechanical ventilation.
2. Unignited hydrogen release in confined spaces with limited ventilation.
3. Unignited hydrogen release in a tunnel with natural/mechanical ventilation.
4. Hydrogen jet fire in confined spaces with limited ventilation.
5. Hydrogen jet fire and vehicle fire in a mechanically ventilated confined space (maintenance shop/underground parking).
6. Hydrogen jet fire impingement on a tunnel.
7. Hydrogen jet fire and vehicle fire in a tunnel.
8. Fire spread in underground parking.
9. Hydrogen storage vessel rupture in a tunnel.
10. Hydrogen storage vessel blowdown with delayed ignition in a tunnel.

Each scenario is described in terms of fixed factors and accident variables that combine to describe the scope and range of the scenario. Several key aspects have been identified through this approach.

The credible transportation modes that are assessed here are cars, H_2-fueled buses and trucks; as well as trains. Buses and truck are grouped together as the vessel pressure (350 bar) and storage volumes are comparable. These three modes of transport represent those sectors that are likely to see the largest uptake. These modes also encompass a wide range of onboard hydrogen storage quantities (5 to 400 kg) which if assessed fully, will allow a more thorough understanding of the consequences, and allow the project to make robust conclusions and recommendations for stakeholders.

It has also been identified that blowdown volumes following TPRD initiation by fire may, in the worst case, lead to the discharge of the full hydrogen inventory simultaneously. Where TPRDs are interconnected, then a prolonged discharge through a common vent may occur. In some situations, delayed opening of one of the TPRDs connected to the same discharge line could block (due to higher pressure) release from the previously opened tank. This and similar safety issues should be addressed through a proper hydrogen safety engineering of a storage and release system.

These identified scenarios were based on current best available knowledge and research experience; they include processes of release and dispersion of unignited hydrogen, the interaction of hydrogen jet fire with structures and materials, pressure and thermal loads from explosions, including tank rupture in a fire, in the event of TPRD failure to operate in localised fire or blockage from fire during an accident, *etc*. The scenarios were targeted at the determination of critical time to reach harm or tenability criteria for safe evacuation and structural damage. It is worth noting that the scenario with hydrogen tank rupture in a fire essentially affects existing evacuation strategies in tunnels making them less efficient due to the short duration of the blast wave and high velocity of fireball propagation in a tunnel. This is why the tank rupture in a tunnel must be prevented by all means. As one possible solution, HyTunnel-CS project has demonstrated, by testing, the efficacy of a TPRD-less self-venting storage tank design.

1.3 Structure of recommendations

Section 2 presents the basic principles of hydrogen safety design for vehicles in confined spaces, in terms of general recommendations and safety strategies.

Section 3 presents the recommendations to deal with unignited hydrogen releases and jet fires in confined spaces. This section covers hydrogen concentration decay in under-expanded jets using the similarity law for a choice of release orifice size; hydrogen release and dispersion in tunnels with emphasis on the effect of tunnel slope, counter and co-flow of air on hydrogen flammable envelope size; the effect of release direction, especially downward hydrogen releases, on hazard distances; and discusses the requirements for TPRD orifice sizes and release directions for underground parking, garages and maintenance shops (including the effect of PPP); and tunnels. The section also discusses the mitigation of hydrogen jet fires using water sprays and mist systems, explains the contribution of hydrogen combustion to the heat release rates of a vehicle fire and presents an example of the hydrogen release effect on a car fire in underground parking.

Section 4 looks at hydrogen explosions, their prevention and mitigation. This covers hydrogen deflagrations, DDT and detonations in confined spaces, prevention of hydrogen tank rupture in a fire and the analysis of the blast wave and fireball dynamics after a hydrogen tank rupture in a fire. The section also discusses blast wave attenuation by absorbing materials, water sprays and mist systems, approach to the choice of onboard storage, and safety technology of explosion free in a fire use of a TPRD-less self-venting tank.

Section 5 presents the impact of hydrogen vehicle incidents on structures, such as erosion of tunnel materials by jet fire, concrete spalling; and the effect of hydrogen tank rupture on tunnel structural integrity.

Section 6 describes examples of applications of the QRA methodology for potential accident scenarios in road tunnels, rail tunnels and underground parking.

Appendix 1 lays out proposed harm criteria, Appendix 2 presents existing RCS information and Appendix 3 discusses the various hydrogen safety engineering models and tools for hazard assessment as well as the design of prevention and mitigation measures. Appendix 4 refers to the scaling technique by HSE for investigating blast waves and fireballs resulting from tank rupture in a fire (further details are also published within HyTunnel-CS D4.4, 2022).

2. Principles of hydrogen vehicle safety design

Usage of hydrogen-powered vehicles should not entail any greater risk than that of fossil fuel vehicles, including their operation in underground infrastructures like tunnels and other confined spaces such as underground parking, garages, maintenance shops, *etc*. The main difference between hydrogen and other fuels is higher onboard storage pressure. This defines differences in safety strategies to be applied. The hazards of HPVs in confined spaces include momentum-controlled releases in the form of under-expanded jets, which could form a flammable cloud if not immediately ignited or jet fire if ignited at the moment of release. Another potential hazard is the deflagration of an ignited highly turbulent jet or flammable cloud and its potential transition to detonation. Finally, hydrogen storage tank rupture in a fire can result in a blast wave, fireball and generation of projectiles. All these hazards can be eliminated or mitigated through proper safety design of the hydrogen-powered vehicle, as it would be difficult to redesign existing tunnels.

Hydrogen safety strategies for confined spaces are numerous. Because the most challenging release with the highest mass flow rate of hydrogen is from the TPRD, the TPRD parameters and direction of release should be designed in a way that no flammable cloud can be formed under the ceiling of underground parking. This would consequently exclude potential deflagrations and detonations, especially in ducts of the ventilation system. Thus, the release should not lead to accumulation of hydrogen above the LFL, i.e. 4% volumetric concentration of hydrogen in air, without the requirement for changes in the ventilation rates.

The ignited hydrogen release in the form of a jet fire from a TPRD should not compromise the ventilation system of the confined space. A strategy thus could be to prevent temperatures exceeding 300^{o}C developing under the ceiling, this being the most likely location of ventilation. It must be stressed that the safety strategy for the design of TPRD and discharge line, if any, should be to prevent flame blow-off.

Both of these goals can be achieved via the reduction of the TPRD diameter. This would mitigate PPP in a garage or a maintenance shop structure as well. The HyTunnel-CS project, for the first time, developed and validated a model to calculate the lower limit for TPRD diameter that would exclude a tank rupture in an engulfing fire. This is now available to OEMs for incorporation into their design processes.

If a vehicle is properly designed to prevent the formation of a flammable cloud in underground parking, it could enter the majority of tunnels without a problem, since tunnel ceiling heights are usually significantly larger than that of underground parking.

The most severe hazard associated with a hydrogen vehicle in a confined space is the rupture of a high-pressure hydrogen storage tank in a fire. In addition, data on the likelihood of tank rupture is still scarce for emerging technologies like hydrogen. This would have catastrophic consequences, including blast wave(s), fast propagating fireballs, and projectiles (the largest of which may be the vehicle itself). Unfortunately, TPRDs could fail to operate in a localised fire; or be thermally isolated from the fire by accident debris, and thus more reliable systems should be proposed. The HyTunnel-CS project therefore carried out further validation testing of a TPRD-less self-venting tank.

3. Dealing with unignited hydrogen releases and jet fires

High-pressure hydrogen storage tanks are currently equipped with TPRDs, which permit hydrogen release, in a fire event, to prevent the tank from rupturing as a result of burn-through of the tank wall, which is typically constructed from composite material. Important features for the proper design of a TPRD are its orifice size, its position relative to the vehicle and the release orientation. TPRD orifice size and release direction should be optimised to minimise the flammable envelope volume and flame length, in order to mitigate the risk to passengers or passing drivers/pedestrians.

The strategy for inherently safer use of HPVs in underground parking is to eliminate the formation of a flammable cloud under the ceiling preventing the potential of cloud ignition and destructive deflagration/ DDT/ detonation. In the case of upward unobstructed release from a TPRD at any angle, the similarity law, as described in Appendix A3.1.1 (Molkov, 2012) can be used to calculate the TPRD diameter that would allow the jet decay to below the LFL before reaching the ceiling. Once the hydrogen concentration under the ceiling is below the LFL, the formation and build-up of a flammable hydrogen-air cloud there can be generally discounted.

Hydrogen at concentrations below the LFL disperses further in the surroundings and should not represent hazards in tunnels and underground parking. Care should therefore be taken for small scale enclosures to exclude accumulation. The validated CFD models accounting for complex geometry and distributed over walls and ceiling vents can be applied for hydrogen safety engineering in such scenarios.

The TPRD release diameter for current hydrogen-powered vehicles is in the range of 2 mm to 6 mm. The use of diameters smaller than 2 mm is preferable and has been under investigation in HyTunnel-CS because it can reduce considerably and can even prevent the accumulation of a flammable cloud under the ceiling of a confined space.

3.1 Hydrogen concentration decay and choice of release orifice size

Unignited hydrogen release in the form of an under-expanded jet is a credible scenario across a wide range of hydrogen applications including accidents with hydrogen vehicles. In many situations, the safety analysis of unignited releases requires assessment for maximum propagation distance of a flammable hydrogen-air composition, i.e. the flammable envelope. The similarity law for hydrogen concentration decay along the momentum-dominated jet axis (Molkov, 2012) is a reliable tool that can be used to determine the distance to a position where hydrogen concentration decays to the LFL. The correlation is thoroughly validated for both expanded and under-expanded releases.

The similarity law states that the distance to a particular hydrogen concentration is proportional to release diameter and the square root of the storage pressure. In other words, the decrease of release diameter by 5 times will reduce the size of flammable envelope by 5 times. This fundamental functional dependence may guide the design of TPRD diameters employed on hydrogen vehicles. Description of the similarity law, its formulation to find the distance to LFL in a free jet and references to its validation are detailed in Appendix A3.1.1.

It must be stressed that the minimum TPRD diameter should be defined accounting for other conditions, especially the prevention of storage tank rupture in a fire.

3.2 Hydrogen release and dispersion in tunnels

3.2.1 Hydrogen releases in tunnels

The general safety strategies for tunnels and underground parking are similar. The design of HPVs and especially TPRD diameter and direction of release could account for the presence of ventilation, however the worst-case scenario in sense of ventilation to be considered is “stagnant atmosphere”, e.g. due to a fire nearby. Though tunnel ceilings are generally expected to be higher than in underground car parks, the safety design for large vehicle TPRDs, e.g. that for trucks, buses and trains, may be challenging due to the significant amount of hydrogen inventory onboard. Whilst larger vehicles may have many tanks and hence multiple TPRDs, a localised fire may not trigger all TPRDs to release the heated/ pressurised gas in order to prevent tank rupture. The ultimate aim is to ensure that hydrogen accumulation under the ceiling of a tunnel is avoided.

In HPVs, hydrogen is stored in composite pressure vessels in the gaseous state under high pressure, to provide driving range comparable with fossil-fuelled vehicles. The compressed hydrogen storage system (CHSS) is equipped with a TPRD that permits hydrogen release when it is activated in a fire, to prevent the storage vessel from rupturing in a fire. As previously mentioned, important parameters for the proper operation of a TPRD are its release diameter, its

position relative to the vehicle and to potential fire, the release direction and the presence and parameters of the discharge pipe, if any. TPRD diameter and release direction should be designed in such a manner as to minimise the hazard distances defined by flammable envelope and flame length; to mitigate the pressure peaking phenomenon; to exclude the formation of flammable cloud and hot combustion products with a temperature above 300^{o}C under the ceiling; and last but not least, to exclude tank rupture in a fire of any possible intensity (heat release rate per unit area), HRR/A.

The TPRD diameter of current HPV passenger cars is typically about 2 mm. It increases to about 6 mm for heavy-duty vehicles and trains. The use of TPRD diameters smaller than 2 mm is the subject of studies in HyTunnel-CS because it can considerably reduce the hazards of HPVs used in confined spaces. The CFD simulations (HyTunnel-CS, D2.3, 2022) performed for scenarios inside a tunnel, with and without inclination, showed that:

- Release through TPRD diameters in the range 2-4 mm leads to the formation of a flammable volume that increases with the increase of TPRD diameter. Moreover, in the case of 2 mm TPRD, the maximum near-stoichiometric fast burning mixture cloud of 25-35% vol. is much smaller than that of the case of 4 mm TPRD. It should be noted, however, that, after a certain time, TPRDs with a smaller diameter may exhibit larger hydrogen cloud volumes within a wide concentration range of 10-75% vol. due to the longer release duration. The release duration is dependent on inventory and other factors.
- For the vertically downwards release (from 700 bar storage pressure), the flammable cloud did not reach a distance of 4 m behind the car, for TPRDs with diameters in the range of 2-4 mm. The hazard distance and associated risk, however, decrease with decreasing TPRD diameter.
- The ventilation inside a tunnel affects the flammable cloud. The size of the flammable cloud and its dispersion towards the direction from which ventilation occurs reduces significantly. However, ventilation generally does not have a significant effect on the total volume of the more hazardous fast-burning near-stoichiometric mixture because it is located for under-expanded jets in the momentum-dominated area of the jet. To exclude the formation of fast-burning mixture under the vehicle, it is wise to direct the release away from/out of this area.
- Hydrogen tends to rise by buoyancy under the ceiling regardless of the release orientation. However, proper design of TPRD diameter and release direction could help ensure that hydrogen under the ceiling is at concentrations below the LFL and thus does not pose any hazard.

TPRDs are typically placed at the bottom of light-duty vehicles (LDV), while for large vehicles such as buses, it is usually located on the roof. In the case of a release beneath a car, the hazards and associated risks might increase if hydrogen can be trapped and accumulate below the car. The CFD simulations (HyTunnel-CS, D2.3, 2022) examined the effect of TPRD orientation on hydrogen distribution inside a tunnel of maximum height 7.1 m from a TPRD located 20 cm above the tunnel floor. The vertically downwards and upwards, as well as horizontally backwards directions were numerically investigated for a configuration comprising two vehicles. The results showed that:

- Flammable clouds lasted longer in the upwards release case.
- Maximum flammable volume was 3 times smaller in horizontally-backward release compared to vertically downward release case. It is worth mentioning that these two cases are not considered as practical; and this result is rather for general knowledge purposes.

- The maximum near-stoichiometric cloud (25-35% vol.) was 70 times higher in the vertically downwards release case, which therefore cannot be recommended.
- Release directions at an angle are shown to be safer practice (Shentsov *et al.*, 2021).

3.2.2 Effect of tunnel slope

The vast majority of tunnels are actually inclined (Zhao *et al.*, 2019) mainly due to physical restrictions, like for example in undersea tunnels. Usually, the slope of tunnels is a few percent. According to the current EU Directive 2004/54/EC, new tunnels are not allowed to have a slope greater than 5% (1:20 gradient, or 2.86°), unless no other solution is geographically possible. Slopes under 2% (1:50 gradient, 1.15°) are considered to be small. An inclined tunnel may be lower in the middle ('V' shape), e.g. when beneath a river, higher in the middle (inverted 'V'), or straight ascent/descent. For single-way tunnels, the straight-line tunnel is mentioned as ‘ascending’, when the vehicles move towards the higher end of the tunnel and ‘descending’ otherwise.

The most important physical consequence of the slope of a tunnel in the dispersion of hydrogen or smoke is the ‘stack effect’, or ‘chimney effect’ due to buoyancy: for straight-line shaped tunnels, lower density gases have the tendency to rise, towards the higher end of the tunnel due to buoyancy effects.

There are a limited number of studies related to hydrogen dispersion in sloped tunnels. Tunnel inclination has attracted scientific interest especially concerning its effects on fire and smoke propagation. Due to the buoyancy of both smoke and hydrogen, their dispersion is expected to present several similarities. It is worth mentioning however, that there is a significant difference between smoke and hydrogen. While smoke remains harmful and hazardous throughout the process, hydrogen decaying below 4% vol. in air is no longer more flammable and thus no longer hazardous to people and structures.

Smoke propagation studies at naturally-ventilated inclined tunnels have revealed that the smoke reaching the ceiling initially expands towards (more or less) both directions, like in the horizontal tunnel case (Tuovinen *et al.*, 1996). Then the ‘stack effect’, due to buoyancy, increases the propagation speed towards the upper end of the tunnel (Woodburn and Britter, 1996), affecting both the flow and the dispersion field (Ji *et al.*, 2015), especially at high inclinations and long tunnels (Fan *et al.*, 2017).

In mechanically-ventilated tunnels, as the slope increases, the critical velocity (in order to avoid back-layering) also increases, but only slightly (Musto and Rotondo, 2014). However, several times greater pressure increase should be provided from the ventilation system, in order to achieve the required critical speed in descending tunnels, due to the significant flow resistance that the stack effect imposes (Du *et al.*, 2018).

In general, the case of descending tunnels is one of the most unfavourable concerning safety (Ballesteros-Tajadura *et al.*, 2006) and should be carefully examined, especially due to the fact that in some cases, confusion may be created about how to act in an emergency (Zhao *et al.*, 2019).

Mukai *et al*. (2005) performed simulations of hydrogen dispersion in sloped tunnels of several longitudinal shapes. The results revealed that in all cases, the potential risk due to a hydrogen-air

mixture above the lower flammability limit is minimal, since only the core of the upward jet close to the car has volume concentrations above 4%. The leak rate of this specific study was very low though. Seike *et al.* (2019) examined the thermal fume behaviour of an HPV on fire in a non-ventilated tunnel. As the slope increases, at the downwind side the fume propagates faster, while at the upwind side the fume propagation distance decreases.

CFD simulations have been performed within HyTunnel-CS for a hydrogen car release from a downwards-pointing 2 mm (and in some cases 4 mm) TPRD at the centre of a 200 m long tunnel (HyTunnel-CS, D2.2, 2020; HyTunnel-CS, D2.3, 2022; Koutsourakis *et al.*, 2021). These showed that:

- TPRD characteristics like the release **diameter** and **orientation of release** have a much more important influence on hazards than the tunnel slope.
- Tunnel inclination up to 5% has, in general, a small effect on the velocity and concentration field around the car, which is usually the most dangerous region, and negligible effect during the first stages of the release, which are considered the most critical. Inclination has also a small effect on the total volume of the most hazardous nearly-stoichiometric concentration cloud. Thus, in straight sloped tunnels of short length, no special treatment regarding inclination is currently considered necessary for safety. There are, however, cases where adverse effects may exist in inclined tunnels. For example, the volume of flammable clouds can be bigger in the case of inclination at specific time ranges, depending on the release parameters and the slope.
- The **long-term** influence of the inclination is positive: that is, in the case of straight sloped tunnels, the greater the inclination, the sooner hydrogen will reach near-zero concentrations. However, the time we refer to here is long after the release stops and is of low interest in terms of safety.
- The ventilation effect in sloped tunnels is similar to non-sloped tunnels. However, in cases where the ventilation flow is against the ‘stack effect’ and its rate is small, part of the hydrogen may remain inside the sloped tunnel for a longer time, especially if the ventilation stops for some reason.
- The flow velocity and concentration fields are unsteady, especially during the initial stages and close to the impingement regions. Thus, high variations of the actual concentrations can be expected.
- At different parts of the tunnel, concentrations may continue to vary significantly, even after a long time due to various reasons (HyTunnel-CS, D2.3, 2022). For example, in a sloped tunnel, the upper (longitudinally) half may become free from a flammable cloud near the ceiling for several minutes, but after the “air curtain effect” ends, the second wave of flammable cloud (that was previously trapped at the lower (longitudinally) half of the tunnel) may pass along to the upper half of the tunnel again. This is more pronounced in the case of comparatively smaller TPRD diameters (yet not small enough to exclude concentrations above LFL under the ceiling as per the recommended safety strategy) due to a longer release duration. Another example is the end of the ceiling-impingement period that will result in resettlement of hydrogen and thus concentration variations in the ceiling area above the car (this can occur in both sloped and non-sloped tunnels). Thus, regions may exist where at some time the concentrations fall below

flammable and continue decreasing, but after several minutes (or possibly even longer, for longer tunnels) they increase above flammable limit again (but not much above the LFL of 4% by volume).

These specific conclusions are expected to be valid for the cases examined. It should be mentioned that these scenarios with flammable cloud migration under the ceiling would be discounted, if the release decays below LFL before reaching the ceiling, especially when taking into account the dynamics of pressure drop in hydrogen storage during blowdown.

3.2.3 Effect of counter-, co- and cross-flow ventilation on the flammable envelope

Mechanical ventilation is a safety measure to prevent hydrogen accumulation inside enclosures and confined spaces and mitigate the consequences in case of an unscheduled leak. The configuration of ventilation is a factor that might influence its efficiency in hazard reduction. The ventilation configuration of co-flow, counter-flow and cross-flow relative to hydrogen release direction were studied experimentally (Grune *et al.*, 2021), and numerically for the case of co- and counter-flow (Giannissi *et al*., 2021) resulted in validation of two CFD models against the experiments. It is demonstrated that the ventilation reduced the size of the flammable envelope for all three studied configurations and regimes that were characteristic for release from a pipeline supplying hydrogen to the propulsion system.

As for the cross-flow experiments, the results can be found in Appendix A3.1.8, with full details in HyTunnel-CS D3.3 (2022).

The conclusions on the effect of airflow from mechanical ventilation in a tunnel are:

- Both co- and counter-flow ventilation led to a reduction of the flammable envelope length compared to the no ventilation case (up to 30% for hydrogen jet with a mass flow rate of 5 g/s through a 4 mm nozzle). This is supported by both the experiments and simulations.
- Cross-flow ventilation can also produce strong turbulence and effective mixing. The dimensions of both 4% and 10% by volume of hydrogen clouds are reduced by the ventilation airflow in a cross-direction, leading to a smaller flammable cloud. Thus, cross-flow ventilation is the most effective way to reduce the flammable length by, e.g. more than 50% in some cases with airflow velocity of 3.5 m/s.
- The CFD models were validated against experimental data and recommended for use as contemporary tools for hydrogen safety engineering (Giannissi *et al*, 2021). However, fan-generated turbulence should be properly modelled, either by imposing high turbulence or a non-uniform velocity field across the inflow boundary to mimic the fan flow.
- The similarity law for concentration decay is a conservative tool not accounting for pressure losses in a pipeline. In these tests with comparatively low storage pressures, the similarity law, which is valid for momentum-dominated jets, overpredicted the concentration at distances further from the nozzle in both the co-flow configuration and in the no ventilation case. The concentration decay in the counter flow was not well reproduced. Whilst the similarity law can be used as a conservative tool for cases with ventilation, validated CFD models are recommended as hydrogen safety engineering tools for cases of comparatively low release pressure and counter-flow ventilation.

It should be highlighted that some catastrophic releases from high-pressure storage and equipment cannot be mitigated by mechanical ventilation. Prevention safety measures should be implemented to avoid such scenarios, where possible. In addition, ventilation in the tunnels is designed to deal with air quality and it reduces to about 3 m/s during fire to assist evacuation. Thus, the ventilation strategy in tunnels cannot be changed.

3.2.4 Dynamics of release and dispersion of hydrogen in a tunnel

A number of experiments have been performed in the HSE 70 m steel tunnel. These have generated measurements of hydrogen concentrations following TPRD releases, simulating those from cars, buses and trains. The measured data was compared with CFD predictions. Overall good agreement was found between simulation results and experiments, at most of the sensor positions. The successfully validated CFD codes can be used as a reliable tool in hydrogen safety engineering. The outcomes from this activity will likely include recommendations on TPRD orifice size.

3.2.5 Results of large-scale experiments on unignited releases in a real tunnel

Four experiments were performed by partner CEA at Tunnel du Mortier (5.2 m ceiling height) with 60 to 70 MPa helium tanks of 78 L volume following a preliminary experimental campaign of seven tests with 20 MPa 50 L tanks. Helium was used instead of hydrogen to exclude hazards and associated risks from the formation of a flammable cloud. Helium was proven to be a good substitute to hydrogen for dispersion characterisation. It has almost the same density, and experimental comparisons between hydrogen and helium releases performed at INERIS confirmed similar behaviour (Bernard-Michel and Houssin, 2016). The paper discusses how to calculate the equivalent flowrates of He versus H_2 and shows that there is little difference due to the similarity in the reduced gravity values of both elements. Several experiments were simulated using the Large Eddy Simulation (LES) technique. The results are presented in HyTunnel-CS D2.3 (2022) and they demonstrated that TRPD diameters above 2 mm will lead to the formation of a flammable cloud in the tunnel (not only in the jet volume), whatever the orientation of the TPRD release.
Results for a 2 mm TPRD release showed the formation of near to 4% cloud under the ceiling of this real tunnel, localised at the injection's vertical axis for vertical release or shifted by around 6 m in the case of a downward 45° release. In the latter case, concentration might briefly exceed 4% (reaching 6%). Therefore, it is recommended **not to use a TPRD diameter equal or above 2 mm**. It is worth mentioning that the situation with the same TPRD diameter in underground parking will be worse due to lower ceiling heights in underground parking.

The experiments showed that **TPRD diameter below 1 mm is preferable** since the formation of a flammable atmosphere is only restricted to the released jet/plume except for a vertical downward release (0^o from the vertical axis), which **always leads to a flammable atmosphere** under the chassis whatever the TPRD diameter is.

It is therefore concluded from the experiments (relevant to tunnels but not always to underground parking):

- Avoid a release from TPRD vertically downwards.
- Releases vertically upward from smaller TPRD diameters or releases downwards at an angle, e.g. 45° to the vertical, could be considered subject to prevention of flammable

cloud formation under the ceiling of confined spaces and prevention of high-temperature combustion products higher than 300°C under the ceiling.

- TPRD diameters below 2 mm could allow the prevention of flammable cloud and high-temperature under the ceiling for tunnels; however, because of the 1mm limit found for underground parking, the commonly applicable TPRD diameter would be 1 mm for both configurations. Note: consideration should still be given to the fire resistance of tank-TPRD systems with comparatively small TPRD release diameters.

The natural ventilation in the tunnel between -0.9 m/s and +0.9 m/s showed no influence on the maximum concentration level and therefore on the dispersion process. However, it affects the concentration distribution far away in the tunnel (more than 50 m) in a way that the cloud is transported in the direction of the ventilation flow with only a small reduction of the concentration. It is recommended that firefighters follow the existing ventilation strategy in the case of a fire with HPV. The use of validated CFD tools is recommended to evaluate dispersion in a tunnel with and without ventilation.

3.3 Hydrogen release in underground parking, garages and maintenance shops

3.3.1 Underground parking

Underground car parks are typically more stringent in safety provisions than tunnels due to lower ceiling height, unless the tunnel is a narrow mine or rail tunnel.

Underground parking has mechanical ventilation for air quality control. The parameters of the TPRD to satisfy safety requirements for the current ventilation arrangement should include its diameter, release location and angle and it should be designed based on:

- Prevention of flammable cloud formation under the parking ceiling.
- In case of ignited release in the form of a jet fire, the temperature of combustion products under the ceiling should be below 300°C (see Section 3.3.1.1).
- The release should not obstruct the self-evacuation or rescue from an HPV.
- The rupture of onboard storage should be prevented at all costs.

It is highly unlikely that PPP will affect the structural integrity of most of the underground parking systems with multiple entrances and exits but must be assessed for enclosures such as small private garages, including underground, and maintenance shops with limited natural ventilation.

3.3.1.1 Requirements for ventilation and TPRD sizing and orientation of release

The rate of ventilation in underground parking is defined by national standards. For example, British Standard BS7346-7:2013 requires 6-10 ACH, Norwegian Standard requires 6 $m^3/h/m^2$, *etc*. The CFD simulations (HyTunnel-CS, D2.3, 2022) were performed by partner NCSRD, examining two ventilation rates, 11.25 ACH as per ANSI/ ASHRAE Standard 62-1989 (Krarti and Ayari, 2001) and doubled to 22.5 ACH assuming two different TPRD release diameters, i.e. 1 mm and 2 mm. The simulations showed that:

- The effect of TPRD size is much more significant than the effect of ventilation.
- Releases from TPRD diameters of 2 mm leads to a flammable cloud that covers a substantial volume of the garage. Halving the TPRD size, i.e. to 1 mm, leads to 2-3 times lower maximum flammable volume for both ventilation rates.

The effect of doubling the ventilation on the maximum flammable volume is found to be insignificant. The testing of the ADREA-HF CFD code (HyTunnel-CS, D2.3, 2022) against a

HyTunnel-CS experiment with hydrogen release through TPRD=0.5 mm and 10 ACH ventilation showed good predictive capabilities. Thus, validated CFD models can be used as predictive tools for hydrogen safety engineering in underground parking with mechanical ventilation.

The general recommendations for the design of HPVs to mitigate thermal and pressure effects of hydrogen release in underground parking or similar confined spaces are based on the following principles:

- The foreseen hydrogen release, if ignited, should not lead to violation of current regulations and their requirements for mechanical ventilation systems. In the case of underground parking, the hot products of hydrogen jet fire should not have a temperature above 300°C at the entrance of the ventilation systems for a ventilation rate of 10 ACH according to British standard BS 7346-7:2013. It should be highlighted that the criterion "not to exceed 300°C under the ceiling" is conservative and that hydrogen jet fires will have a much shorter duration compared to the fire resistance time for ventilation fans of at least 60 minutes to 300°C required for a general car fire scenario.
- The hydrogen jet fire contribution to the total heat release rate (HRR) of a vehicle fire should be negligible.

The dimensionless flame length correlation can be used to assess hazard distances for unobstructed hydrogen jet fires (Appendix A3.1.7). However, in the case of complex geometry and impinging jets, only validated CFD models can be recommended as contemporary tools for hydrogen safety engineering, for example, to assess the effects of a hydrogen jet fire directed downwards at some angle to the vertical, in an underground parking structure, including its interaction with structural elements, the mechanical ventilation system, *etc*.

UU performed simulations in underground parking structures with dimensions 23.5×45×3m for downwards unignited and ignited releases from TPRDs of different diameters and different release angles (releases were directed towards the rear of the vehicle) from an onboard storage tank of 62.4 L volume and NPW=70 MPa. The conclusions of this study are in line with those from experimental and numerical studies of other partners:

- Mechanical ventilation with a rate of 10 ACH does not affect the distribution of the hot combustion product under the ceiling and hazard distances for TPRD of 0.5 mm diameter.
- A downward release at angle 45° to the vertical through a TPRD of 0.5 mm diameter does not obstruct the vehicle evacuation and reduces the hot combustion products (300^{o}C) height compared to release angles of 0-30°, and hazard distances compared to release at angle of 60° to the vertical. Ignited releases at an angle of 0° may obstruct self-evacuation and rescue operations from the vehicle. For release angles below 30° the formation of hot products with a temperature of 300°C at a height of 2 m is observed. This height is comparable to the minimum height of 2.1 m recommended for underground parking by IStructE (2002).

A downward release at angle 45° to the vertical should be through a TPRD of 0.5 mm diameter to not exceed 300^{o}C at the entrance to the ventilation system in underground car parks with height 2.1-3.0 m and to not significantly affect an HPV heat release rate (+15% for a short period, see Section 3.5). Release diameters equal to or larger than 0.6 mm may result in the formation of hot products with a temperature greater than 300°C, at heights equal to or smaller than 2.5 m. This statement is valid for storage pressures equal to NWP and above. In addition, it should be mentioned that the duration of the hydrogen blowdown through the TPRD for vehicles is generally less than the minimum 60 minutes period indicated for the operability of fans at 300 °C (class F300).

The conclusions presented above are valid for a hydrogen jet fire not impinging on the walls or ceiling of the underground parking structure. These observations for a TPRD release diameter and angle are in line with results obtained for unignited releases but are more restrictive with regards to the maximum allowable TPRD release diameter.

Reduced and comprehensive CFD models were compared within the HyTunnel-CS project for the design of mechanical ventilation in underground parking. It was demonstrated that hydrogen release from HPV onboard storage may lead to a highly non-uniform and transient hydrogen distribution, which usually contradicts the assumptions of the reduced models, e.g. on mixture uniformity, and leads to loss of predictive capability of such models. The CFD models do not need simplifying assumptions typical of the reduced models and may be recommended as contemporary tools for hydrogen safety engineering for scenarios with unignited and ignited releases in mechanically ventilated underground parking. The CFD models can account for highly dynamic release scenarios, i.e. blowdown of the storage tank, a large volume of parking, presence of obstacles in the vicinity, including vehicles, location of ventilation ducts, flow losses and heat transfer in ducts, *etc*.
For downward jet direction, it was demonstrated (Shentsov *et al.*, 2021) that unignited releases from the TPRD do not lead to accumulation of flammable composition under the parking structure ceiling provided the TPRD diameter is less than 0.75 mm and when the release angle is 45° to the vertical.

The experimental investigations of hydrogen releases from a TPRD of 0.5 mm and a TPRD of mm diameter with 70 MPa storage into a 40-foot ISO container confirmed the conclusion of numerical studies that the ventilation rate does not influence the maximum concentration level (Lach and Gaathaug, 2021). The ventilation rates 6 ACH and 10 ACH were investigated following recommendations of BS 7346-7:2013. The duration of the time when the cloud was flammable was reduced with the increased ventilation rate. The experimental acquisition system comprised 38 hydrogen sensors, a mass flow meter, a transducer for measurement of tank pressure and thermocouples for temperature measurements. This dataset can be used to validate CFD simulations on vertical downwards release and dispersion on hydrogen in an enclosure with mechanical ventilation (it can be found at https://doi.org/10.23642/usn.14405903). A TPRD diameter should be less than 1.0 mm for a hydrogen jet fire to comply with current ventilation systems requirements. This conclusion does not consider the added effect of a burning car.

The recommendations are limited to the release of gaseous hydrogen at atmospheric and cryogenic temperatures. It has been demonstrated that the Similarity Law and the dimensionless flame correlation work for cryogenic temperatures for free jets. The release of liquid hydrogen is out of the scope of the HyTunnel-CS project (it is recommended that the reader refers to the results of the PRESLHY project for studies involving liquid hydrogen). It has been concluded that a TPRD diameter of the order of 0.5 mm would be sufficient to reduce hazards and associated risk to the level of fossil fuel vehicles (see later in the recommendations on the fire resistance of tanks with a TPRD diameter of 0.5 mm). Recommendations do not require the introduction of changes to existing tunnel and underground parking systems if the design principles described in these recommendations area applied. This underpins the inherently safer deployment of hydrogen-powered transport in Europe and beyond.

The effect of jet impingement was studied experimentally in a large-scale experimental system (Lach and Gaathaug, 2020) and (Lach and Gaathaug, 2021). The experimental data can be used to validate hydrogen safety engineering models and tools (see Appendix A3.2.4). The experiments on hydrogen releases in underground parking were carried out in a 40-foot ISO container simulating underground parking. The blowing type ventilation was used and a vehicle was simulated by a steel model. The model was scaled to 40% of a Toyota Mirai car. The release was from nozzles of diameter 0.5-1.0 mm from 6-70 MPa storage with mass flow rates 1-8 g/s. The recommendations from this study and safety strategies are:

- Underground parking has complex geometries and no general scaling criteria have been found. **It is recommended to use CFD tools for assessing the consequences of unintended releases of hydrogen in specific parking systems.** The correct modelling of the hydrogen source is important. The CFD models can be validated against the detailed experimental concentration measurements obtained in the HyTunnel-CS project (Lach and Gaathaug, 2021a). It includes detailed measurements of concentrations under the simulated car.
- In agreement with numerical studies, the ventilation rates in the investigated range, do not affect the maximum concentration under the ceiling. The influence of the TPRD nozzle diameter is critical. In this series of tests in the container, even a TPRD of 0.5 mm diameter resulted in about 8% of hydrogen concentration under the ceiling. **The recommendation is to use as small a TPRD diameter as possible** (sufficient to prevent tank rupture in a fire).
- The change of ventilation rate from 6 ACH to 10 ACH influenced the duration of the flammable hydrogen cloud presence (see Table 3-1). The blowdown time is the duration of the release, while P_{tank} and P_{end} were the start and end pressure of the hydrogen reservoir. The total flammable time (in seconds) was the duration of when there was an ignitable atmosphere inside the container. **It is recommended to use high ventilation rates in case of unintended hydrogen releases.** It should be noted that propagation of a flammable mixture to ventilation ducts could cause deflagration and even detonation.

Table 3-1. Duration of flammable atmosphere during hydrogen releases (Lach & Gaathaug, 2021b)

Test No.	P_{tank}	ACH	Blowdown Time	P_{end}	Total flammable time t_f
22	209 bar	6.0	900 s	6 bar	11 s
23	359 bar	10.2	900 s	12 bar	83 s
21	362 bar	6.2	900 s	10 bar	195 s
19	721 bar	10.2	900 s	16 bar	285 s
20	713 bar	6.2	900 s	17 bar	336s

The experimental investigations of hydrogen jet fires in a 40-foot ISO container showed that the temperature in the ventilation was below 300°C (HyTunnel-CS, D3.3, 2022, 2022 and Lach and Gaathaug, 2021b)). This was the contribution from the hydrogen jet fire mostly from 0.5 mm nozzle, but at realistic pressure in the storage tank of 70 MPa. When compared to the 1.0 mm nozzle, the temperature was above 300°C at the inlet to the ventilation system. These experimental observations are in line with the conclusions of numerical studies.

The experiments in a 40-foot ISO container, which simulated ‘super-small’ parking (HyTunnel-CS, D3.3, 2022) were used to assess the direction of the TPRD release in such an arrangement,

with walls close by on all four sides). While the angle of TPRD release did not affect the measured temperature under the ceiling, in the case of the largest angle of 45°, the temperature along the floor behind the car was higher. This is in line with the predictions of numerical simulations.

3.3.2 Example of hydrogen release effect on car fire in underground parking

The fire spread in a car park has been investigated (Markert and Giulani, 2019). The opening of the TPRD is triggered on HPVs adjacent to the vehicle which originally caught fire, when the parking distance is close, e.g. 60 cm, and the TPRD diameter is comparatively large. The reduction of the TPRD diameter was modelled in the study carried out by DTU and this showed the tendency of this effect to stop with the decreasing TPRD diameter below 4 mm. Although the increase of the release duration and the duration of the jet fire may have a role to play as in the simulation, the TPRD of a neighbouring car was surprisingly not triggered for diameters below 4 mm all the way down to 0.5 mm (release vertically downwards) with the exception of the 1 mm case[1]. This also influences the ceiling temperatures and thus the impact on the concrete structures. The design of the TPRD diameter should consider such effects to minimise impact.

Safety in underground parking is not compromised by the burning of a single hydrogen car. Nevertheless, as very large fire incidents involving multiple vehicles have recently been seen in car parks, perhaps it is worth giving more consideration to this aspect. This is of course more of a question of improved fire safety design of such infrastructures, independent of the type of fuel a vehicle is using. In the case of hydrogen-powered vehicles with protection against fire by TPRD, a very large fire could simultaneously trigger the TPRDs of several nearby vehicles. This could generate a substantial hydrogen flammable cloud that could deflagrate. In the event of the failure of a TPRD to open, a storage tank rupture may occur. Both scenarios are extremely hazardous. It should be assured that the hydrogen safety engineering of a vehicle is properly performed to allow it to be safely parked in underground garages. The underground parking arrangements should ensure that only very few vehicles may be on fire at the same time[2]. This is also the intention of current regulation [DCLG (2010), Schleich, *et al*. (1999), Tohir and Spearpoint (2013)], but these may need to be revised. It has to be reiterated that this is important for all types of vehicles and is as such, is not a unique safety issue of hydrogen vehicles.

3.3.3 Garages, maintenance shops, CHSS enclosures

Garages, maintenance shops, enclosures for compressed hydrogen storage system (CHSS) onboard of vehicles, trains, airplanes and similar enclosures have somewhat different hydrogen safety considerations compared to underground parking and tunnels, as discussed in the subsections that follow.

[1] The reason for this anomalous behaviour is unclear. One hypothesis could be that for the larger diameters, the release is very fast and even though the HRR is high, the very short heating time means the components cannot reach the 110°C within that duration. As for the 0.5mm TPRD diameter, the HRR is too small even though the release time is long. So, the combination of a TPRD diameter of approximately 1mm provides a sufficient HRR and a sufficient time period for the TPRD to reach 110°C.

[2] Note that the scope of the project does not include escalation to vehicles using other fuels, i.e. does not consider that a H_2 jet fire escalates to an adjacent vehicle with gasoline fuel, leading to a gasoline pool fire that could affect further vehicles.

3.3.3.1 The pressure peaking phenomenon

Recommendations for the provision of safety of HPV in garage-like enclosures differ from those for tunnels and underground parking. Due to a limited area of vent(s), the comparatively small volume of garage-like enclosures, and close proximity of walls to releases in any direction, it is not always possible to follow safety strategies formulated for tunnels and underground parking, i.e. prevention of flammable cloud formation under the ceiling and restriction of temperature to a maximum of 300ºC at the entrance to a ventilation system. By the same reasoning, compact enclosures are subject to PPP, as revealed earlier at UU (Brennan *et al*., 2011). This is a constituent part of any hydrogen safety engineering of any application.

In the case of a hydrogen release from high-pressure storage or equipment, e.g. TPRD failure or full-bore pipe rupture, in an enclosure like a garage or room with hydrogen tanks onboard a train, ship, or airplane, PPP could occur, demolishing the enclosure. A typical civil structure can withstand overpressures of around 10–20 kPa but during PPP, much higher pressures could be generated, depending on the area of the vents in the enclosure, in just 1–2 s. Therefore, a tank-TPRD system should be designed to withstand any fire without rupture whilst reducing the rate of release of hydrogen through the TPRD to prevent PPP and subsequent risk of enclosure demolition.

The PPP overpressure inside an enclosure of known volume, area of openings (vents) and hydrogen release flow rate (depends on storage pressure, volume and temperature) can be calculated using the tool described in Appendix A3.1.5 and available online (free of charge) in the e-Laboratory of Hydrogen Safety (https://elab.hysafer.ulster.ac.uk/). Mitigation of PPP can be achieved by either the decrease of TPRD diameter or the increase of vent area. However, such PPP mitigation measures cannot be considered separately from the requirement to prevent storage tank rupture in any fire.

The theoretical, numerical and experimental studies undertaken demonstrated that PPP from a jet fire is more hazardous than an unignited release from the same source, i.e. release from a TPRD (Makarov *et al*., 2018; Lach *et al*., 2020; Lach and Gaathaug, 2021c). The overpressure from an ignited hydrogen release corresponds to that of an unignited hydrogen release with about 22 times larger mass flow rate.

3.3.3.2 Experimental study of unignited releases

Experimental investigations of unignited releases in confined space were carried out. Hydrogen was released from storage at 70 MPa through 0.5 mm or 1.0 mm diameter nozzles. Hydrogen concentration was measured inside a 40-foot ISO container with a mock-up car inside. Hydrogen was released vertically downwards under the car. Tank pressure, temperature and hydrogen mass flow rate were measured. Experimental data can be used for the validation of CFD models and are available at: https://doi.org/10.23642/usn.14405903.

The investigation showed that a 0.5 mm nozzle at storage pressures 20 MPa and 70 MPa produced approximately the same mass flow rate as a 1.0 mm nozzle at lower pressures 6 MPa and 20 MPa respectively. The larger nozzle diameter resulted in higher concentrations of hydrogen under the ceiling even when the mass flow rate was reduced by use of a lower storage pressure. This experimental observation is in line with theoretical understanding that flammable envelope and flame length are proportional to both nozzle exit diameter and mass flow rate.

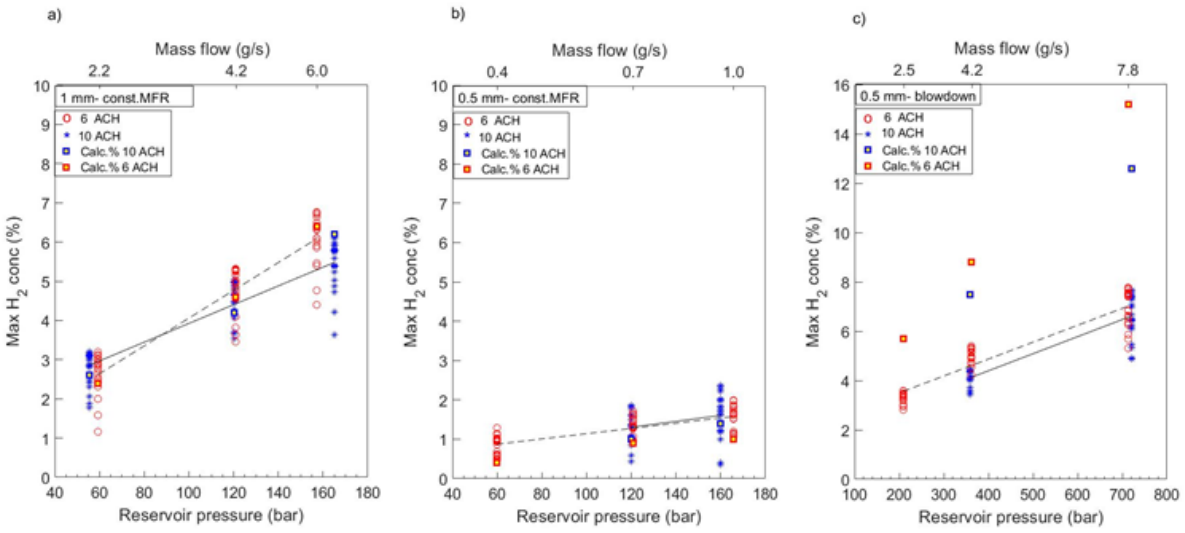

Figure 3-1. Maximum hydrogen concentration under the ceiling as a function of reservoir pressure and nozzle diameter: a) 1.0 mm nozzle, constant mass flow rate; b) 0.5 mm nozzle constant mass flow rate; c) 1.0 mm nozzle tank, blowdown (reducing in time mass flow rate). Release is vertically downwards under the mock-up car

Experiments (see *Figure 3-1*) confirmed that for studied scenarios the maximum concentration was not affected by ventilation rate in the range from 6 ACH to 10 ACH. The only observed effect of the ventilation rate was a decrease of time during which the cloud of hydrogen in the air was flammable.

The main recommendations derived from this series of experiments on unignited releases in garage-like enclosures are:

- Smaller release orifice diameter reduces hydrogen concentration in the flammable cloud. The nozzle of 0.5 mm diameter resulted in concentrations below 10%.
- A higher ventilation rate reduces the duration of the flammable cloud existence.
- Validated CFD models are recommended for carrying out hydrogen safety engineering in complex geometries.

3.3.3.3 *Experimental study of ignited releases*

The ignited release investigations used the same experimental setup as for the unignited releases. The majority of tests were performed with a nozzle of 0.5 mm diameter. Both downwards vertical jet fire under the car and 45° backwards jet fire were investigated (Lach, Gaathaug and Vågsæther, 2022). A sketch of the experimental setup is shown in Figure 3-2. The ventilation system is an extracting-type ventilation where air comes in via the open doors and is removed at the closed end.

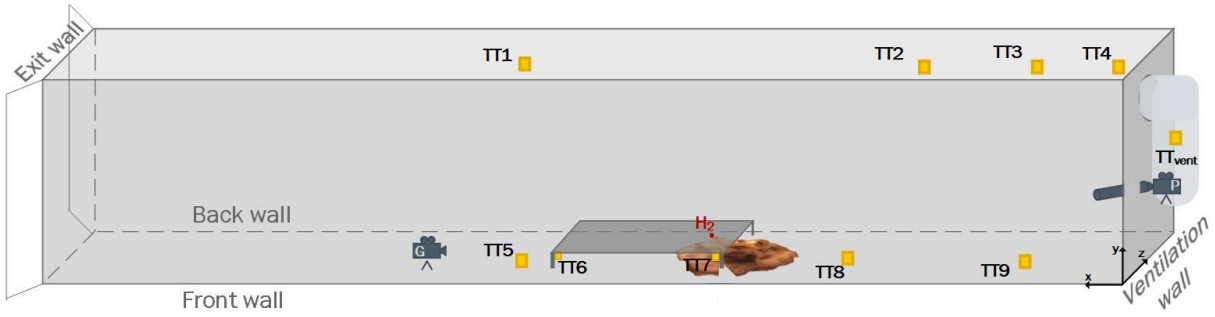

Figure 3-2. Sketch of the container used for experimental study of ignited releases. TT shows where the sensors were placed in the tunnel mock-up

Temperature and heat flux were measured in these experiments (see Figure 3-3). The main result of these tests is that, for investigated mass flow rates, the temperature under the ceiling and in the vent did not exceed the standards-mandated temperature of 300°C. The jet fire from the nozzle of 1.0 mm diameter from 35 MPa storage pressure resulted in a temperature of 270°C in the ventilation shaft, and it is expected that 70 MPa would result in a temperature higher than 300°C. Testing with a nozzle of 0.5 mm diameter showed that the temperature was below 200°C for a release from 70 MPa storage.

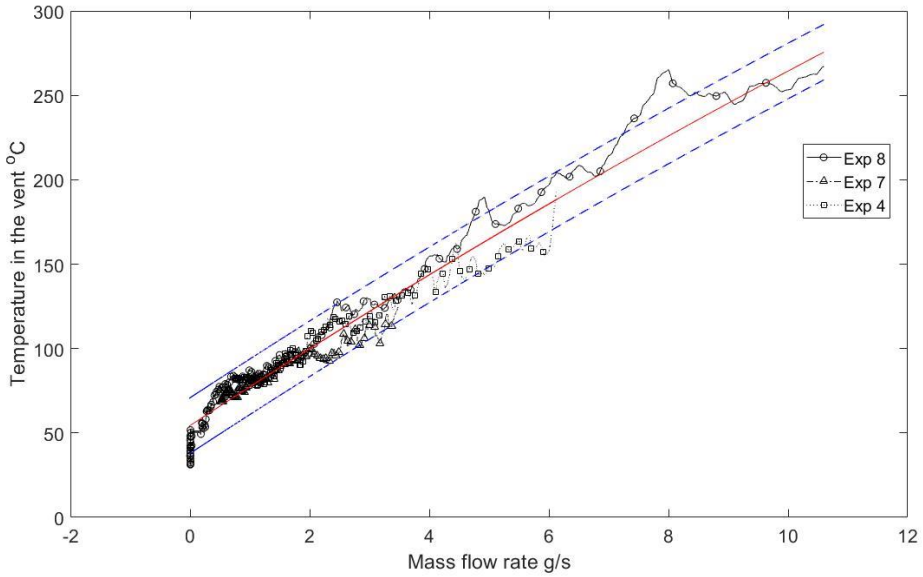

Figure 3-3. An experimental relationship between the hydrogen mass flow rate and the temperature in the vent (1 mm nozzle, 35 MPa storage pressure)

An ignited release directed vertically downwards resulted in higher temperatures around the car and could make self-evacuation and rescue from the HPV impossible. The experiment with the

jet fire from the TPRD directed at a 45° angle to the vertical backwards demonstrated that it is possible to get out of the car and evacuate passengers in the back seats. This is illustrated graphically in Figure 3-5 where a firefighter walks all the way up to a 70 MPa blowdown hydrogen jet fire located under a mock-up car.

The higher ventilation rate of 10 ACH compared to 6 ACH showed that the overall temperature exposure is reduced with increased airflow rate as expected. This effect can be seen in Figure 3-4. The temperature exposure, i.e. time integral of the temperature, showing that increased ventilation reduces to some extent the temperature exposure at the ceiling where the time integral of the temperature is calculated. There was no reduction in visibility due to the formation of water vapour from the jet fire in all experiments, as per camera records. No general scaling methods were identified, and thus it is recommended to use validated CFD models for hydrogen safety engineering of such systems.

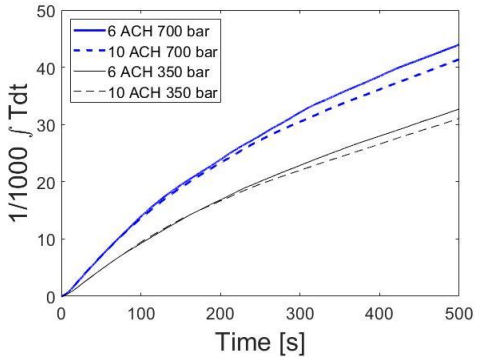

Figure 3-4. The temperature exposure, i.e. time integral of the temperature, showing that increased ventilation reduces to some extent the temperature exposure at the ceiling

The conclusions from this series of experiments are:

- The use of a 0.5 mm nozzle reduces the temperature under the ceiling and in the vent.
- The release backwards from TPRD at a 45° angle on passenger cars enables self-evacuation and rescue.
- A higher ventilation rate reduces the thermal exposure of the system.
- The generated experimental data can be used to validate CFD models.

Figure 3-5. Firefighter kneeling next (on the left) to the ignited release from a 0.5 mm nozzle in 40-feet container with the open door (note: the length of the 40-ft container may not be evident from photo)

3.3.3.4 Concluding remarks

The HyTunnel-CS project closed several important knowledge gaps related to hydrogen ignited and unignited releases. It is now well understood that the TPRD diameter plays a crucial role in the provision of safety for hydrogen-powered vehicles in confined spaces. Therefore, to enable safety analysis and inherently safer design of garages, maintenance shops, underground parking and similar confined spaces, to inform the development of fire intervention strategies and tactics, suitable rescue plans by firefighters, and general guidance for the public, OEMs must provide in the public domain, information on TPRD diameters used in their vehicles, as well as the direction of release, discharge line, if any, and response time in fires of different intensity, HRR/A. Without this important data, safety of individual hydrogen-powered vehicles cannot be adequately assessed by regulatory authorities responsible for authorising their placement onto the market.

3.4 Mitigation of hydrogen jet fire with water sprays and mist systems

Field tests performed previously by French Fire Brigade during the HyResponse project led by ENSOSP demonstrated that it is nearly impossible to extinguish a high-pressure hydrogen jet fires using water jets.

3.4.1 Interaction with water sprays and mist systems with hydrogen fires

Water in form of a jet, spray or mist is a common means of firefighting. A special tactic for gas firefighting in confined spaces is "gas cooling" (Svensson and Veire, 2019). The use of water spray or mist does not extinguish hydrogen jet fires. The main hot reacting zone (temperature above 1200°C) of hydrogen jet fires has minor sensitivity to water spray or mist. Nevertheless, a "gas cooling" effect of the combustion products takes place. Water mist, i.e. droplets of smaller

size**,** has a higher cooling effect than water spray composed of larger size droplets. However, the use of mist systems in enclosures with ventilation would be not efficient as mist will follow the gas flow rather than be directed to the fire.

3.4.2 Remarks on the effect of water supply on hydrogen fires in confined space

Conclusions from numerical studies on the effect of water supply to hydrogen fires in confined space:

- Water sprays are NOT recommended as a good extinguisher of hydrogen jet fire.
- Water sprays can mitigate the hot atmosphere effectively, i.e. reduce the hot gas temperature from hydrogen fire in a tunnel.
- Water sprays with smaller droplets have a better cooling effect than those with larger droplets, e.g. 100 μm is better than 300 μm. Mist with fine droplets is recommended instead of sprays of large droplets. However, the effect of ventilation on mist dispersion and propagation should be taken into account.
- Oxygen depletion decreases hydrogen flame temperature but cannot effectively suppress the hot atmosphere in the tunnel.

Tests on hydrogen fires with water spray supply were performed at KIT. The conclusions from this series of experiments (HyTunnel-CS, D3.3, 2022) are:

- Visible hydrogen flame length is reduced by water injection by 34–64%.
- Maximum hydrogen flame temperature is decreased by water injection by 140-240°C, from 1220°C to 980–1080°C.
- Water mist has a better cooling effect than water sprays.
- In one of the tests with a release through a nozzle of 4 mm diameter with hydrogen mass flow rate of 1 g/s and water sprays with a flow rate of 40 kg/min, hydrogen combustion was intensified by the spray, which resulted in higher flame temperature. This is thought to be due to: (i) suppression of the rising hydrogen jet tail downwards by the sprays, that resulted in the increased hydrogen concentration, (ii) intensification of combustion by sprays induced turbulence (flame acceleration).

3.5 Contribution of hydrogen to the heat release rate of a vehicle fire

Hydrogen jet fires from a TPRDs contribute to the transient HRR of a vehicle fire. The decrease of TPRD release diameter would result in the decrease of this contribution. Figure 3-6 shows the dynamics of contributions of hydrogen combustion to a passenger car fire HRR from TPRDs of diameters 2 mm, 1 mm and 0.5 mm during blowdown of 70 MPa, 62 L tank.

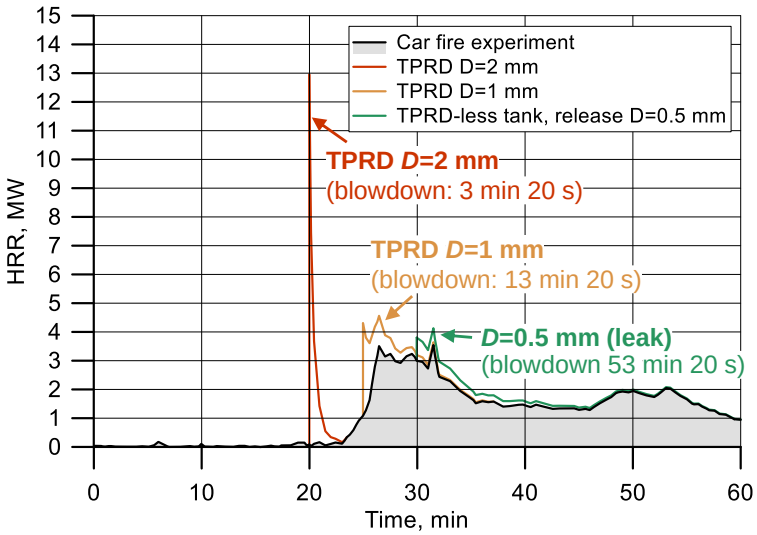

Figure 3-6. Contribution of hydrogen combustion to HRR in a passenger car fire (Okamoto et al., 2009). Example of hydrogen blowdown from 70 MPa, 62 L tank through TPRD of diameter 2 mm, 1 mm and 0.5 mm

Figure 3-6 shows a typical car fire with the peak HRR=3.55 MW (Okamoto *et al*., 2009). The use of TPRD=2 mm increases the HRR peak to 13 MW (3.7 times of the car fire HRR peak) although for a short duration of a minute. The TPRD of 1 mm and 0.5 mm diameters increase the HRR peak compared to the peak of the ordinary car fire to about 4.6 MW, i.e. by 30%, and 4.1 MW, i.e. by 15%, respectively. As expected TPRD=0.5 mm gives the least "addition" to the burning car HRR.

To minimise the contribution of jet fire from a TPRD to an overall fire HRR, it is recommended to reduce TPRD diameter to as low as reasonably practical and safe, i.e. so as to prevent tank rupture. It is also essential to design the TPRD in such a way as to exclude flame blow-off and consequent accumulation and deflagration of a flammable cloud. These measures will together minimise the jet fire contribution to the overall vehicle fire HRR. Explosion free in fire, self-venting TPRD-less tanks can be used to exclude the possibility of rupture in a fire (Molkov *et al*., 2018).

3.6 Experiments on hydrogen jet fire from TPRDs in a real tunnel

HyTunnel-CS Partner CEA performed 14 tests, 4 of them in the presence of a burner representing a source of fire from a nearby vehicle. The detailed results are presented in (HyTunnel-CS, D3.3, 2022). Whenever possible, these results were compared to the preliminary experimental campaign of CEA in 2019 with 20 MPa hydrogen storage tanks.

3.6.1 Flame length

The dimensionless correlation for free hydrogen flame length is recommended for use (Molkov and Saffers, 2013). Comparisons of the correlation with CEA experiments in a real tunnel on high-pressure vertical hydrogen jet fires showed very good agreement (see *Figure 3-7*). More details can be found in (HyTunnel-CS, D3.3, 2022).

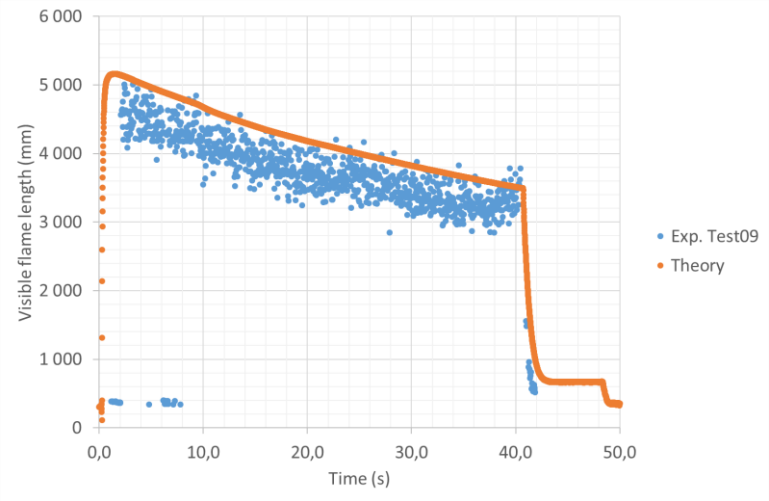

Figure 3-7. Test No.09: visible experimentally measured in a tunnel flame length compared to the correlation (Molkov and Saffers, 2013) for free hydrogen jet flames developed for the open atmosphere

For an upward release from a 2 mm nozzle from 70 MPa storage, the flame hardly reaches the ceiling of the 5 m height tunnel. For the case of a 4 mm nozzle, the flame hits the ceiling of the tunnel and therefore the model/correlation for flame length of free jet fires cannot be applied. In the case of a downward release at an angle of 45° beneath the vehicle, a 3.5 m long attached horizontal flame is observed (see *Figure 3-8*).

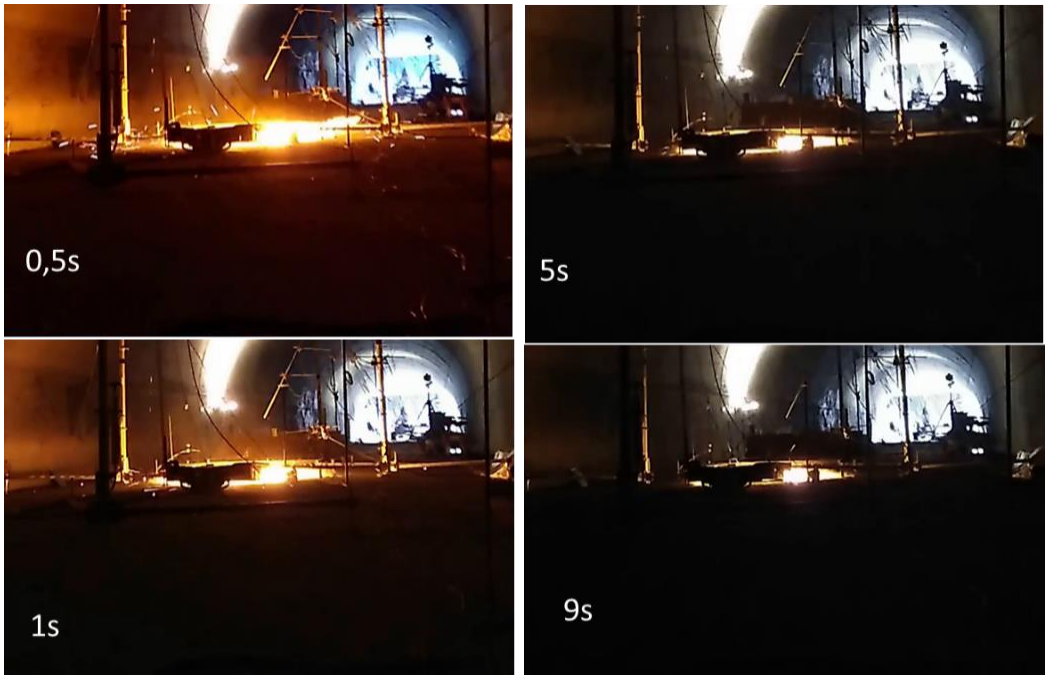

Figure 3-8. Test No.22 (2020 campaign). Hydrogen jet fire shape viewed from the rear side: the nozzle diameter 2 mm, downward 45°

3.6.2 Radiative heat flux

A model (Hankinson and Lowesmith, 2012) was used by CEA to determine the radiative characteristics of jet fires. Single-source and multiple-source approaches showed good agreement with the radiative heat flux measurements by sensors made during CEA tests.

Nevertheless, it should be pointed out that this model is not conservative since measured fluxes were sometimes higher than those calculated by the model.

Different release directions, i.e. vertically upward and downward, downward at an angle 45° to the vertical, and locations of release nozzle, i.e. under or over a chassis, were tested. **Radiative fluxes for human presence are not a challenge beyond 2 m away from the source** for storage pressure up to 70 MPa and TPRD diameters up to 2 mm, since radiative heat fluxes are below 2 kW/m^2 (see Appendix 1 for further information on heat flux limits for human exposure).

For a vertically downward release, almost immediately after the TPRD opening, an explosion was audible. This is thought to be due to the deflagration of a highly turbulent impinging hydrogen jet initiated by an electrical arc. This supports the recommendation made earlier not to direct hydrogen TPRD releases vertically downward under a vehicle.

The reduction of TPRD diameter decreases the radiative heat flux (but which is mostly not a problem anyway). At the same time, a smaller TPRD will increase the exposure time and probably the thermal dose. Care should be taken during hydrogen safety engineering that small diameter TPRD does not lead to residual safety problems, such as potential for catastrophic tank rupture, *etc*.

3.6.3 Temperature

Upward release through a TPRD of diameter below 2 mm has very localised impacts on tunnel structure, i.e. the ceiling. The temperature might reach 1000°C at the tip of the flame. However, no temperature exceeding 300°C at the ceiling level was registered for horizontal releases (thermocouples were measuring temperature in the vertical direction 6 m away from the release point (see *Figure 3-9*). Therefore, hot combustion products would have little or no impact on a ventilation system in similar arrangements, except very locally. For a downward 45° inclined release, the temperature around 100°C at the ceiling, shifted about 6 m away from the chassis (but the 1000°C hot point near the ceiling no longer exists).

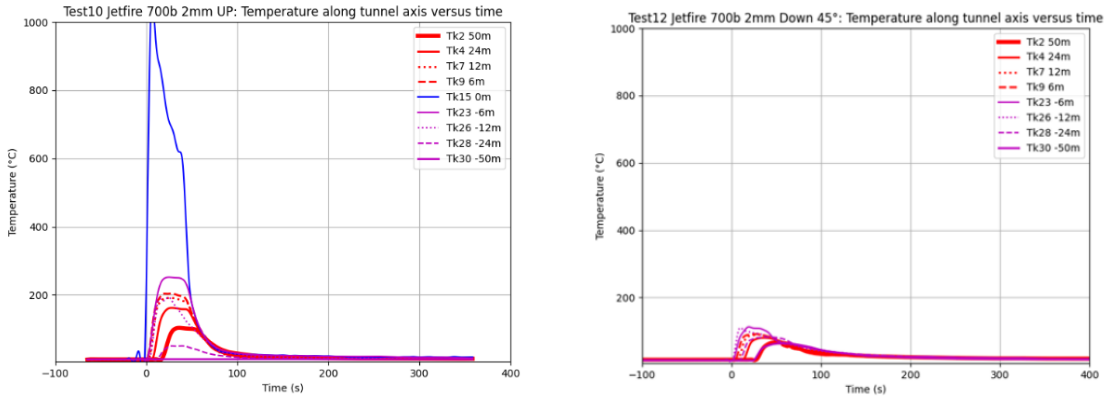

Figure 3-9. The gas temperature along the ceiling (thermocouples were located at a distance of 20 cm from the ceiling) for release from TPRD=2 mm: left – release vertically upwards, right – release downward at an angle 45°

TPRDs of larger diameter, e.g. 4-6 mm currently used in large vehicles (HGVs, buses, *etc.*), should be studied in greater detail, since the increase of released energy and a possible higher location of the TPRD in a vehicle would change these conclusions. It is clear that for each

particular vehicle design, in the sense of arrangements relevant to onboard hydrogen storage, should undergo detailed hydrogen safety engineering, e.g. with the use of validated CFD models.

In the case of an ignited release, the temperature distribution is impacted by TPRD release orientation. If a peak of temperature is to be avoided on the ceiling on 5 m height tunnel, the downward release at an angle of 45° would be preferable. If the existence of a "near to the ground" flame of 3.5 m is to be avoided, then the upward release could be considered.

Reducing the TPRD diameter down to 1 mm or 0.5 mm will reduce the maximum temperature and flame lengths but attention has then got to be paid to the potential thermal dose which could be higher for smaller TPRD diameter, and the higher possibility to ignite the asphalt road surface due to longer exposure to the flame from TPRD (downward release only). Explosion free in a fire self-venting TPRD-less tank can exclude this hazard, due to micro-flames that are localised near the tank surface and after fire extinction, will be substituted by microleaks with concentration decay below LFL close to the tank surface.

In the experiments performed to study the parameters of storage pressure, TPRD diameter and orientation indicate that firefighters' intervention strategy and tactics would not change, with respect to the temperature distribution field, compared to a conventional car fire - since hazard distances for hydrogen jet fires for recommended TPRD parameters are relatively short.

3.6.4 Interaction of a car fire with hydrogen flame from a TPRD

Figure 3-10 below shows, for an example test, the visible hydrogen flame length in the presence of a car fire, compared to the flame length of a free jet fire correlation.

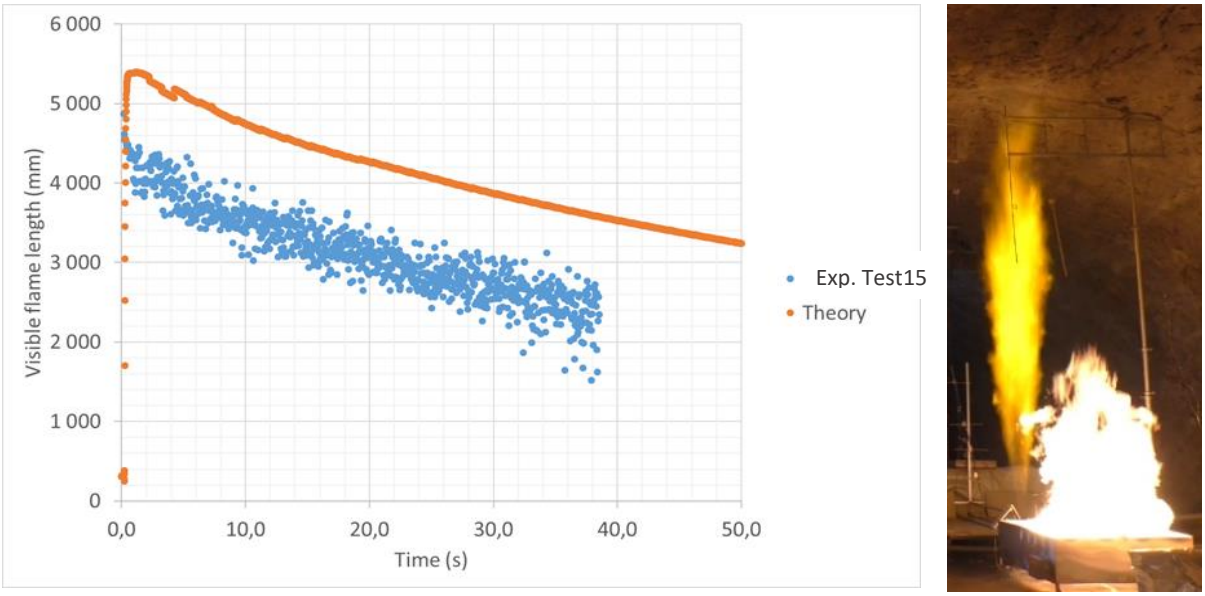

Figure 3-10. Test No.015: visible hydrogen flame length in presence of car fire compared to flame length of free jet fire correlation (Molkov and Saffers, 2013)

The radiative heat flux from the car fire is increased during hydrogen release. Nevertheless, for a TPRD=2 mm release, values of the flux are not a problem at a distance of a few meters from the burning car (see *Figure 3-11*). Note that in *Figure 3-11*, t= 0 s is at the start of the jet fire. Fx1 to Fx7 are names of the different flux meters. Flux Meters Fx1 to Fx7 positions and detailed results can be found in (HyTunnel-CS, D3.3, 2022).

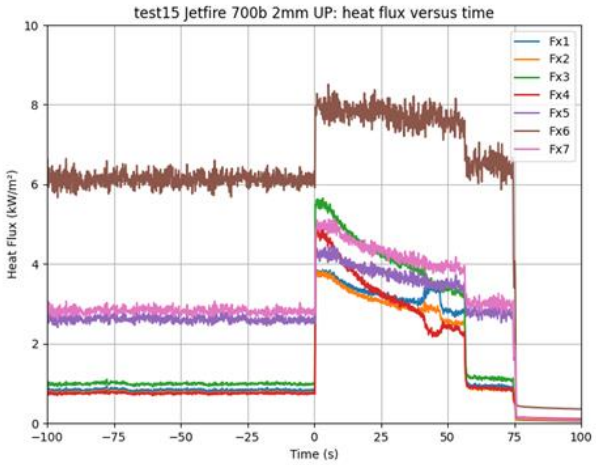

Figure 3-11. Test No.015: measured radiated heat flux

Figure 3-12. 2021 Test 015: Jet-fire shape viewed from the rear side

The jet-fire remains well below the tunnel vault and decreases almost continuously (Figure 3-12). Post-processing of the images shows that the flame height is well below the theoretical prediction (Figure 3-11).

4. Hydrogen explosions prevention and mitigation

The recommendations of section 4.1 address the following types of explosions:

- deflagrations;
- detonations; and
- structure demolition by PPP (see Section 3.3.3.1).

Section 4.2 gives recommendations on consequences and prevention of high-pressure hydrogen storage tank rupture in a fire.

All types of explosions are characterised by pressure and thermal effects. Confinement and congestion are known conditions that aggravate the consequences of deflagration and facilitate its transition to detonation (DDT). There is little opportunity to mitigate deflagrations in tunnels, if this happens, by the application of the most widespread venting of deflagration technique. This is why the focus should be on prevention of deflagration and prevention or minimisation of a flammable hydrogen-air cloud that could deflagrate. It is not possible to exclude turbulent high-pressure hydrogen jet deflagration, but it can be mitigated, for example, through the reduction of TPRD diameter.

Hydrogen storage tank rupture in fire is the worst-case scenario for a hydrogen-powered vehicle, even in the open atmosphere. The hazards of tank rupture in a fire in a tunnel and its consequences, drastically increase due to the one-dimensional characteristic of blast wave decay in a tunnel compared to three-dimensional decay in the open. The microleak-no-burst (LNB), for prevention of tank rupture is validated further, in addition to previous studies, by experiments carried out by CEA, USN and HSE.

The HyTunnel-CS project has developed innovative safety strategies targeting first of all, the prevention of explosions. The mitigation techniques are, however, presented as well.

4.1 Prevention and mitigation of hydrogen deflagrations, DDT and detonations

Experimental work, undertaken by partners HSE, CEA, PS and USN, includes evaluation of the phenomena relevant to deflagration of non-uniform hydrogen-air clouds in a tunnel; spurious operation of TPRD safety devices; DDT and detonation. Consideration was given to the attenuation of combustion and DDT events by foam and by water and the attenuation of shock waves by absorbing materials. The results from these experiments were used by partners UU and KIT to undertake analytical studies and to develop and validate engineering tools. Numerical studies and simulations by partners NCSRD, CEA, KIT, UU and USN will also be evaluated against the achieved experimental data.

4.1.1 Experimental studies of non-uniform deflagrations in HSE tunnel

The cases studied experimentally by partner HSE (HyTunnel-CS, D4.4, 2022) are those associated with cars, buses and trains. In all tests, the entire content of the hydrogen storage cylinders was released to understand the process dynamics. The releases were undertaken both with and without scaled vehicle models being present in the tunnel, with both unignited and ignited (jet fires) releases being undertaken. Hydrogen concentrations were measured together with over-pressures and flame propagation, supported by high-speed video recordings. The findings of HSE experimental work were reported alongside the details based on the scaling technique (Appendix 4). The data collected will be used to aid the validation of models for

hydrogen safety engineering, as well as showing what may happen should these scenarios occur in practice and inform the development of prevention and mitigation techniques.

4.1.1.1 Non-uniform hydrogen-air cloud deflagrations in a tunnel

The tools to predict the burning characteristic of non-uniform hydrogen-air clouds in large semi-confined tunnel geometry are limited (HyTunnel-CS, D4.3, 2022). The deflagration of stratified hydrogen-air layers in tunnel geometry is different from uniform hydrogen-air mixture combustion. For uniform hydrogen-air layers the possible combustion regime is determined by the hydrogen concentration and the layer height, while for a stratified hydrogen-air layer it depends mainly on the maximum hydrogen concentration and the flammable layer height. For stratified hydrogen-air layers the amount of hydrogen can be less than for uniform hydrogen-air layer deflagration to generate comparable or even more severe consequences during combustion. The key conclusion is to avoid formation of near-stochiometric clouds as they are responsible for highest overpressures of non-uniform deflagrations.

4.1.2 Overpressure during spurious operation of TPRD

HSE has performed experiments in its 70 m tunnel from hydrogen storage pressures up to 700 bar. Experiments comparing instantaneous and delayed ignition has been performed to assess the effect of turbulence intensity on deflagration overpressure. Recommendations on hazard distances relative to nozzle size can be found in HyTunnel-CS D4.4 (2022).

4.1.3 Deflagrations of ignited spurious hydrogen releases

The delayed ignition of a highly turbulent, under-expanded hydrogen jet from high-pressure equipment or storage tanks causes a deflagration generating a blast wave able to harm people and damage property. Experiments demonstrated that the deflagration overpressure produced can be as high as 20 kPa at a distance of 4 m from the release point for a 65 MPa storage pressure and free jet from 10 mm nozzle diameter (Takeno *et al*, 2007). This pressure is above the serious injury threshold of 16.5 kPa (LaChance *et al*, 2011). The recommended correlation for blast wave decay after under-expanded hydrogen jet deflagration (presented in Appendix A3.2.2) allows the calculation of the maximum blast wave overpressure at different distances by knowing the hydrogen release parameters, i.e. storage pressure and the release diameter. The correlation is applicable to free jets in the open atmosphere and confined spaces with dimensions comparable to the jet axial distance to LFL. However, the effect of jet impingement on generated deflagration pressure is yet to be quantified, this will only be possible when sufficient experimental data is available- further work will be required outside of the HyTunnel-CS project.

HyTunnel-CS demonstrated that for a leak from hydrogen storage with NWP=70 MPa, the “no-harm” distance for humans (assessed by overpressure from deflagration of hydrogen turbulent jet) reduces from 10.5 m to 2.6 m when a TPRD diameter decreases from the 2mm figure currently applied by several OEMs to 0.5 mm. This means that the reduction of TPRD size leads to a “no-harm” distance comparable with vehicle size and is recommended as a measure to mitigate pressure effects from a delayed ignition of a turbulent hydrogen jet.

4.1.4 Prevention of hydrogen-air flame acceleration and DDT in train tunnels

For a scenario of a hydrogen-powered train in a rail tunnel that is essentially narrower than a typical road tunnel, hydrogen releases from a TPRD of larger diameter would require sufficient air entrainment to assure the effective reduction of hydrogen concentration above and on the

sides of the train. High train speed and smaller TPRD diameter could ensure a decrease of flammable cloud. For a stationary train in a tunnel, a smaller diameter TPRD can reduce hydrogen concentration and the size of a flammable envelope to some extent. It is recommended to use LNB tanks onboard hydrogen-powered trains to exclude the formation of a flammable mixture in the comparatively narrow space between train and tunnel that could result in DDT.

The details of the correlation for DDT in horizontal and vertical channels with non-uniform hydrogen-air mixtures in the presence of obstacles are presented in Appendix A3.2.4. The correlation is based on thorough studies carried out by KIT in this area before and within HyTunnel-CS.

For trains travelling in a tunnel, a larger release will form a large flammable mixture. Figure 4-1 shows the hydrogen mass flow into the air above the train to produce an average 30% hydrogen-air mixture as a function of air volumetric flow rate. The airflow rate of 80 m^3/s corresponds to about 55 m/s train speed for 0.5 m height between train and tunnel ceiling and 6 m width and assuming a linear profile (see Figure 4-1). For this scenario, the accidental release of hydrogen with a mass flow rate over 2 kg/s would be required to produce a 30% hydrogen-air mixture along the length of the train. The train speed of 55 m/s (200 km/h) was chosen as it is typically the maximum allowable speed through a train tunnel in Norway [Sautter *et al*. (2007)] and was assumed as an upper boundary to see the effect on flame acceleration. Smaller gradients in velocity will give a smaller effect on flame acceleration, so this was seen as a worst-case. In the UK, maximum hydrogen train speeds are more likely to be in the order of 40-45 m/s (Lipscomb, 2022).

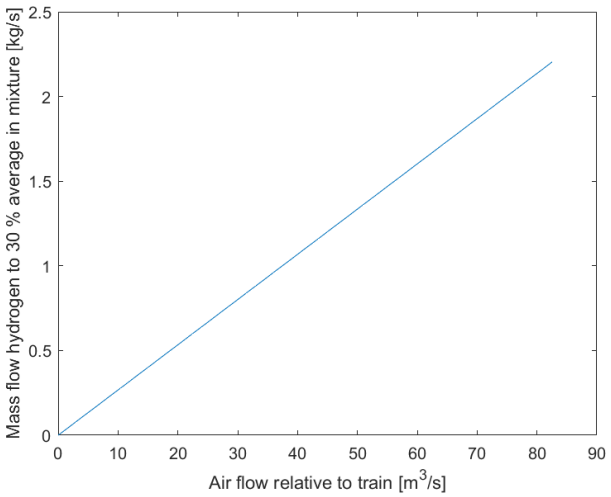

Figure 4-1. Hydrogen mass flow rate into air volume above the train to form 30% vol. hydrogen-air mixture as a function of volumetric air flow rate above the train in the tunnel, assuming 6 m × 0.5 m free area above the train

Simulations on flame acceleration and DDT in a train tunnel were performed by USN for inhomogeneous clouds and homogeneous clouds in velocity gradients (HyTunnel-CS, D4.3, 2022). Velocity gradients (110 (m/s)/m) do not produce significant flame acceleration as the flow of gases ahead of the flame due to expansion dominates the flow field due to the flame speed being much higher than 55 m/s. The results also show that concentration gradients alone can provide flame acceleration to DDT in a simulated rail tunnel geometry.

Effects of the concentration gradient

Figure 4-2 shows the concentration gradient applied in the USN simulations. The results show that stratification of the mixture with concentration gradients can significantly accelerate the flame even in the case of "lean" in the average mixtures.

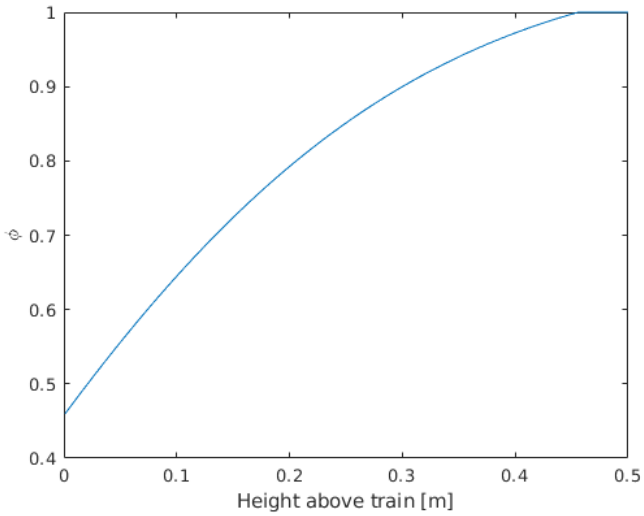

Figure 4-2. Hydrogen concentration distribution (gradient) used in the USN simulations (shown in terms of the equivalence ratio). A "lean" in average hydrogen-air mixture is used to keep reactivity low in simulations

Figure 4-3 shows three snapshots of simulated pressure during flame acceleration in a rail tunnel volume above the train from the initial vertical concentration gradient shown in Figure 4-2. Ignition is at the top and centre of the geometry. The middle frame (9.2 ms) shows destructive Mach-stems are forming towards the train roof. In the last frame (10.1 ms) DDT is seen on both sides, producing pressure up to 9 MPa due to detonation in the pre-compressed mixture. This is far above the 1.35kPa no-harm limit for human exposure: threshold for serious injury is 16.5 kPa; maximum survivable blast 0.17 - 0.21 barg; 1% fatality 0.25 - 0.35 barg; and 50% fatality 0.5 - 1.0 barg.

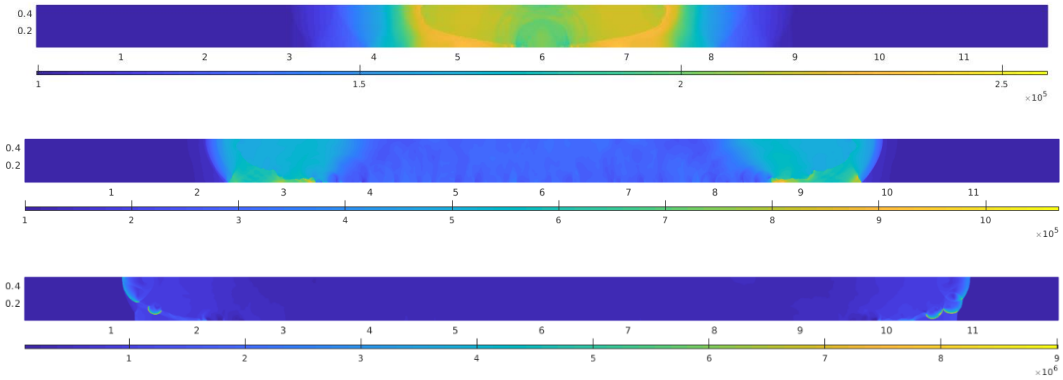

Figure 4-3. Three snapshots of simulated pressure during flame acceleration in a rail tunnel volume above the train. Ignition is at the top and centre of the geometry. Top: 7 ms after ignition; middle: 9.2 ms; bottom: 10.1 ms. The lower scale is the pressure in Pascal

Effect of the velocity gradient

The simulations of partner USN were performed in 2D domain of 0.5 m height and 12 m for concentration gradients and 32 m long for velocity gradients. The domain is discretized using a spatial resolution of 1 mm. A velocity gradient of 110 m/s/m was applied based on a typical train velocity of 55 m/s in a tunnel leading to a strained flow field in the space between the train and the tunnel walls. A typical height between train roof and tunnel ceiling is 0.5 m for standard tunnel and train sizes. Figure 4-4 shows a pressure contour where the flame is close to the domain exit.

The pressures in the domain reach 0.1 MPa (1 barg) as the flow field in front of the propagating flame dominates over the initial strained flow field. Such a pressure is much higher than required for glass window rupture and represents a fatality threshold. If the duration of over-pressure is longer than 10 ms, then such pressure load may lead to 50% of brick or concrete wall demolition (Yanez *et al.*, 2015).

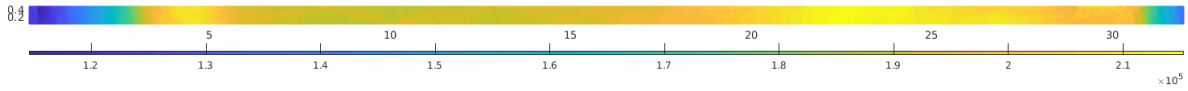

Figure 4-4. Simulated pressure during accelerated flame propagating in velocity gradient of 110 s^{-1} (0-55 m/s over 0.5 m) at 69 ms from the ignition. The domain is 32 m long

Since the initial velocity field of strain rates of 110 m/s/m will not, significantly, contribute to flame acceleration up to DDT, the recommendation could be to keep high train velocity through tunnels for dilution of hydrogen during accidental release.

4.1.4.1 Deflagration of stratified hydrogen-air clouds

Hydrogen release, dispersion and deflagration with and without ventilation in a road tunnel were simulated by several partners, including KIT with in-house COM3D code. The conclusions from the simulations could be summarised as:

- For the hydrogen momentum-dominated supersonic jet near the release nozzle the effect of ventilation, for which velocity is limited to a few meters per second, is negligible.
- With velocity drop further from the nozzle and after impingement, the ventilation can strongly influence the dispersion of hydrogen in a tunnel. Typical for tunnels ventilation velocity of 3 m/s blows this part of the hydrogen cloud downstream. It is worth repeating the need to provide decay of hydrogen concentration below the LFL at the distance similar to the ceiling height by proper design of the TPRD vent diameter and orientation.
- It was found that the hydrogen accumulation and deflagration overpressures are not much different between tunnels with horse-shoe or rectangular cross-sections of the same cross-sectional area.
- For cases without ventilation, the deflagration overpressure is higher than those with ventilation. The local pressure near the ceiling even exceeds 1.04 bar abs. for a simulated scenario (TPRD=2 mm, 5 kg of hydrogen in 125 L, 70 MPa tank, vertical upwards release at location 1.15 m above the ground into a tunnel with a cross section of H×W=6.3 m ×8.7 m). A lower overpressure is recorded at the lower part of the tunnel.
- The simulation results demonstrated that combining longitudinal and transverse ventilation is beneficial.

4.1.4.2 Water injection effect on hydrogen combustion

A discrete Lagrangian particle model was developed at KIT to simulate the transport of the water droplets. The thermal-hydraulic effect of a liquid water phase on hydrogen combustion is simulated. The mitigation effect of mist presence on the hydrogen-air mixture deflagration overpressure is apparent, e.g. in the case of 5.1 s ignition delay time, the overpressures were reduced by 24-35% depending on the ventilation conditions.

Due to ventilation, hydrogen propagates in most cases downstream. In some situations, this creates larger hydrogen flammable clouds with a higher fraction of fast-burning near-stoichiometric concentrations than in a scenario without ventilation. Thus, ventilation causes a higher deflagration overpressure for such scenarios. However, a fast-burning flammable hydrogen cloud and corresponding deflagration overpressure start to decrease as the ventilation becomes stronger (3 cases of ventilation velocities, i.e. 0 m/s, 1.25 m/s and 2.4 m/s, were simulated, which correspond to the computed peak overpressures of 2.1 kPa, 5.3 kPa and 4.9 kPa, respectively, in the worst-case scenario with an ignition delay of 5.1 s). It is therefore recommended that hydrogen safety engineering using contemporary validated CFD models is undertaken for scenarios of interest.

4.1.4.3 Numerical study of fine mist effect on hydrogen deflagration

NCSRD performed 2D simulations to study the effect of water mist on hydrogen deflagrations. A uniform hydrogen-air mixture of 30% was considered in the HSE tunnel geometry (70 m length and maximum height of 3.25 m). The mixture was assumed to occupy an area of 10 m length around the centre of the tunnel. Ignition at the centre of the tunnel was considered, 1.2 m above the ground. Water concentration of 0, 0.05, 0.10, 0.20, 0.50 and 1.00 kg/m^3 were studied. Water was distributed uniformly inside the hydrogen-air mixture.

For the simulations the ADREA-HF CFD code was used. The Homogeneous Equilibrium Model (HEM) was applied for modeling a two-phase mixture, assuming that both liquid and vapor phase have the same temperature. The phase distribution was estimated using the Raoult's law. As a result, the evaporation of water droplets occurs instantaneously. This assumption is valid in a very fine water mist (very small droplet size, approximately <25μm). The effect of liquid phase on the velocity field due to the imposed drag is neglected in this study, because NCSRD only examined the case of very fine water mist, thus, no water droplet diameter needed to be defined. Simulation details can be found in (HyTunnel-CS, D4.3, 2022).

Figure 4-5 shows the effect of water concentration on maximum overpressure and on maximum temperature. The overpressure is reduced almost linearly with increasing water concentration. Maximum overpressure in the 0.2, 0.5 and 1.0 kg/m^3 cases is 1.27, 1.75 and 4.7 times smaller compared to the dry mixture case. The more pronounced effect on pressure is achieved with 1.0 kg/m^3 water concentration. The reduction of mixture temperature is also significant. The water cooling effect is very strong and it is the main reason for the decrease of overpressure.

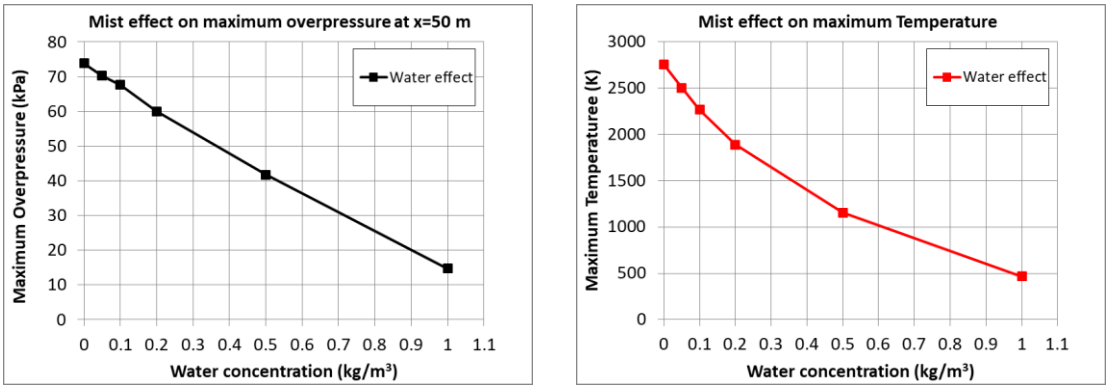

Figure 4-5. Effect of water mist on maximum overpressure (at x=50 m) and on maximum temperature

Due to the assumptions made, the observed pressure reduction can be considered as one of the best-case scenarios that can occur corresponding to the case of very fine water droplets and uniform mixture. The maximum overpressure in the no-mist case was equal to 73 kPa, whereas in the mist case (with water concentration equal to 1 kg/m^3) the overpressure was significantly reduced to 15 kPa.

4.1.4.4 Flame acceleration and transition to detonation

The methodology to evaluate the critical hydrogen concentrations for flame acceleration (FA) and deflagration-to-detonation transition (DDT) is based on the known "sigma" (expansion ratio) and 7λ (λ - detonation cell size criteria developed by KIT for channel and layer geometries, in particular for tunnels. The method takes into account the blockage of tunnel cross-section, stratification of the mixture, and dimension (elongation) of hydrogen cloud. The method was validated against large-scale experiments and reproduced by CFD simulations.

Critical conditions for FA and DDT in a tunnel are evaluated in the case of uniform and stratified hydrogen-air mixtures. The elimination of conditions for supersonic flame propagation and thus detonation by keeping the maximum hydrogen concentration below the critical level for a certain hydrogen distribution in a tunnel cross-section provides a significant reduction of the blast wave overpressure in the case of delayed ignition of the flammable cloud. The following observations from these numerical studies may be of value in the development of safe design:

- For the unlikely uniform distribution of hydrogen inventories in the range 2-10 kg throughout the entire tunnel cross-section, no detonation is foreseen.
- Keeping hydrogen concentration below the critical 10% by the ventilation system is still not sufficient for the provision of safety, as deflagration pressure of 0.3-0.5 MPa may be generated.
- In stratification of the layered hydrogen-air mixture, the flammable cloud becomes elongated.
- The detonation of a stratified (non-uniform concentration) layer of hydrogen-air mixture with inventory above 10 kg is possible for hydrogen concentrations above 20%.
- For rail tunnels characterised by a higher blockage ratio, e.g. blockage ratio BR=40%, hydrogen concentrations above 15% in the flammable cloud should be avoided, to exclude transition to detonation in the case of a 100 kg onboard hydrogen inventory.

Partner USN applied in-house CFD code for flame acceleration, detonations, and shock waves, using a centred TVD (Total Variation Diminishing) scheme, FLIC (Flame with Implicit Convection) including combustion models for turbulent flames and chemical kinetics and

viscous stresses allowing the simulations of flame acceleration, DDT, detonation propagation, blast waves and shock-flow interactions, to scenarios of hydrogen release from a train in a tunnel. The effects of a moving wall relative to the train, and concentration gradients were taken into account. The narrow gap between the train and tunnel ceiling in addition to a moving train can form a large flammable hydrogen-air mixture and lead to a severe explosion.

The simulations looked at the effects of concentration gradients and moving walls (a moving train). A typical train velocity can be up to 55 m/s through a tunnel, leading to a strained flow field in the gaps between train and tunnel walls was assumed. A typical height between train roof and tunnel ceiling is assumed as 0.5 m for standard tunnel and train sizes. From the simulations, flow velocity, pressure, density and reaction variables were calculated for the whole domain. The results showed the pressure build-up, flame acceleration and possibility of DDT. To ensure sufficient spatial resolution, 2D simulations of the domain above the train were carried out. Simulating DDT by the USN code requires a mesh size below 1 mm, preferably much smaller. More details can be found in Appendix A3.2.4. Due to complexity, including moving walls or train, and resource limitations, no experiments were conducted within HyTunnel-CS to validate these informative simulations.

4.1.5 Blast wave attenuation by water sprays, mist and absorbing materials

4.1.5.1 Effect of spray droplet size and mist density on mitigation of deflagrations and DDT

HyTunnel-CS D4.3 (2022) describes the hardware and software used by partners KIT and PS to investigate the effect of water sprays and mist on deflagrations and DDT potential. The study of partner USN found that most of the droplets in the mist are in the >50 µm region, however when considering the Sauter mean diameter of the spray the value can be up to 100 µm. The conclusions of these studies are as follows.

The droplet size distribution can affect the mitigating properties of water in a hydrogen explosion scenario. Different droplet sizes can have dissimilar mitigation mechanisms depending on the application. In general, the number-based droplet size distribution can be fairly monodispersed. However, it is worth bearing in mind that the volumetric size distribution can range from fine mist to about 200 µm for the nozzle investigated in this case.

Research publications often present a range of droplets or a mean diameter, but the detailed distribution can be crucial when using the data, e.g. for safety engineering or validation of CFD models. The HyTunnel-CS study was performed using the shadow-imaging technique. This technique offers the possibility of quantifying the measurements to give an idea of the performance of the method. This fundamental study on the characterization of parameters of mist does not produce an immediate recommendation of the mitigation properties of the mist for deflagrations, but the results can be used as an input to CFD models subsequently used for hydrogen safety engineering.

It is important to note that water sprays can actually aggravate the consequences of deflagration in some circumstances. For example, it was observed in experiments in a large-scale cylinder of 5 m height that a hydrogen-air mixture at concentrations close to LFL generated large deflagration overpressures when water sprays were applied from the top of the vessel (Shebeko *et al.*, 1990). The reason for this “unusual” result is thought to be because the near-LFL quiescent mixture can propagate flame only upwards and thus only a small fraction of the mixture could be burnt out. The introduction of water sprays makes the mixture turbulent and provides conditions for a larger fraction of the mixture to react. The increase in risk created by mixture fractions that combust more easily, is greater than the mitigating effect of sprays due to

cooling the combustion products. It should also be noted that evaporation generates water vapour that would contribute somewhat to increase in pressure.

Note that for mist systems with low liquid density, the influence on the dynamics of a hydrogen-air deflagration is minor. Only a slightly lower flame speed was observed in the presence of light density mist compared to dry conditions; a flame quenching effect was not observed. In short, significant impact is only observed for heavier, sufficiently high-liquid-density mist systems.

4.1.5.2 Deflagration propagation through fire extinguishing foam

The application of extinguishing foam is one of the means of firefighting. The knowledge of the behaviour of hydrogen-enriched foam is very limited (HyTunnel-CS, D4.3, 2022). In a medium foam, built by using a uniform hydrogen-air mixture, the flammability limit for downwards flame propagation lies in the range of gaseous hydrogen-air mixture. The hydrogen-air mixture, e.g. that from a decaying jet from a TPRD, would be "fixed" on the ground inside the foam applied by firefighters. A significant flame acceleration to values close to the speed of sound in such foams can be observed for a wide range of hydrogen concentrations in air. This means that the injection of foam can initiate flame acceleration and therefore is not a good choice as a risk mitigation measure.

4.1.5.3 Blast wave attenuation by absorbing materials

The explosion shock wave attenuation effects of different soft materials were investigated via experimental measurement in KIT by measuring the pressure amplitudes and the positive impulse of the reflected shock waves for different layers of soft materials.

Three sorts of soft materials with different thicknesses were tested: polystyrene, glass wool fibre, and polyurethane foam. Samples thickness for each material was 2 cm, 12 cm, or 20 cm thick. The experiments demonstrated that:

- The pressure amplitude of the reflected shock wave is reduced by 50% using glass wool fibre, by 40% using polyurethane foam, and by 20% using polystyrene compared to the case of reflection of the shock wave by a solid steel wall without any soft layers.
- The efficiency of attenuation of the pressure amplitude of the shock wave is not relevant to the layer thickness of soft materials between 2 cm to 20 cm.
- The positive impulse of the reflected shockwaves is attenuated more effectively by thicker layers.

It can be concluded that glass wool fibre is the most effective soft material among the tested samples, to attenuate shock waves.

4.1.5.4 Blast wave attenuation by water sprays and mist

Water spray and mist have the potential to attenuate blast waves due to energy absorption. The effect is comparatively small for the amounts of water supplied usually from stationary extinguishing systems.

The interaction between hydrogen detonation shock wave and water mist with different droplet sizes was simulated using the KIT in-house code (HyTunnel-CS, D4.3, 2022). A discrete Lagrangian particle model was developed to simulate the transport of the water droplets. The thermal-hydraulic effect of the liquid phase on hydrogen combustion was modelled. A droplet

break-up model was developed to simulate the attenuation effect of mist when the detonation shock front encounters individual droplets. The simulation results demonstrated that:

- The detonation shock wave pressure is reduced by 10-20% in the presence of mist.
- Larger droplet size and large liquid phase fraction have better attenuation effect for the detonation peak pressure.

These results require more investigation and numerical studies. Experimental studies were out of the HyTunnel-CS scope due to resource limitations.

4.2 Hydrogen tank rupture in a fire: consequences and prevention

4.2.1 Blast wave and fireball after hydrogen tank rupture in a fire

4.2.1.1 Blast wave decay after hydrogen tank rupture in a tunnel

There is a non-zero probability of TPRD failure in a fire. The TPRD cannot be initiated by localised fire if the fire affects only a part of the tank where there is no TPRD, e.g. smouldering fire. The TPRD can also be thermally isolated from a fire during an incident. Additionally, TPRD response time depends on fire intensity and could thus be extended for a lower intensity fire. The device could also fail to open or may equally could spontaneously open without fire due to fatigue stress as a result of numerous pressure cycles during service life, or as a result of a shock resulting from vehicle collision. Therefore, the knowledge of the blast wave decay for a tank of a particular volume and NWP is required for first responders and design of inherently safer HPVs. The universal correlation for the assessment of blast wave decay in a tunnel (Molkov and Dery, 2020) is presented in Appendix A3.3.2.

Because the blast wave decays in a tunnel extremely slowly, the general recommendation is to prevent hydrogen tank rupture in a tunnel fire by all means necessary. The most promising technology that excludes disadvantages of storage systems with a TPRD is an explosion-free-in-a-fire self-venting TPRD-less tank, which could be presented as a tank with a virtual “TPRD” distributed over the whole tank surface and providing release in a form of harmless microleaks.

4.2.1.2 Fireball behaviour in a tunnel: a numerical study

A hydrogen storage tank rupture in a fire leads to the formation of a fireball. The fireball propagation dynamics in a tunnel is different from that in the open space. At the initial stage after tank rupture, it was observed for the first time in simulations performed by UU that the fireball “freezes” for a while between the original tank location and tunnel walls (See Figure 4-6, left). The combustion at the contact surface continues while the starting shock has multiple reflections from walls and the quasi-plane blast wave propagating through the whole tunnel length is formed. The same behaviour of hydrogen combustion in a fireball was registered by high-speed video in experiments of CEA (see a snapshot in Figure 4-6, right) in the real tunnel. This is the verification of UU’s CFD model for assessment of consequences of hydrogen tank rupture in confined spaces like tunnels (Molkov *et al.*, 2021a).

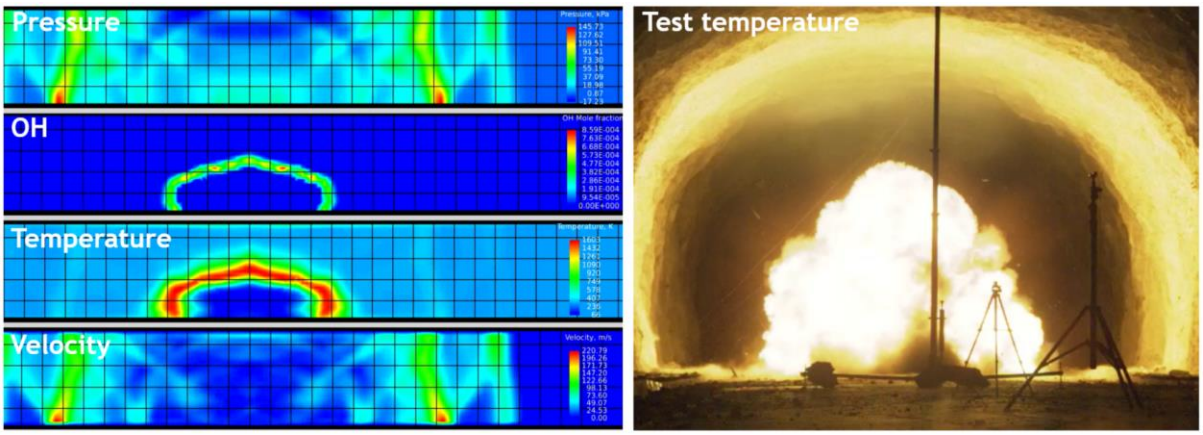

Figure 4-6. The initial stage of fireball development after hydrogen tank rupture in a fire: left - simulations by UU model (Molkov et al., 2021a); right – HyTunnel-CS experiment by CEA

The "unusual" and extremely hazardous behaviour of a fireball in a tunnel is its propagation with a high velocity as high as 20-25 m/s behind the blast wave. This creates additional hazards to people and vehicles, i.e. thermal and asphyxiation hazards for people, and thermal effects on vehicles. This must be taken into account in the design of a hydrogen-powered vehicle and assessment of consequences of a tank rupture in a tunnel. The engineering solution should exclude tank rupture in any circumstance to eliminate this new hazard.

The fireball dynamics depends on the location of the incident in a tunnel. The worst-case location is close to the tunnel exit, which is known as a place with the highest probability of a traffic incident in tunnels. The fireball then propagates into the tunnel towards the opposite tunnel exit dragged by the flow created by the blast wave. The hazard distance created by fireball propagation along the tunnel will depend on the parameters of the ruptured tank and the tunnel dimensions.

A hydrogen fireball in a tunnel, unlike fireballs in the open atmosphere, may propagate a substantial distance along the tunnel. *Figure 4-7* shows an example of simulated temperature distribution in a centre-plane cross-section of a 2-lane 500 m tunnel 36 s after rupture of a 120 L tank containing 5 kg of hydrogen inventory at 94.5 MPa (temperature before burst in a fire is 385K). The vehicle is located at a distance of 50 m from the right entrance to the tunnel. The layer of hot combustion products propagated towards the left tunnel exit to a distance of around 140 m. With further time advancement after 36 s, the combustion products will continue to move and start to cool down.

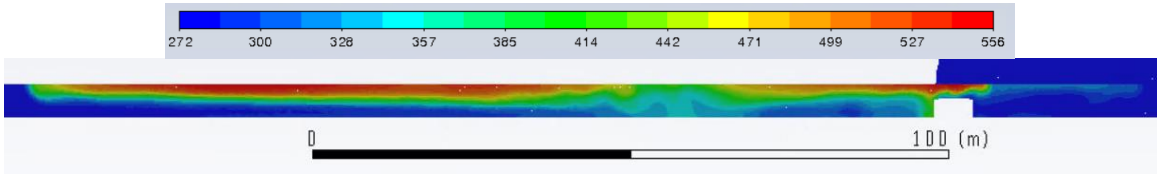

Figure 4-7. Temperature contours of fireball in a 2-lane, 500 m tunnel 36 s after rupturing of 120 L, 94.5 MPa (5 kg hydrogen inventory) tank for the scenario of a car accident at 50 m from the right tunnel entrance

4.2.1.3 Large-scale experiments on fireball after hydrogen tank rupture in a scaled tunnel

HSE have carried out a number of tests looking at the catastrophic failure of a hydrogen storage vessel and the ensuing blast wave and fireball propagation. The outcomes from this activity are

reported in HyTunnel-CS D4.4 (2022) and include recommendations on the use of TPRD and their sizing.

4.2.1.4 Large-scale experiments on fireball after hydrogen tank rupture in the real tunnel

Partner CEA has performed 9 successful tests during the 2021 experimental campaign (2 tests failed due to an electrical problem arising from the blast wave effect). Results for the 2020 experimental campaign were used whenever useful for the development of correlations, assessment of reproducibility, *etc*. Detailed results on fireball studies are given in (HyTunnel-CS, D4.3, 2022), including the progression of the hot gas along the ceiling of the tunnel.

To clarify the dependence of blast wave strength on hydrogen combustion (at the contact surface between air heated by the starting shock and expanding hydrogen), the experiments were performed by rupture of tanks filled with helium (mechanical energy only) and hydrogen (mechanical and chemical energy). To estimate the effect of the detonation cord used to initiate tank rupture, on blast wave strength, the tests were also performed with empty tanks. Based on experimental results and their agreement with previous numerical studies of UU, it was concluded that hydrogen combustion reaction contributes to the blast wave strength.

Fireball dynamics were recorded by a high-speed camera. The derivation of the hemispherical radius of the fireballs was performed by the use of the pictures taken by the high-speed cameras during fireball development. The initial phase of fast fireball growth slows down, similar to what was seen previously in the simulations by UU. The fireball “breathing” phenomenon due to the interaction of the fireball with reflected from tunnel walls shock waves, observed for the first time in the simulations, was confirmed by experimental observations.

It is recommended that the validated CFD models are used, e.g. (Molkov *et al*., 2021a), for the assessment of tank rupture in a fire and its consequences due to complicated fireball behaviour in a tunnel rather than fireball models developed for the open atmosphere, e.g. (Zalosh and Wayandt, 2005), (Makarov *et al*., 2021b), *etc*.

4.2.1.5 Blast wave after hydrogen tank rupture: experiments of CEA in a real tunnel

Tests on blast wave after tank rupture were performed in the real tunnel du Mortier (5.2m ceiling height) at a distance of 220 m from the main entrance on the Autrans side. Two straw walls were installed at each end of the tunnel to limit natural convection and to mitigate the blast waves exiting from the tunnel. To capture the pressure wave propagation along the tunnel, PCB blast wave pencil transducers were located in seven locations. Full details of the blast wave experimental studies are presented in HyTunnel-CS, D4.3 2022.

Figure 4-8 shows the dynamics of the blast wave in the tunnel after a 9 MPa, 78 L hydrogen tank of Type IV ruptures in a “fire” (imitated by high-temperature combustion products of a detonation cord used to initiate the tank failure). The blast propagates with a velocity of 350 m/s. This is slightly higher than the acoustic velocity of 341 m/s in the tunnel.

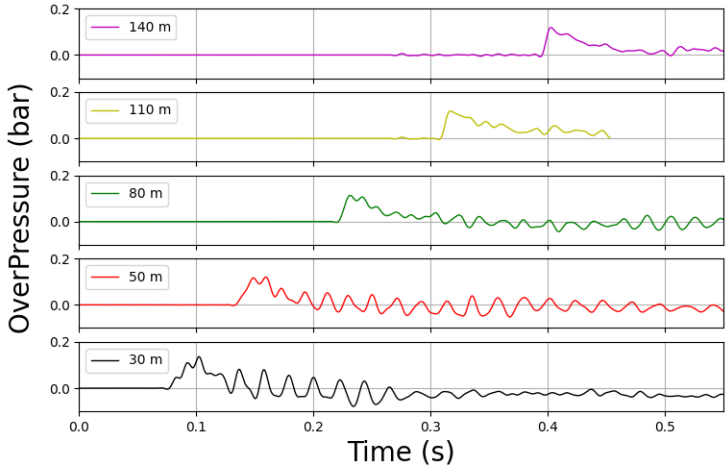

Figure 4-8. Test No.5: Overpressure dynamics at different distances from hydrogen tank (9 MPa, 78 L, Type IV) rupture in a "fire" (mimicked by a detonation cord)

The most important observation and conclusion is that ***there is almost no reduction of the pressure peak throughout the entire tunnel length***. In contrast to fire safety regulations, there is ***no notion of safety distance*** in a tunnel in the case of a tank explosion. The entire tunnel is a hazardous zone and it is very unlikely that a no-harm distance defined by overpressure of 1.35 kPa can be designated in the event of tank rupture, no matter the length of the tunnel. The only safe location is outside of the tunnel, at some distance away from the tunnel mouth. This experimental confirmation of theoretical and numerical studies stresses the need to implement safety strategies and engineering solutions to exclude any chance of hydrogen storage tank rupture in a tunnel.

The second observation is that the pressure level is very high and ***far above the 1.35kPa no-harm limit*** for human exposure, even in the case of a hydrogen tank at a very moderate pressure of 9 MPa. Recorded in these tests overpressures were ranging from 8 kPa up to 33.6 kPa for the different tested tanks. The threshold for serious injury is 16.5 kPa.

The experimental results are in excellent agreement and thus validate the universal dimensionless correlation for blast wave decay after hydrogen tank rupture in a tunnel (Molkov and Dery, 2020). This correlation was developed using methods of similitude analysis and numerical experiments. The numerical experiments were performed using the validated CFD model that accounts for both the mechanical energy of compressed gas and the chemical energy of hydrogen reaction with air at the contact surface behind the starting shock (Molkov *et al.*, 2021a).

Figure 4-9 shows the comparison of CEA experimental results with the correlation for blast wave decay developed at UU. The fraction of chemical energy contributing to the blast wave is accounted for and taken as 12% (Molkov and Dery, 2020). Most of the experimental data (see

Table 4-1) are close and slightly below the best fit line of the correlation. Therefore, despite its slightly conservative character, the best fit correlation is recommended for the assessment of blast wave decay in a tunnel after a hydrogen tank rupture in a fire. The conservative fit correlation can be used if conservative estimates are mandatory.

Table 4-1. The parameters of ruptured tanks in CEA tests

Test No.	Tank type	Pressure, MPa	Temperature, °C	Mechanical energy, MJ	Chemical energy, MJ
5	Type IV	9	15	1.60	66.92
6	Type II	19.4	15	2.09	86.94
7	Type IV	52.0	15	7.39	306.14
8	Type IV	61.0	15	8.31	344.13
20	Type II	4.7	10	0.56	24.41

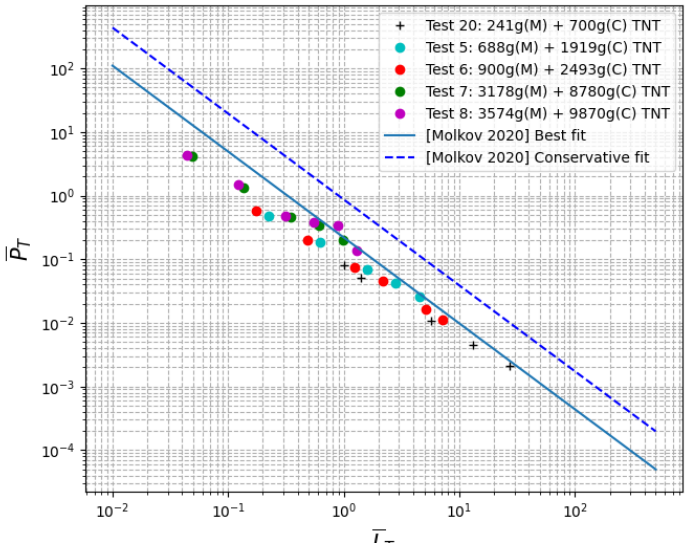

Figure 4-9. Validation of UU's correlation for blast wave decay after hydrogen tank rupture in a tunnel (Molkov and Dery, 2020) against the CEA experiments. The legend indicates the amount of mechanical energy (M) and chemical energy (C) expressed in Trinitrotoluene (TNT) equivalent

The correlation can be developed further to account for the loss of mechanical energy absorbed by a vehicle. However, the presence of a vehicle, e.g. above the ruptured tank, could not only decrease the amount of mechanical energy transmitted to the blast wave, but could increase the fraction of the chemical energy released due to combustion under the vehicle at higher pressure conditions compared to the case of tank rupture in an open space. This study was not performed within HyTunnel-CS and can be done in the future to improve understanding in the field of hydrogen safety engineering.

4.2.2 The model to design an inherently safer tank-TPRD system

There were no models for the design of an inherently safer tank-TPRD system before the HyTunnel-CS project.

The comprehensive physical model (Molkov *et al*., 2021b) of non-adiabatic thermal behaviour of a composite tank-TPRD system in an engulfing fire accounts for all main underlying physical phenomena, i.e. convective and conductive heat transfer, effects of mass and heat transfer during hydrogen blowdown from the tank, the composite resin degradation and liner melting. The model developed at UU is based on the original failure mechanism of a composite tank rupture in a fire, stipulating that the composite loses the load-bearing ability where the resin is decomposed and thus fibre layers become loose and can no longer bear the hydrogen pressure load.

The model can be applied to design a tank-TPRD system with any storage tank size, volume and pressure, any tank wall thickness and properties and any TPRD release diameter and response time to a fire. A blowdown through the TPRD can be simulated using the model with known TPRD activation time, i.e. immediate, or with a delay or even without activation, leading to tank rupture in a fire. The time to tank rupture in a fire is named the fire-resistance rating (FRR). The model provides transients of:

- Pressure and temperature of hydrogen inside the tank.
- Temperature distribution in the tank wall.
- Propagation of the resin decomposition and liner melting fronts.
- Fraction of the wall thickness that is able to bear the transient hydrogen pressure load.
- Tank FRR in a fire of particular intensity, HRR/A (when TPRD failed to be open).
- Dynamics of safe hydrogen blowdown from the tank without rupture (can be designed for selected tank using TPRD release diameter and response time as input parameters).

The full model details are described in the paper (Molkov *et al*., 2021b). The model is referenced in Appendix 3.1.4. The methodology is applicable also for a system of tanks.

4.2.3 Breakthrough safety technology of explosion free in fire self-venting (TPRD-less) tank

The HyTunnel-CS project tested UU's explosion-free in a fire self-venting (TPRD-less) tank. The concept of the invention (V. Molkov, D. Makarov, S. Kashkarov. European Patent Application No 18706224.5 "Composite Vessel for Hydrogen Storage", 2019) is the microleak-no-burst (μLNB) behaviour of TPRD-less tank, i.e. melting of tight to hydrogen liner and initiation of release through the composite wall before the tank composite wall loses its load-bearing capability (Molkov *et al*., 2018). The technology has already been proven to exclude hydrogen storage tank rupture in a fire. Figure 4-10a shows the scheme of the μLNB tank and its components, i.e. liner, bosses, fibre reinforced polymer (FRP) and thermal protection layer (TPL) that can be as load-bearing as the FRP.

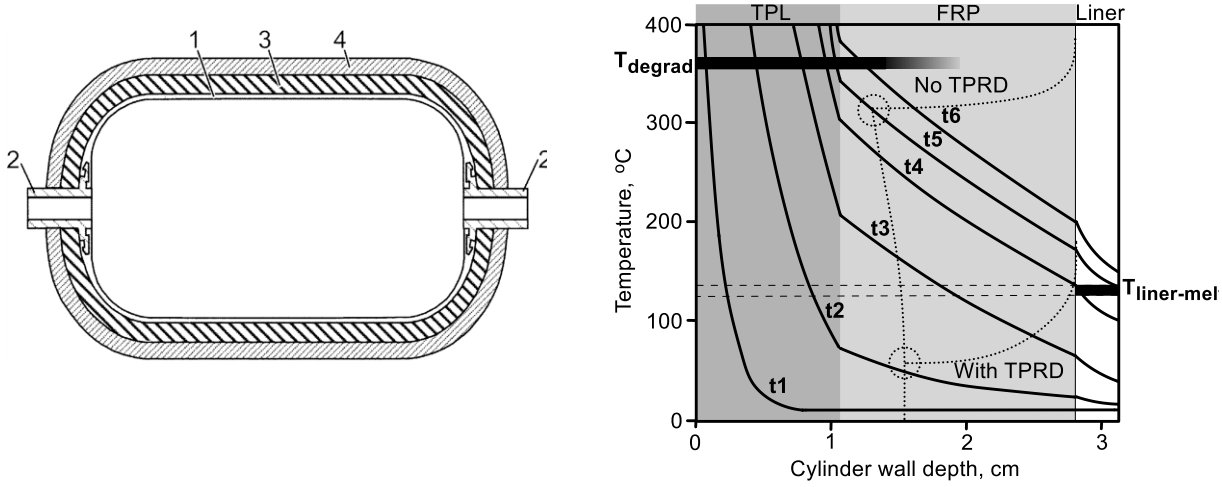

Figure 4-10. (a) - a cross-section of the explosion free in a fire self-venting μLNB tank and its components (1 - liner, 2 - bosses, 3 - FRP, 4 - TPL); (b) - schematic diagram of μLNB tank operation in a fire (Molkov et al., 2018)

*Figure 4-10*b schematically demonstrates the operation of the μLNB self-venting TPRD-less tank in a fire. The marking of "TPL", "FRP" and "Liner" for the vertical layers (dark grey, light grey and white) shown on the top demonstrates the widths of the corresponding materials in the overall tank wall thickness. The TPL layer is on the outer side of the tank and subject to a fire from the left side (not shown in the diagram). The purpose of the liner is to prevent hydrogen

permeation. The liner is located on the inner side of the tank and exposed to hydrogen (not shown in the diagram). The Y-axis in *Figure 4-10*b represents the temperature (temperatures are the highest on the left due to heat transfer from a fire). The X-axis represents the tank wall thickness. The horizontal bar on the left, next to "T_{degrad}" describes the resin decomposition temperature range typical for TPL and FRP composite materials. The horizontal bar on the right, next to "$T_{liner-melt}$" describes the liner polymer melting temperature range. The dotted curves represent the tank wall load-bearing thicknesses (LBT), i.e. that part of the tank wall thickness which is sufficient to bear the load of transient hydrogen pressure. The curve marked "No TPRD" indicates dynamics of LBT for the tank without a TPRD or faulty/not operational TPRD as time progresses from t1 to t6. The dashed line marked "With TPRD" indicates the dynamics of LBT for the tank equipped with a TPRD, which opens at time t2; as hydrogen pressure decreases the LBT decreases too, which is shown in *Figure 4-10*b by the dotted line "With TPRD" leaning to the right. Solid black curves marked "t1"–"t6" indicate temperature distribution through the wall thickness and liner as time progresses from t1 to t6.

Tank original failure criterion behind the μLNB safety technology is based on the understanding that the composite material loses its load-bearing ability when its temperature is above T_{degrad} , i.e. the resin is thermally decomposed and different plies are no longer being bonded, i.e. becomes loose. In the example in *Figure 4-10*b the part of the wall thickness where the temperature is above T_{degrad} is not capable to bear any load according to the failure criterion. The degraded in a fire fraction of wall thickness increases as the time progresses from t1 to t6.

The dotted curve under "No TPRD" bending to the left with time (as it intersects with temperature distribution for different times t1-t6) means that the initial LBT increases with time. This happens due to the growing hydrogen pressure in the tank (which increases together with temperature due to the heat transfer from a fire). The higher the hydrogen pressure in the tank the thicker LBT should be to bear it. If the dashed curve intersected the "T_{degrad}" bar this would mean that thermal degradation front reached the minimum LBT required to bear the hydrogen pressure load and the tank rupture would occur.

For the tanks built using μLNB technology the rupture does not occur: at time t5 the temperature in the entire liner increases above its melting temperature $T_{liner-melt}$, the liner melts, allowing hydrogen to leak through the tank wall and the tank depressurises safely. As the pressure decreases, the LBT starts to decrease as well, which is reflected in the dotted "No TPRD" curve changing direction to the right after time t5. Further tank wall degradation is no longer hazardous – TPL and FRP degradation bar marked "T_{degrad}" does not catch up with the dotted LBT line, i.e. the tank doesn't rupture in a fire.

The μLNB technology may also work alongside a TPRD installed on hydrogen tanks. Another scenario schematically illustrated in *Figure 4-10*b is associated with a tank equipped with TPRD which starts to operate at time t2. The LBT dashed curve marked "With TPRD" starts deviating at the intersection with temperature gradient t2 and bending inwards (to the right), demonstrating the LBT decrease as the pressure decreases inside the tank. This means that a TPRD could activate at some time and blow-down without rupture would take place. This mechanism is described in (Molkov *et al.*, 2021).

The prototypes tested previously demonstrated self-venting capability in different possible incident conditions, including the extinction of fire by water sprays. The experiments showed

that the explosion free in a fire TPRD-less tank continued to leak and the pressure inside the tank dropped to atmospheric. This allows first responders to apply the same intervention strategies and tactics as with fossil fuels vehicles, i.e. to extinguish the fire as soon as possible to exclude hazards from smoke and further fire propagation to other vehicles.

This technology resolves all main concerns of using high-pressure hydrogen storage tanks onboard vehicles, especially in confined spaces, where the use of a TPRD does not provide an acceptable level of safety. Self-venting tanks provide an improved level of safety by eliminating rupture risk and making hydrogen vehicles potentially safer than those using gasoline or diesel, where fuel tank rupture is still a possibility. Benefits can be characterised as:

- No blast wave;
- No fireball;
- No projectiles;
- No long flames (microflames);
- No formation of a flammable cloud;
- No pressure peaking phenomenon;
- No life and property loss, *etc*.

4.2.4 Validation of UU's explosion free in fire self-venting (TPRD-less) tank technology

Partner CEA has conducted tests on the two μLNB tank prototypes manufactured in the USA to UU's designs. Two tests were performed with NWP=70 MPa, 7.5 litres μLNB tanks. The tanks had the same wall thickness (2+ mm) but used different fibres-resin compositions. The scenario selected by CEA was: the TPRD-less tank was subject to a localised fire of HRR/A=1 MW/m^2 up to the time when it started to vent hydrogen through the composite wall after the liner has melted with a distinguishable hissing sound; then, the burner fire was shut down (no water sprays were applied to the tank surface as in the previous experiments performed by UU within national projects) and the depressurisation of the μLNB tank was monitored as well as the behaviour of the gaseous atmosphere around the tested tank. A detailed description of the experimental protocol and results of CEA tests can be found in (HyTunnel-CS, D4.3, 2022), and results of USN and HSE tests in (HyTunnel-CS, D4.4, 2022).

Both prototypes at CEA series followed the same test sequence that can be divided into several phases:

- Phases 1 to 3: filling of μLNB tank to stabilised pressure of around 55 MPa.
- Phase 4: fire starts, degradation of the μLNB tank by the localised fire with HRR/A=1 MW/m². This phase ends when the μLNB tank starts to leak in the localised fire.
- Phase 5: depressurisation (self-venting) of the μLNB tank after the liner has melted. Just after the start of the leakage, the localised fire was switched off and the pressure decrease inside the μLNB tank was monitored. This phase ends when the pressure inside the μLNB tank decreased down to only 4MPa and remains almost constant after that (self-closing of microleak channels due to tank contraction during essential pressure drop) for at least 10 minutes (the tank is no longer emptying).
- Phase 6: the burner is switched on to imitate restart of the fire. The leakage process starts again and finally fully depressurises the μLNB tank to atmospheric pressure.

Time zero has been set at the start of Phase 4. The same behaviour was observed for both tank prototypes even those manufactured with the use of different fibres and resins, but with the same liner material. Only the timing of the event was varied slightly. Events timing is summarised in Table 4-2.

Table 4-2. Time of the occurrence of the main events

Event	Time	
	Test No.1	Test No.2
Start of the burner	0 s	0 s
Start of leakage	402 s	319 s
Stop of the burner	433 s	332 s
Stop of flames on the tank	761 s	600 s
Restart of the burner	1882 s	1195 s
Restart of the leakage	~2480 s	~1700s

The temperature and pressure in the nearest measuring chamber were used to determine the mass flow rate during the blowdown of the tank. This mass flow can be compared with a simulation of a hydrogen release through a calibrated orifice using the sonic nozzle method. However, in the absence of data on the C_D coefficient for the cases of leaks through a porous membrane, the value C_D=1 was accommodated. The values of equivalent microleak orifice diameter found by CEA with this method are 0.58 mm (Test No.1) and 0.65 mm (Test No.2); and in UU's estimation of the equivalent orifice size is assessed as 0.4 mm (Test No. 1 and 2).

The technology is shown to be efficient and reproducible for a selected scenario. It is promising as the tank becomes intrinsically safe, i.e. explosion free due to self-venting in a fire. Furthermore, the equivalent "TPRD diameter" of the microleaks through the composite wall is below 1 mm, i.e. smaller compared to used currently TPRD diameters and in line with requirements for parking in garages as well as underground parking.

Partner USN conducted the fire test with a TPRD-less tank prototype. The tank filled to 70 MPa was subject to a localised fire of HRR/A=1 MW/m^2. The prototype leaked in the fire, as anticipated. One of the aims of this test was to quench the fire and measure hydrogen concentration decay around the tank after fire extinction (expected to dip below the LFL, in a few millimetres/centimetres). However, the water sprinkler that was installed above the tank was unable to entirely put out flames of burning hydrogen below the tank. In order not to damage hydrogen concentration sensors, the concentration was not measured. The USN experiment described above with the µLNB tank prototype indicate that water sprinklers arrangements need to be modified to ensure that all the flames are extinguished.

In the USN test, the sequence of events is presented in *Table 4-3*.

Table 4-3. Time of the occurrence of the main events – USN fire test with the leaked prototype

Event	Time
Start of the burner	0 min
First resin combustion was observed	1 min 19 s
Start of leakage	5 min 32 s
Stop of burner fuel supply, resin and hydrogen burning continues	5 min 39 s
Start of water sprinkler	5 min 55 s
Extinction continues, resin and hydrogen burning continues	6 min 30 s
Seconds after sprinkler stopped – small combustion is slightly visible	13 min 30 s

5. Impact of hydrogen vehicle incidents on structures

5.1 Hydrogen jet fire effect on tunnel structural integrity

In some cases, fires in underground infrastructures such as road and rail tunnels as well as underground parking are triggered by vehicle accidents as well as arson, severe battery malfunction (ignition/ explosion) *etc*., and consequent ignition of a spill, vehicle itself or part of it, followed by an explosion of the fuel tank in a fire. Due to the inherent design of these infrastructures, the starting fire may easily spread to adjacent vehicles and become a large, long-lasting fire. However, even if the fire remains localised to a single vehicle, a typically lower ceiling height may aggravate the incident development. Very hot flames may directly impinge the structural elements and expose them to high temperatures.
The severity of such fires has been increasing in the past decades, as a consequence of the increased size of modern cars and a greater amount of plastic material used in the interiors. This is evidenced by several very large car-park fires, e.g. in Liverpool and at Stavanger airport in 2018 and 2020 respectively. In the Liverpool fire alone approximately 1400 vehicles were damaged. Therefore, in the case of car parks a general fire safety issue may have to be addressed regardless of the type of vehicles that are using these infrastructures. The general situation in tunnels seems improved since some major tunnel fires, e.g. 1999 Mont Blanc fire, triggered research and development of safety engineering solutions for tunnels.

Nevertheless, the number of alternative fuelled vehicles such as electric and hydrogen-fuelled cars is rising (IEA, 2017). These may change the potential fire accident scenarios and the potential impact on structures and people. Therefore, the use of new vehicles such as HPV in tunnels and confined spaces needs to be investigated.

This is one of the objectives of the HyTunnel-CS project. In the following sections of this chapter, some general findings are reported and recommendations are given to prevent and mitigate fires involving hydrogen vehicles in tunnels and other confined infrastructures such as underground parking. Hydrogen fires may be hazardous for these structures because of the jets from high-pressure storage, generally higher temperature of hydrogen combustion products and higher heat flux from the under-expanded impinging jet flame to the structure.

5.1.1 The state of the art

Explosion and fire-resistant structures are often designed according to simplified design methods, where both the action and the structural system are strongly simplified to obtain analytical solutions readily available for practitioners (HSE, 2006; De Cesare *et al*., 2010). However, these methods are hardly applicable to complex structures such as tunnels, where interactions and other sources of nonlinearities affect both the action (confinement, blast waves, triggering or generated fires, *etc*.) and the structural response (material nonlinearity, thermal expansion, thermo-plastic degradation of the mechanical properties, damage, *etc*.), i.e. action/structure interaction.
More advanced design methods resort to finite element (FE) models of different complexity. Three-dimensional FE models with shell or brick elements, e.g. such as (Sorelli and Toulemonde, 2005) or (Anau and Molins, 2011), are though mostly confined to the research field and rarely used in common practice. Furthermore, structural materials and soil are generally considered elastic, although some authors also treated them as non-linear (Cavalaro *et al*., 2011; Arnau and Molins, 2011; Winkler *et al*., 2004). Further limitations of most structural models concern the lack of consideration of thermal solicitations directly due to the explosion

but also caused by a concurrent fire. This approach is in line with what is required by current regulations (EN1990, 2002), where the occurrence of exceptional actions (explosions, fires, impact) is considered using an accidental design situation, where one exceptional action at a time is assumed, in reason of the low probability of occurrence of two exceptional actions at the same time. If this assumption is reasonable for two statistically independent actions, such as e.g. vehicle impact and arson, it is not justified in the case of exceptional actions triggered by previous ones, such as fire triggering or following explosions. As a consequence, a structure designed to resist explosion and fire separately may be at high risk of collapse in the case of a fire acting concurrently with an explosion.

Few researchers have attempted to include both explosion and fire in finite element models of structures, but they either refer to different structures, e.g. (Crosti *et al*., 2012), or use simplified models (Colombo *et al*., 2015). A comprehensive and reliable method for designing tunnels against explosion and fire using a coupled CFD/ FEM simulations is at present not available and would greatly advance knowledge beyond the state of the art of research and practice.

5.1.2 Vulnerability of concrete

Tunnel structures are often made of concrete elements, either in the form of precast tunnel sections (often used in submerged tunnels) or in the form of wall linings (drilled tunnels) and partitions (such as reinforced concrete slabs carrying the ventilation system).

Concrete elements are known to be quite vulnerable to fire and especially to rapid heating rates, such as those possible in the case of hydrogen fires of high intensity. As such, the investigation of the structural response of tunnel concrete elements to the fire of hydrogen-fuelled vehicles is paramount to ensure both a safe evacuation and limited economical repercussion due to structural damages and infrastructure downtime during reparation.

The term vulnerability is here intended as the easiness of a structural element to be damaged as a direct consequence of the exceptional action, e.g. comparatively large hydrogen fire. The reasoning for such vulnerability of concrete or reinforced concrete elements is twofold:

- **Explosive spalling**: spalling is a phenomenon where pieces of fire-exposed concrete are projected away at high velocity, as a consequence of the evaporation of the water in the concrete and sudden rise of the pore pressure. The phenomenon typically occurs in the first phases of a fire and can therefore represent a serious hazard for safe self-evacuation and rescue operations. Furthermore, spalling can expose the steel reinforcement, leading to premature structural failure. The risk of spalling is particularly high in case of very rapid fires, as well as high-strength concrete and concrete subjected to compressive strain (Hertz, 2003), as typically occurs in tunnels.
- **Structural integrity**: in the case the fire spreads to other vehicles and lasts longer, the damage to the concrete elements may not be limited to the outer surface, but may penetrate the concrete core and endanger the structural stability of the element or the whole structure. Due to the low conductivity of the concrete and the long time needed by the heat to penetrate the concrete core, the structure may be at risk of structural failure or collapse long after the fire has been extinguished. Such a situation is particularly critical for compressed elements, where the contribution of the concrete core to the resistance is predominant in terms of the steel reinforcement. An example of such delayed collapse is provided by the Gretzenbach underground parking,

Switzerland (2004), where the ceiling floor of the carpark collapsed and caused the death of 7 firefighters.

Both vulnerability aspects represent a potential danger not just for the structure, but also for the safety of people. In particular, while spalling typically occurs in the first phase of the fire, structural failures may also occur long after the extinction of the fire, when firemen and car owners may re-enter the tunnel, e.g. to inspect the scene or move their cars and belongings.

5.2 HSE experiments on hydrogen jet fire erosion of tunnel materials

A high-pressure hydrogen jet fire resulting from an accident involving an HPV will provide a short duration jet fire with flame temperatures greater than a typical hydrocarbon pool fire encountered in accidents involving fossil-fuelled vehicles. As described in Section 5.1.2, high strength grades of concrete are liable to explosive spalling due to the heat transfer associated with fire exposure. Furthermore, exposure to elevated temperatures can lead to irreversible loss of stiffness and strength. Existing design criteria for tunnel construction materials are based on standard fire curve, e.g. RWS (Rijkswaterstaat) or HCM (hydrocarbon modified), that describe peak exposure temperatures of up to 1370°C with test duration >60 minutes, whereas a hydrogen jet fire may reach higher temperatures, e.g. 1600°C, but for a shorter duration of 10–20 min. Therefore, investigation of the material response is required so that appropriate safeguards or mitigations can be identified if required.

The effect of high pressure and temperature hydrogen flames on the integrity of typical tunnel materials was investigated using a simulated ignited hydrogen blowdown from a storage vessel. The initial vessel conditions were 70 MPa and 100 L which is representative of the hydrogen storage found in HPVs. Two vent pipe orifice diameters were investigated, i.e. 2 mm and 0.5 mm, where the former is typical of current vehicle TPRD diameter while the latter has been investigated to avoid the formation of a flammable atmosphere under the underground parking ceiling if an unignited release were to occur. The tunnel construction material examined by partner DTU was a high strength grade of concrete with and without polypropylene fibres present. These are described in the sections that follow and recommendations are also given. Qualitative inspection of the material following the jet fire was used to assess the occurrence of spalling while ultrasonic microstructure analysis was used to determine if the internal structure of the cement or aggregate had been modified. In addition to the material testing, the temperature and pressure distribution was assessed in separate experiments to allow quantification of the jet fire characteristics.

5.2.1 Erosive effects of hydrogen jet fires on tunnel structural materials

The experimental setup for HSE's test programme aimed to mimic a high-pressure release from a fuel cell hydrogen (FCH) vehicle as a result of activation of the thermal pressure relief device (TPRD) on the fuel tank, which is impinged on tunnel structural material. These devices typically have a release opening of 2 mm and thus, a nozzle diameter of 2 mm was used. A 0.5 mm diameter nozzle was also used, as a TPRD with that diameter has been suggested as a potential option to increase safety i.e. by reducing the magnitude of the resultant flammable cloud build-up in the event of a tank blowdown event. Two tanks (each with a volume of 49 L) were pressurised to 700 bar to replicate parameters of those of a hydrogen fuelled vehicle, a car specifically. The resultant releases were ignited using a propane pilot light and samples were placed at a standoff distance of 1 m approximately.

A series of release scenarios were designed, where different parameters were measured:

- Free jet release – temperature measurements made along the axial length of an unimpeded jet.
- Impeded jet release – jet was impinged onto two sensing plate; the first was instrumented with pressure sensors and the second with temperature sensors.
- Impeded jet release – the jet was impinged onto structural samples and the erosive effects investigated using imaging and post-test material analysis.

Thirteen jet fire experiments were conducted in total.

5.2.1.1 Jet release characteristics

The axial temperature readings from the unimpeded jet releases for both nozzles showed that the highest recorded flame temperatures were 1650 °C, and more likely to be 1800 °C (Molkov & Saffers, 2013). For the 0.5 mm nozzle, this maximum temperature was recorded by the closest thermocouple at 0.5 m from the nozzle, whereas for jet fires where the 2 mm nozzle was used, the maximum temperature was recorded 3 m downstream.

When the jet fire was impinging upon the temperature plate, the maximum temperature reading, for a standoff distance of approximately 1 m, was found to be 1200 °C at the jet centre, rising to 1400 °C at the surfaces adjacent to the first strike spot of the jet. When the jet fire using the 2 mm nozzle was impinged onto the pressure plate the maximum pressures were measured at the initial stage of the release. The maximum pressure reading was recorded by the most central pressure sensor where the jet was incident, giving a value of 92 mbar. The pressure readings from the adjacent surfaces gave a range of readings from 15-52 mbar at approximately 100 mm from the centre of the plate. The pressure readings over the duration of the release appeared to decay in the same way as the vessel pressure decay with blowdown.

The duration of a hydrogen release would be limited by the inventory of the vehicle, and the development/duration of a representative fire curve for a hydrogen jet fire would be of the order of a few minutes rather than 1-2 hours as is typical of the standard fire curves. **Error! Reference s ource not found.** shows an overlay of the free jet test results from the axial measurement of the 2 mm nozzle, 49 L, 700 bar release with the RABT-ZTV car fire curve. The duration of the releases when considering the full inventory (98 L at 700 bar) for a 2 mm nozzle was approximately 3 minutes 45 seconds. Thus, a representative fire test curve for a hydrogen jet release from a car would be characterised by a rapid and intense temperature increase, up to potentially 1650 °C, lasting on the order of 3 - 5 minutes.

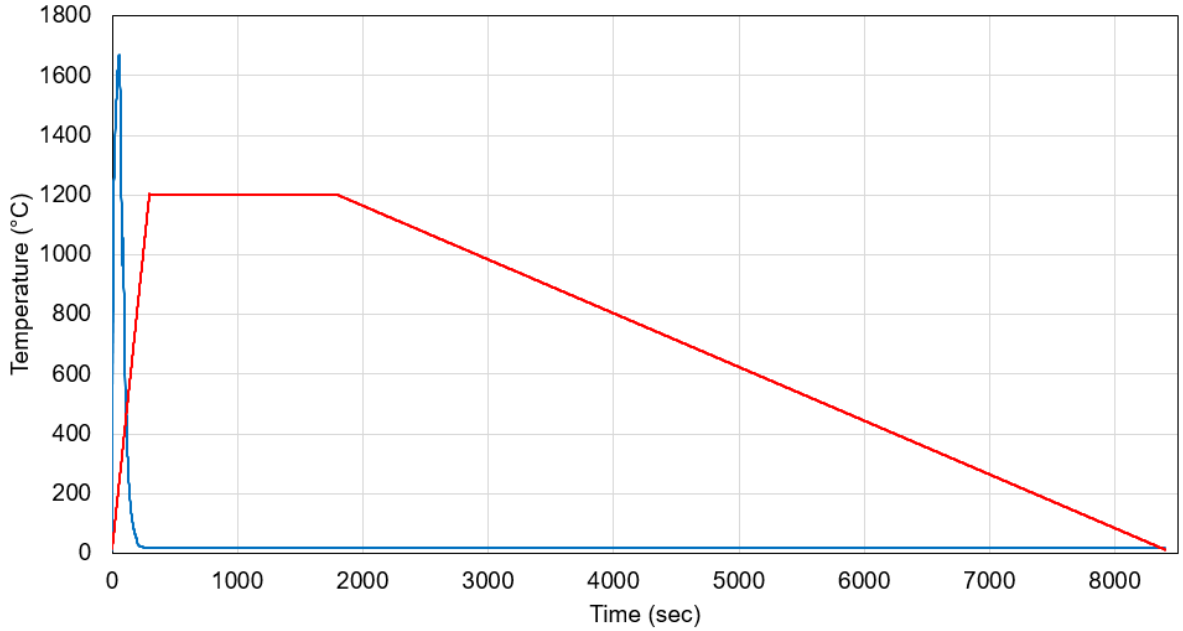

Figure 5-1. Plot showing comparison of temperature progression of 2 mm nozzle, 700 bar release vs. RABT-ZTV fire curve (car). Both are characterised by rapid initial temperature rises i.e. hydrogen jet temperature increases to a maximum of 1650 °C after 70 seconds approximately, whereas the fire curve, which assumes a hydrocarbon fuel reaches a maximum temperature of 1200 °C after 30 minutes.

The work in this test programme considered hydrogen jet releases to be the sole fuel source in the fire scenario, whereas in reality it is possible that other hydrocarbon fuelled vehicles may be involved. To account for this scenario, the fire curves could be designed to include this progression; it is expected that this portion of the scenario i.e. hydrocarbon fuelled fire, would then be accounted for using the typical fire curves profiles.

In terms of the jet light up, it was also noted that ventilation affected the ignition source i.e. gusting could move the ignition flame out of the jet path temporarily, resulting in a delayed ignition; this had consequences in terms of how mixed the jet was at the time of ignition and thus the resultant light up pressure and noise. A more informed fire curve could be developed by looking at results from the tunnel experiments in other work packages.

5.2.1.2 Jet effects on structural material

It was observed that spalling occurred in both non-polypropylene fibre containing concrete samples, even at differing stand-off distances from the jet release point i.e. 1.06 m vs. 2.24 m. The samples containing the polypropylene fibres on the other hand, whilst sustaining a scorch mark in each case, did not appear to spall, even when using the 0.5 mm nozzle, which gave a longer impingement time than the 2 mm nozzle (40 minutes vs 3.5 minutes). For the most severely spalled sample, the maximum depth of the spalling was approximately 30 mm and the spalling appeared deepest in the central region of the sample. **Error! Reference source not found.** shows a laser scan and visible image of (a) the non-polypropylene fibre containing sample and (b) the sample containing polypropylene fibres, where the 2mm nozzle was used for both.

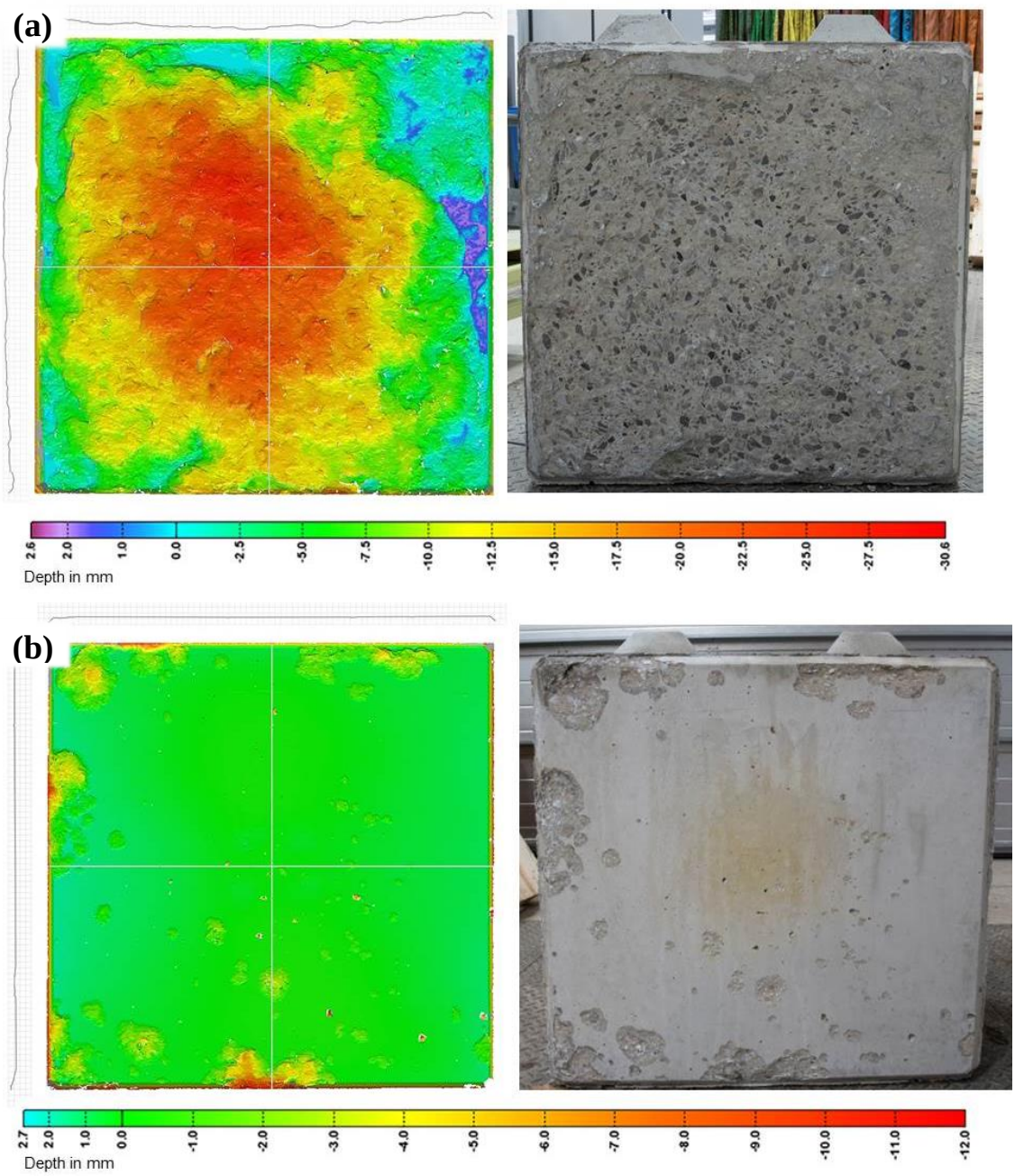

Figure 5-2. Laser scan and visual image of surface of HSE's concrete blocks (a) Sample 1, containing no PP fibres, and (b) Sample 2, containing PP fibres. Release conditions for both, 700 bar, 98 L, 1.06 m standoff, 2 mm nozzle. PP= polypropylene. Jet duration was 3 minutes, 45 seconds

Post-test analysis i.e. pulse velocity measurements looking for defect formation and compressive strength measurements looking at sample strength suggested that the damage sustained by the samples was mostly superficial and would probably not contribute serious engineering repercussions as result of an impingement of this type and duration. The heat transfer measurements suggested that the temperatures at increasing depth into the sample did not appear to approach those temperatures at which pore pressure increases, and spalling is likely to occur i.e. 200-300 °C.

In a similar way, another study (Park, Yoo & Kim, 2021) was carried out, where heat transfer measurements were made within a high strength concrete sample at a standoff distance of 2m. The test had a longer impingement time i.e. 320 secs, and recorded maximum temperatures of up to 1350 °C at a depth of 25mm and 85 °C at a depth of 50mm. The thermocouples in this case were embedded during the curing process (rather than inserted into drilled holes) and so better thermal contact between sensor and concrete is expected.

It is worth commenting that these test methods and results are specific to this setup only. Previous research (Mcnamee & Jansson, 2015) has concluded that a multitude of factors, including the chosen test method, will influence whether spalling will occur, not one property in isolation. For example, it was found that larger samples with the same concrete composition as smaller samples were found to be more likely to spall due to the added load generated by the sample bulk itself (Mcnamee & Jansson, 2015). Previous research has noted that the severity of spalling appears to be greater when the sample is exposed to slower heating rate rather than faster heating (Mindeguia et al., 2009; Phan, 2008). Thus, it is possible that though hydrogen has the potential to reach greater temperatures and faster than that of a hydrocarbon fire, the resultant fire by itself, may not contribute additional risk in terms of erosion of structural materials.

5.2.1.3 Recommendations

It is difficult to conclude a definitive test method for spalling due to the multitude of factors that can affect the resultant behaviour of a structural material when fire impinged. In the case of an unobstructed hydrogen jet, where there is no delay in ignition, with the limited inventory e.g. 2-4 kg hydrogen, temperature rather than pressure appeared to be the most influencing factor.

It is envisaged that other factors such as delayed ignition, and further obstruction by presence of vehicles could contribute to a different fuel/air mixing scenario situation, which may contribute additional pressure effects that were not seen in this test programme. Work package 4 investigates this in more detail and so measured overpressures in this work could be used to inform on representative pressure tests to be considered for structural material.

The key findings and recommendations from this work are:

1. The materials testing results indicate that polypropylene fibres do provide effective fire resistance in concrete samples when impinged upon with a hydrogen burning jet. It was found that the impinging hydrogen jet, over the short duration of venting of a typical vehicle inventory, would be unlikely to cause more severe damage than that of a hydrocarbon fuelled fire.
2. The present test results will be specific to both the jet fire setup used and the composition of the sample itself and the results are not necessarily directly transferable to any arbitrary sample. For example, ventilation will affect the magnitude of the resultant temperature of the burning hydrogen jet, compression/external load on the sample will affect its propensity to spall. Therefore, it is recommended that a wider range of test conditions and material properties are investigated.
3. A representative materials test, similar to existing fire curve scenarios should be developed, e.g. a standard test where a sample is exposed to a temperature profile over a defined time period. In contrast to existing fire curves, a burning hydrogen jet from a vehicle would be characterised as a short duration event with a rapid temperature increase, which then decays with the decreasing jet pressure.

4. The use of the smaller nozzle diameter did result in shorter hazard distances when considering the extent of the temperatures reached. Thus, the use of smaller TPRD sizes will limit the size of the affected zone around a vehicle accident/jet fire.
5. The hydrogen free jet itself is not visible, however when impinging upon a surface, a bright yellow-orange flame was observed. In addition, the noise generated by the momentum driven jet could be heard easily, whether ignited or not. Therefore, it is expected that there would be visual and audible indicator to inform emergency service responders that there is a depressurising vessel and hydrogen jet fire.

5.3 DTU work studying the effect of hydrogen jet fire on concrete spalling

As explained in Section 5.1.2 the reaction of concrete structural elements to fire is related to i) spalling and ii) loss of fire resistance.

Prediction of spalling is in particular very challenging, as it would require also a fully coupled hygro-thermal-mechanical (HTM) analysis and is characterised by several aleatory and epistemic uncertainties, which would affect the reliability of the results. For this reason, the modelling of spalling is often tackled in a simplified way, based on pre-defined spalling criteria evaluated against the thermal map of concrete. In some cases, a mechanical analysis can follow, where layers of concrete are removed, when the spalling criteria are met (Deeny *et al.*, 2008).

This procedure has been applied to the case study of a drilled tunnel with concrete pre-fabricated wall linings and a 35 cm thick reinforced concrete slab placed at 6.5 m distance from the floor and carrying the ventilation system. The slab is 10 m wide and is assumed to be simply supported on the tunnel walls, as shown in Figure 5-3 below. The assumed fire scenario consists of a hydrogen-fuelled bus that has an accident: the TPRD (located on the top of the bus) activates, releasing a hydrogen jet fire that hits the concrete slab just above. The centreline of the flame is assumed to be at 3 m from the left support of the slab.

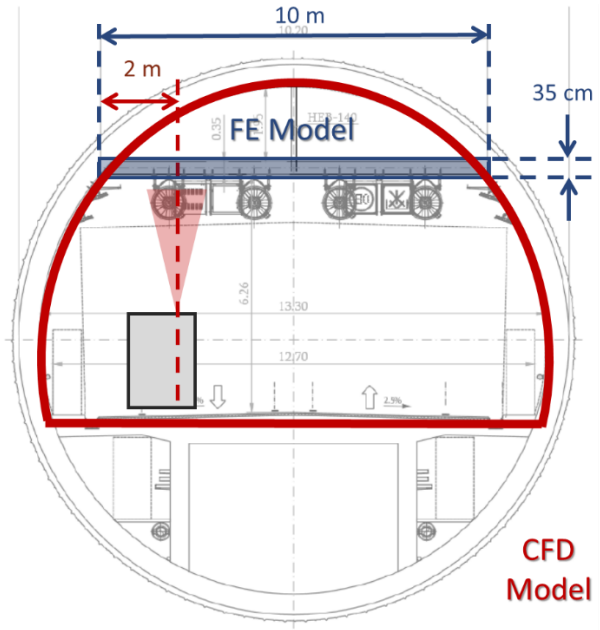

Figure 5-3. Drilled tunnel used as case study and sections of the CFD and FEM simulations. The main dimensions of the latter are shown, as well as the position of the bus and of the vertical axis passing through the TPRD

CFD model

CFD modelling is recommended as a reliable tool to assess the hazardous conditions produced by transient hydrogen jet fires impinging on tunnel structures. CFD simulations can be used in conjunction with FEM analysis for a comprehensive assessment of the tunnel structure response to the hydrogen jet fire.

FE thermal model

A 2-dimensional FE thermal model of the cross-section of the concrete slab just above the flame has been implemented in ABAQUS (Simulia, 2011) and transient thermal analyses have been carried out, with the aim of identifying the maximum heat penetration depth in the slab, an accurate thermal map of such depth, and the maximum temperature of the steel bars. Such outcomes have been used to give some indication of the extent of concrete damage, the possible occurrence of spalling, and the structural response of the slab.

The results of the analyses indicate that in the case where spalling is avoided, the structural resistance of concrete slabs exposed to hydrogen jet flame is not expected to be at risk, due to the short duration of the flame and limited time left for heat penetration into the concrete.

Nevertheless, the results also indicate that the bottom part of the slab is heated very rapidly to high temperatures and suggests that explosive spalling of the outermost concrete is possible. Based on literature indications on a critical temperature of 375°C for spalling (Hertz, 2018), the depth of concrete that is deemed to be susceptible to spalling has been assessed as the bottom 1.5 cm of the slab and further analyses have been carried out on a model with the bottom 1.5cm removed. The results indicate that a slab in which spalling has occurred, can also resist the hydrogen jet fire without significant loss of the load capacity.

Nevertheless, it is relevant to stress that such good fire resistance of the slab is mostly due to the high rebar cover of 5.5 cm, which allows for a further 4.0 cm of concrete protection after the region where assumed spalling has occurred. Many common R.C. slabs of similar dimensions and capacity often present a smaller rebar cover – typically 3.0 cm. In such slabs, the assumed spalling would reduce the depth of the steel to 1.5 cm from the spalled surface and leads to a higher steel heating temperature and a significant reduction of the load bearing capacity.

In order to ensure good fire resistance of tunnel slabs to hydrogen jet fires, it is therefore recommended to avoid spalling in the concrete elements that may be exposed to hydrogen fire and to ensure a high rebar cover of at least 50 mm, in order to limit the heating of the steel reinforcement, if spalling should occur.

It is important to underline that these conclusions only refer to the action considered in this fire scenario and analysed in the CFD model, that is a hydrogen jet flame triggered by the activation of the TPRD. It is however unlikely that this activation is not triggered by a previous car fire or other accidents that result in larger fire. In such cases, the heating of the concrete slab would be much longer and result in much higher temperatures of the steel and decrement of the load bearing capacity. Furthermore, the effect of the spalling possibly caused by the hydrogen flame would not be the same, as the reduction of the concrete cover in a longer fire would lead to much higher maximum steel temperature and likely failure of the slab during the longer broader fire event.

FE mechanical model

The mechanical response of reinforced concrete elements to fire is quite challenging, as it involves the coupling of two different materials (concrete and steel) and the consideration of softening and cracking of the concrete, in addition to the thermal degradation of the material properties. In particular, softening is known to cause stress localisation and issues related to mesh objectivity (Bontempi & Malerba, 1997). Cracking is also a complex phenomenon to be explicitly described (Amorim, Proença, & Flórez-López,, 2014) and is often modelled using a smeared cracking approach. Such an approach is based on the definition of cracking energy, which is defined at the element base. This means that the material model becomes mesh dependent and mesh limits arise from the consistency of the stress-strain models of concrete and steel (Vonk, 1992). Such mesh limitations may affect the convergence of the analysis or the accuracy of the results and therefore require an accurate validation of the model.

Experimental Spalling Tests on concrete (hydrogen jet flame exposure)

After some initial standard cylinder tests (Zaineb, 2020), three types of concretes, all with added PP-fibres, were tested as wall elements (1m × 1m) by exposure to a propane jet flame (Sørensen, 2021) followed by a hydrogen jet flame. These three further tested concretes all had added PP-fibres and an amount of microsilica (1%, 2% or 4%). One of the concretes (Type C) also had 2% fly ash added as well. See Table 5-1 below.

Table 5-1. Concrete recipes for testing of spalling (Sørensen, 2019)

Concrete	Characteristic	w/c-ratio	Microsilica	Fly ash	Plasticiser	PP-fibre	Aggregates
A	Reference	0.45	0%	0%	0	0%	Sea
B	Dense	0.40	1%	0%	+	0% / 1%	Sea
C	Dense +	0.35	2%	2%	+	0% / 1%	Sea
D	Dense + High strength	0.30	4%	0%	+	0% / 1%	Sea

B: Dense concrete. Probably not susceptible to spalling, at least when PP-fibres added.

C: Dense+ concrete. Could be susceptible to spalling, but the amount of fillers are on a relatively low level, so adding of PP-fibres will probably remove the risk.

D: Dense+ and high-strength concrete. Experience has shown susceptible to spalling, but reducing of moisture level, and adding of PP-fibres can probably remove the risk.

The percentages in the table are by cement weight.

The three concretes *with PP-fibres* (concrete B, C, D) were tested with propane and hydrogen jet flames, because none of them showed signs of spalling in the preliminary 1000ºC exposure on standard cylinder test.

Curing of all the concretes should at least be 28 days before testing, however longer curing is better and produces more representative results. We had a curing time of at least 60 days. A water bath (40ºC) can be used for accelerated curing of the cast standard specimen. Control of moisture level is important. The moisture level of the concrete should preferably be lower than 3-4% if used for tunnels. For each of the three test items tested as wall elements in compression, 4 gas burning exposures were performed, 2 with propane gas and 2 with hydrogen.

Based on the test results, **concrete type B is recommended** as it withstood all three test methods without spalling. This was the sample made up of **dense concrete, w/c=0.40 with 1% PP-fibres and 1% microsilica.**

In summary, the work conducted by partners HSE, DTU and USN on a selection of concrete samples, showed that to reduce spalling, it is recommended that less dense concrete with polypropylene fibres is used. The denser the concrete, the more susceptible it is to spalling – superdense concrete with no polypropylene fibres showed the worst damage especially in low moisture conditions in the experiments conducted by DTU. Polypropylene fibres seem to provide effective fire resistance in concrete samples when impinged upon with a hydrogen burning jet. To ensure wider applicability, a representative materials test, similar to existing fire curve scenarios should be developed, e.g. a standard test where a sample is exposed to a temperature profile over a defined time period.

5.4 Effect of blast wave after hydrogen tank rupture on tunnel structure

5.4.1 Tunnel structure reaction to a blast wave from hydrogen tank rupture in a fire

CFD simulation of the maximum overpressure dynamics on the tunnel ceiling surface from stand-alone 62.4 L, NWP=70 MPa tank rupture a the tunnel fire for selected scenario is shown in Figure 5-4. The peak overpressure of 152 kPa was recorded on the surface of the tunnel ceiling in the simulation. The structural strength of the concrete used in this particular tunnel is C35 which is commercial grade heavy duty structural concrete with compressive strength of 35 MPa which means that it will hold 35 N/mm^2, if applied as a compressive load on the section. However, bending capacity of the slab is just 17 kPa, that is 2000 times smaller than 35 MPa and therefore FEM analysis should be performed in order to assess tunnel integrity after high pressure tank rupture in a fire. The current pressure load, shown in *Figure 5-4* below is 0.15 N/mm^2 and is applied as uniform dynamic pressure to the bottom of the slab for performed FEM analysis.

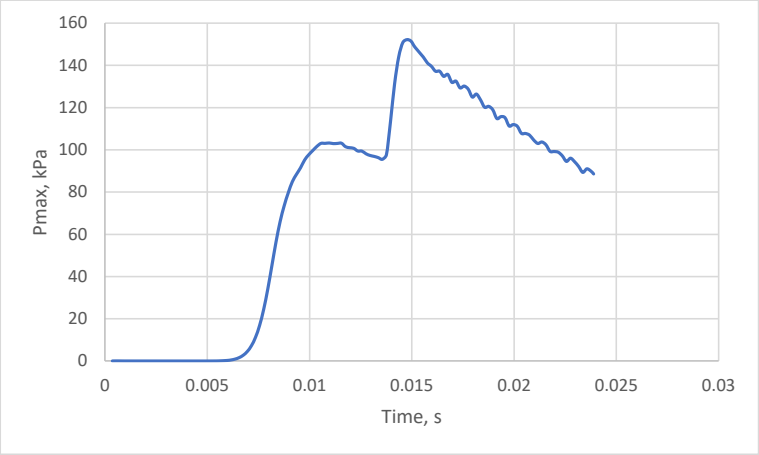

Figure 5-4. Maximum overpressure dynamics on the tunnel ceiling surface for a stand-alone tank of 62.4 L, NWP=70 MPa ruptured in a fire

The ceiling slab is 10 m wide and anchored at the side walls of the tunnel such that rotation of the slab ends is allowed. The slab is 35 cm high and reinforced with 16 mm diameter hot-rolled bars placed every 150 mm in both directions and both at the top and the bottom of the slab. The

top reinforcement is placed at 35 mm from the top and the bottom reinforcement is placed at 55 mm from the bottom. A simple calculation of the static load-bearing capacity of the slab indicates that the slab can resist a uniform distributed load of 17 kN/m^2 in negative bending and slightly less in positive bending.

These values are about 10 times smaller than the peak pressure of 152 kN/m^2 recorded on the surface of the tunnel ceiling, indicating that the slab would completely fail, if such pressure were to be applied in a quasi-static way. Nevertheless, the duration of the dynamic action is very short in comparison of the natural period of the slab and, as a consequence, the dynamic application of the load would cause a significant de-amplification of the response. As a result, the slab would experience significant deformation and residual damage, but it is not deemed to collapse under the assumed impulse.

The results have been obtained by means of a FEM analysis of the nonlinear dynamic response of a 2D model of a transversal section of the slab. The effect of the explosion wave travelling along the length of the tunnel have not been included. Furthermore, the slab section has been uniformly loaded over the transversal length to the explosion pressure of one tank, as shown in *Figure 5-4*.

As such, the validity of the conclusions is limited by the assumptions made on the overpressure dynamics and on the modelling. In particular, the response of the slab could be higher, if:

- some parts of the slab were exposed to a lower but longer overpressure, resulting in a dynamic amplification or at least a lower de-amplification of the response;
- the effect of the pressure wave along the tunnel caused more significant deformations or vibrations in the longitudinal direction of the slab;
- the explosion of more than one tank occurred, as a consequence of the same accident; and
- the tank explosion had been triggered by a large vehicle fire, which had previously or was simultaneously acting on the slab.

If none of the above is relevant, no additional design recommendations would be required to ensure the structural integrity of the tunnel slab in a hydrogen tank rupture in a fire, as it is deemed to resist the pressure loads for considered scenario.

6. Quantitative risk assessment methodology

6.1 QRA methodology for hydrogen vehicles in confined spaces

The hazards and associated risks and implications of the use of hydrogen-powered transport in road and railway tunnels as well as underground parking have to be estimated.

A QRA is a logical and systematic approach to numerically estimate the risk associated with certain hazardous events that are more complex and involve novel processes. It is an assessment that uses special quantitative tools and techniques to establish the risk to people from defined scenarios with a given set of parameters. It involves estimating the likelihood and potential consequences and severity of hazardous events; and expressing the findings as a risk to people.

Several risk assessment models and tools are available in the literature but either they do not include hydrogen as a dangerous substance, e.g. QRAM by PIARC and OECD, or the "low frequency – high consequence" events are not included in the analysis, e.g. QRA developed by Erhart *et al*. (2019).

The QRA methodology proposed in HyTunnel-CS includes incident and fire frequencies, traffic statistics, tunnel geometries, including certain prevention and protection measures such as means of traffic control, monitoring, ventilation and emergency procedures that can control and extinguish the fire, in order to ensure the safety of the tunnel users and the tunnel structure. The flowchart of the proposed QRA methodology, according to PIARC (2008), is shown in Figure 6-1 while a detailed description of all the phases is reported in (HyTunnel-CS, D5.3, 2022).

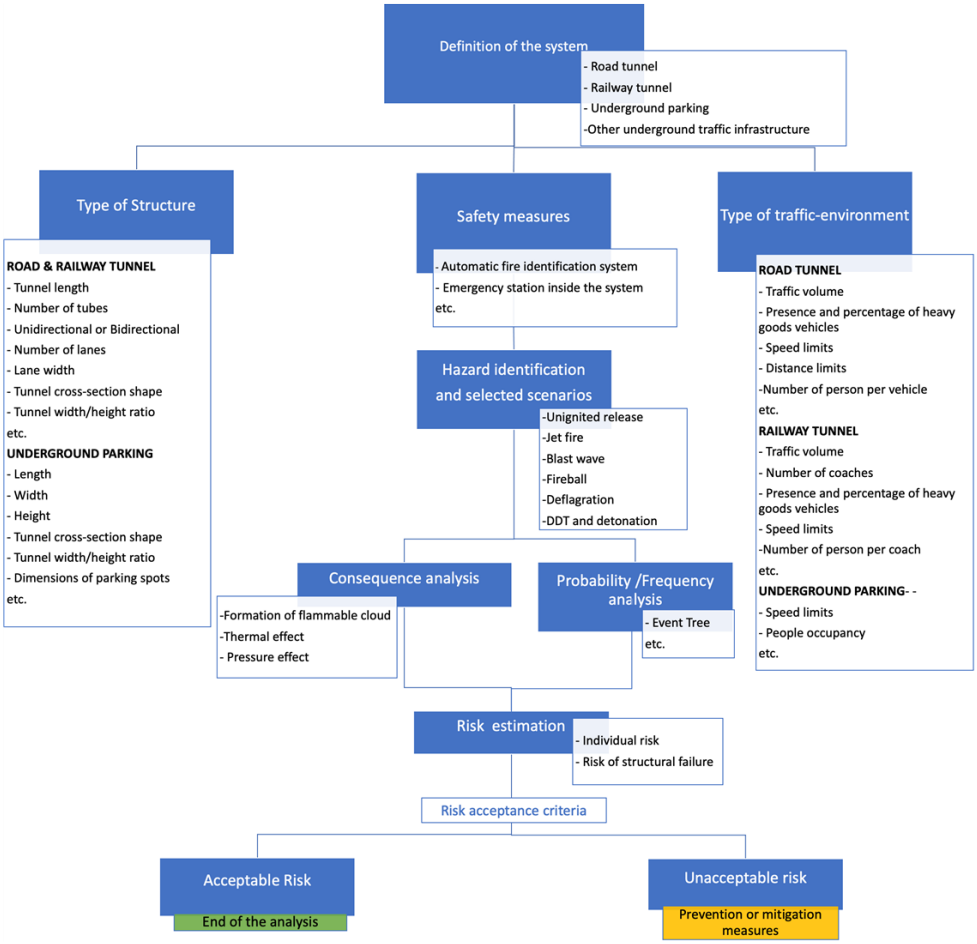

Figure 6-1. Phases of the proposed quantified risk assessment procedure

To demonstrate the application of the suggested QRA methodology, examples have been provided for selected incident scenarios in road and railway tunnels, as well as in underground parking but further applications could also include a ship's hold and other confined spaces.

Event Tree Analysis (ETA) is the technique to estimate the event frequencies. It is a common and widely used technique and tool in the industry to enable event frequencies to be estimated from numerical data such as accident/event data, failure rates and probabilities. Event trees were developed to graphically illustrate all possible outcomes following an accident involving a hydrogen vehicle. It depicts the chronological sequence of events that could occur following the initiating accident, including escalations and mitigation measures, e.g. first responders' intervention at the site of the incident. Figure 6-2 details an example event tree developed within this project. The difficulties in ETA for emerging technologies is a lack of statistics, failure rates and probabilities that make QRA uncertainty very high. Thus, the priority at the initial stages of technology implementation should be given to the development of inherently safer engineering solutions that are supported, rather than substituted by risk analysis.

A detailed analysis of the incident scenarios that are unique to hydrogen vehicles, such as consequences of the initiating events, is included in the QRA methodology. The collision types that may result in a release of hydrogen in a tunnel and the location of such an incident are also considered. As an example, the worst-case incident scenario in a road tunnel is assumed to be a collision of a vehicle at high speed into the last vehicle in a queue. Then both hydrogen release from the hydrogen fuel system and TPRD are considered.

Regarding the latter, the proposed methodology enables the assessment and evaluation of scenarios involving external fires or vehicles that burst into fire because of an incident or other ignition event. The heat impact on the hydrogen storage system is of great importance as it implies the storage tank rupture and gas cloud explosion scenarios. Therefore, both engulfing fire and localised fire scenarios are considered by application of different TPRD failure probabilities in a fire taken from publicly available sources. The reliability of the TPRD is not reported sufficiently. There are very limited literature data available, e.g. in the FireCOMP risk assessment study (Saw *et al*., 2016) and the SANDIA National Laboratories publication (Erhart *et al*., 2019).

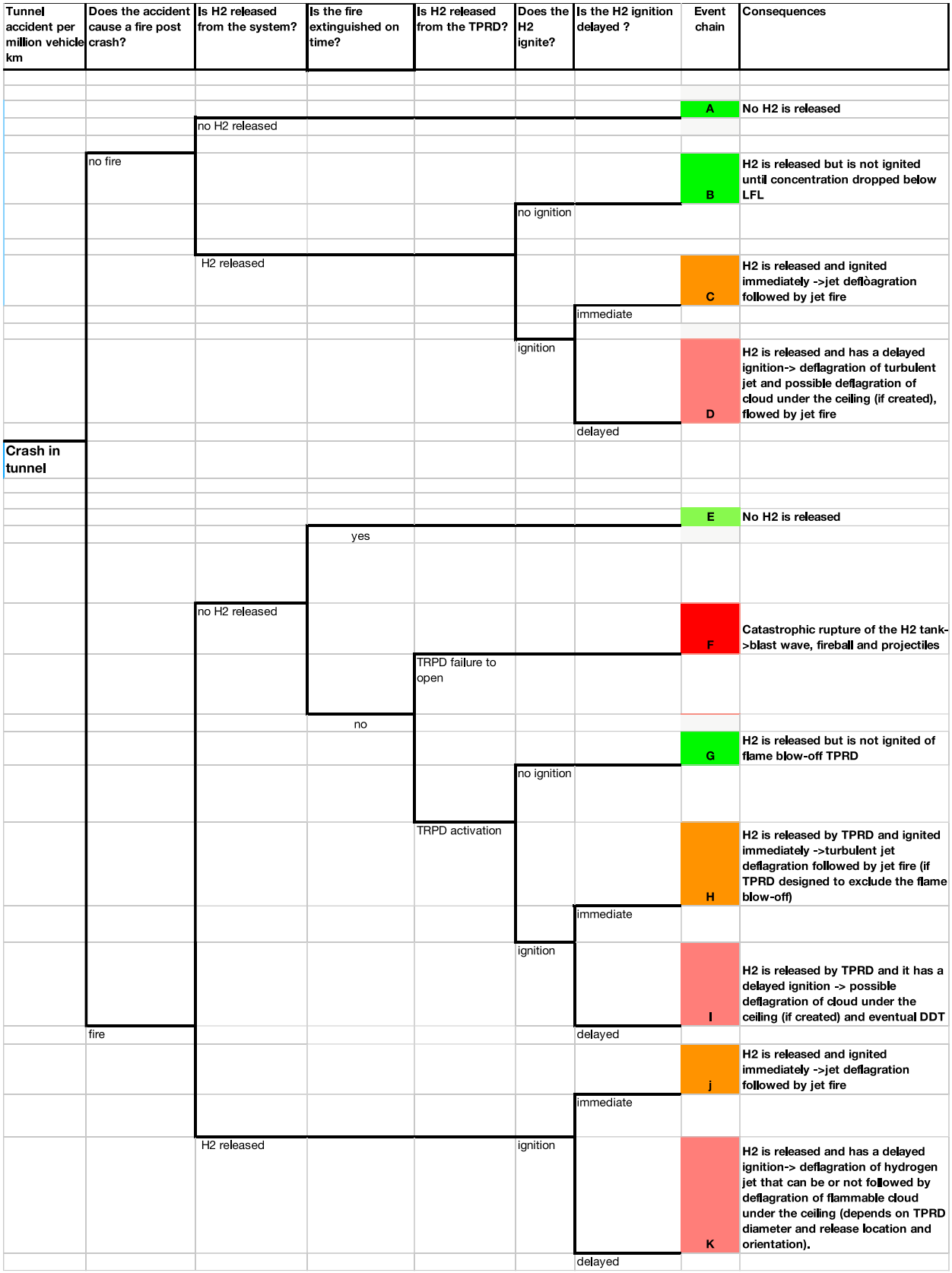

Figure 6-2. Event tree for crash scenarios involving hydrogen vehicles

The consequence analysis, therefore, includes the hazard from unignited release, hydrogen jet deflagration and fire, deflagrations/DDT/detonations of flammable cloud under a ceiling if it is created, blast wave and fireball after hydrogen storage tank rupture in a fire, *etc*. The pressure

peaking phenomenon, which is relevant to enclosures with limited vent area like garages, could be dropped for consideration of hydrogen releases in tunnels and is thus not included in the ETA. For jet fire, the flame length, which depends on the storage pressure and release orifice diameter, can be calculated using the dimensionless correlation for hydrogen jet flames (Molkov and Saffers, 2013) that is available on the free online e-Laboratory of Hydrogen Safety (https://elab.hysafer.ulster.ac.uk/). The correlation is for free jets and applies to hydrogen temperatures down to cryogenic (Cirrone *et al*., 2019). Unfortunately, there are no engineering tools for the assessment of hazards of attached or impinging jets at the moment. In the case of TPRD releases, the impinging jet will be shorter due to loss of momentum and follow-up effect of buoyancy compared to a free jet and therefore the correlation can be considered as a conservative estimate. To assess the effect of radiation from a jet fire, the radiative heat flux may be calculated. Radiant heat flux predictions derived from conventional single point source models have been observed to underpredict measured values by 40% or more, particularly in the near-field (Ekoto *et al*., 2012, 2014). On the contrary, weighted source flame radiation models have demonstrated substantial improvement in the heat flux predictions, particularly in the near-field of the hydrogen jet flame.

As for blast wave in tunnels, the universal dimensionless correlation for the decay of blast wave in a tunnel and thus assessment of the hazard distances (Molkov and Dery, 2020), which was confirmed by CEA experiments, is recommended for the consequence analysis. For fireball after high-pressure hydrogen tank rupture in a fire, the engineering correlations for assessment of hazard distance (defined by the fireball size) are available both for stand-alone and under-vehicle tank rupture in an open atmosphere, but not in confined spaces (Makarov *et al*., 2021b). The HyTunnel-CS research demonstrated the higher hazard of fireball in a tunnel compared to the open atmosphere, i.e. propagation of fireball along the tunnel with velocity up to 20-25 m/s depending on the location of tank rupture in a fire.

The correlations to assess the blast wave and fireball size after a high-pressure hydrogen tank rupture in a tunnel have been proposed by UU for compressed hydrogen tank rupture in a fire. These are submitted as part of HyTunnel-CS D4.4 (2022). The correlations have been compared with the numerical simulation to assess the dynamics of the blast wave and the size of the fireball and propagation of hazard distances. It could be concluded that none of the simple correlations can be easily applied for the fireball hazard distance in a tunnel due to the complex dynamics of its propagation.

Prediction of the consequences of hydrogen detonation is important for hydrogen safety assessment in confined spaces. Partner KIT (Li *et al*., 2021) calculated the hydrogen dispersion in the tunnel to evaluate the risk of flame acceleration and DDT. The detonation in the tunnel is calculated by assuming a strong ignition at the top of the tunnel at an unfavourable time and location. The pressure loads are calculated to evaluate the consequence.

The QRA output for hydrogen-powered vehicles in tunnels is individual risk in terms of human fatality per vehicle per year, for a selected scenario. Probit functions are particularly useful in QRA since they can provide harm probabilities for the range of incidents included in the risk assessments. In the case of a fire scenario, a Probit function translates a thermal dose level to a probability of injury or fatality. Several Probit functions are available to evaluate the probability of injury or fatality as a function of thermal dose. Unfortunately, no Probit function has been generated specifically for hydrogen fires. According to LaChance *et al*. (2011), the Eisenberg Probit function is likely the most appropriate in the harm predictions from radiant heat fluxes.

In the case of tank rupture, possible consequences on humans and structures or equipment include blast wave overpressure effects, impact effects, impact from fragments generated by the tank rupture, the potential collapse of equipment or structural elements, and the thermal effects

from subsequent fireballs. Only the blast wave effects on humans and structures are considered. Fortunately, there are Probit functions available to predict the level of harm to people and structures from the impact of blast overpressures. According to LaChance *et al*., 2011, the HSE model is used to evaluate the probability of harm to people as it provides the most conservative results for low peak overpressures even if it provides lower probabilities than the Eisenberg model at higher overpressures. As for structural failure, the Eisenberg Probit has been chosen as it provides results that agree reasonably well with the data reported by the American Institute of Chemical Engineers (1998).

Finally, hazard distance is evaluated assuming a threshold probability of individual risk. The threshold probability is the *de minimis* risk defining the acceptable risk level (1×10^{-6} fatalities per year) below which society normally does not impose any regulatory guidance. An acceptance criterion of 1×10^{-5} fatalities per year is instead proposed by (EIHP2, 2003) as acceptable level of risk for the first responders in a hydrogen refuelling station. In the following case studies, both values 1×10^{-5} and 1×10^{-6} fatalities per year will be used and results compared.

A detailed description of the QRA methodology is reported in (HyTunnel-CS, D5.3, 2022).

6.2 Examples of QRA methodology application to hydrogen vehicles

6.2.1 QRA of hydrogen vehicle in a road tunnel: Dublin tunnel (Ireland)

European Hydrogen Safety Panel (EHSP) published the guidance document on "Safety planning and management in EU hydrogen and fuel cells projects" (FCH 2 JU, 2021). For the safety provisions within projects, it targets to find and address the key knowledge gaps and technological bottlenecks, as well as set out the activities to provide technical and organisational safety activities. The document describes the preparation, implementation, monitoring and reporting on the project safety plan, an important part of which is the hydrogen safety engineering process and its implementation. The overall flow chart of this process is presented in Figure 6-3.

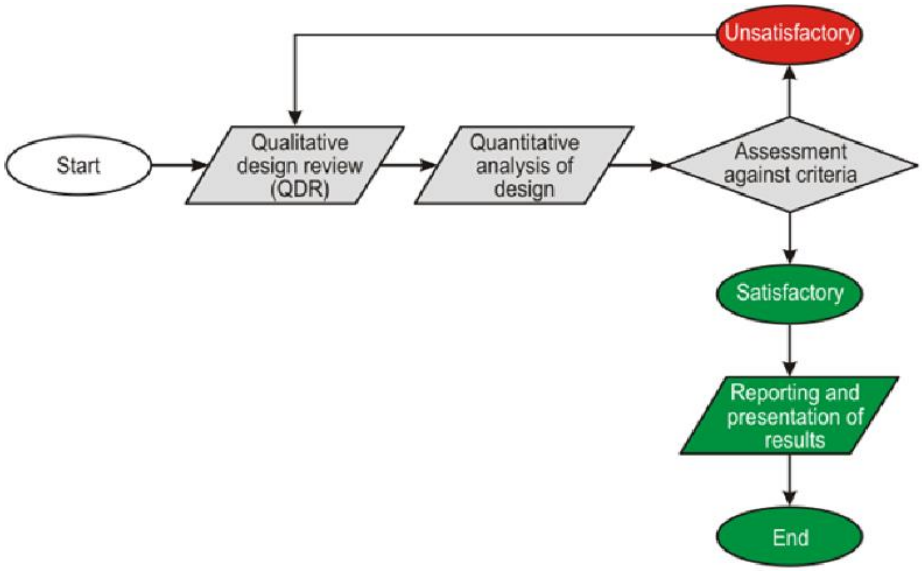

Figure 6-3. The scheme of the hydrogen safety engineering process (FCH 2 JU, 2021; Molkov, 2012)

In this process the three main stages are followed, i.e. qualitative design review (QDR), Quantitative analysis of risk and assessment against criteria. The QDR is done by the safety team that includes project managers, hydrogen safety engineers, representatives from authorities, e.g. emergency services, *etc*., and includes hazards identification analysis and defines incident scenarios for further investigation and safety objectives for hydrogen safety engineering. It

allows its members to discuss a range of safety strategies and propose possible engineering solutions. Then, the quantitative analysis on the selected scenarios and design options is conducted by hydrogen safety engineers having knowledge in the state-of-the-art hydrogen safety science and engineering and exploiting the available tools and validated CFD and FE models. Then, the assessment of hydrogen system performance against the determined acceptance criteria is conducted. The main objectives of hydrogen safety are preservation of life, control loss and protection of the environment (FCH 2 JU, 2021).

With regards to hydrogen safety engineering in confined spaces, firstly the review of the potential hazards from the hydrogen system should be carried out. The recent findings in the HyTunnel-CS project associated with hazards from hydrogen vehicles in confined traffic infrastructure were utilised (Makarov *et al*., 2021a). This paper contains particulars of and the hazards from hydrogen releases from a TPRD and the effect of release orientation, hydrogen dispersion and effect of tunnel slope, hydrogen jet fire heat release rate (HRR) contribution to overall car fire HRR, the blast wave from hydrogen tank rupture in a tunnel, the Pressure Peaking Phenomenon (PPP), flame acceleration and DDT, the performance of a tank-TPRD system in an engulfing fire and performance in any fire, including localised, of innovative explosion free in a fire self-venting (TPRD-less) tank following UU's microleak-no-burst safety technology (Molkov *et al*., 2018). Not all the hazards from hydrogen-powered vehicles would be applicable inside the tunnels, e.g. the PPP is only applicable to confined spaces like garages with a limited vent area. The blast wave and fireball generated inside a tunnel after a high-pressure hydrogen storage tank rupture in a fire will represent the 'new' (characteristic only for high-pressure hydrogen onboard of a vehicle) most hazardous scenario relevant to a hydrogen vehicle. Unlike behaviour in the open space, the blast wave and fireball in a confined space like a tunnel presents high overpressures and more severe thermal hazards to people, vehicles and tunnel infrastructure, practically along the entire tunnel length.

Partner UU developed a QRA methodology for a tank rupture in a tunnel, this is as shown in the flowchart in Figure 6-4. The QRA output for a hydrogen-powered vehicle in a tunnel is a value of risk in terms of human fatality per vehicle per year, and in terms of the cost of human lives per accident. The consequence analysis identifies the dominant hazards in an incident fire and their consequences, which are considered here only as fatalities per event of a tank rupture. The risk in terms of human fatalities per vehicle per year (Figure 6-4a) is calculated based on the frequency of hydrogen tank ruptures per vehicle per year in road tunnels. Following a similar consequence analysis procedure, the risk in terms of monetary losses per incident (Figure 6-4b) is evaluated in this example using the tank rupture probability, accounting for the cost of human life losses in the incident scenario.

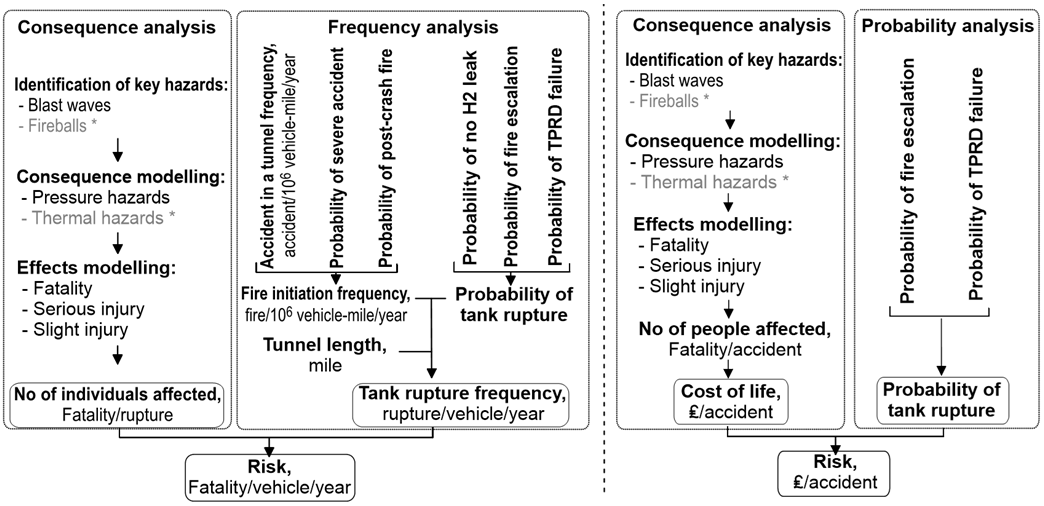

*Figure 6-4. The QRA methodology flowchart for hydrogen-powered vehicles in road tunnels: (a) risk in terms of fatality per vehicle per year; (b) risk in terms of cost of life losses per accident. Note: hazards with * are not accounted for in the current example of the QRA methodology application*

The first step in the consequence analysis is the identification of the key hazards relevant to the selected incident scenario with a high-pressure composite tank in a fire in a tunnel. They are identified as a "new" (compared to fossil fuel vehicles): strong blast wave and fireball following a catastrophic tank rupture in a fire. In this QRA example, only hazards from the blast wave are considered. Other hazards, including jet fires from TPRD and projectiles emanating from a tank explosion, are out of the scope of this QRA study as they do not prevail over the scenario of tank rupture. It has been demonstrated that the safety strategies for inherently safer use of HPVs in tunnels introduced in these recommendations can easily eliminate blast waves from deflagrations and detonations, if proper safety design of a tank-TPRD system is carried out by OEMs using outcomes of HyTunnel-CS. By this reasoning, the blast waves from deflagrations and detonations are excluded from this QRA.

The next step in this QRA methodology is the estimation of hazard distances in a tunnel at which pressure could cause fatality, serious injury, slight injury, and where there is no harm from the blast wave. The universal dimensionless correlation for blast wave decay after hydrogen tank rupture in a tunnel fire (Molkov and Dery, 2020) is applied for consequence analysis to calculate the hazard distances. The harmful effects on people from the blast wave overpressures inside the tunnel are based on the pre-defined harm criteria (Kashkarov *et al.*, 2020).

The Dublin tunnel (Road Tunnel Association, 2019) of 2.89 miles (4.65 km) long was used for this example of UU's QRA methodology. It has 2 tubes with 2 lanes each. The consequence analysis is performed for 1 tube. The selected scenario suggests that an HPV is trapped in an accident inside the tunnel, 50 m from the exit, blocking both lanes of the tube and an accident has escalated to a fire. The HPV has two onboard storage tanks, whereas only the rupture on the larger tank of 62.4 L, NWP=70 MPa (Yamashita *et al.*, 2015) is considered. The onboard hydrogen tank's state of charge (SoC) will normally be below 100%, which is expected to be immediately after fuelling. The maximum SoC for HPV is up to 59% before refuelling (Mattelaer, 2020). Thus, the value of SoC=59% resulting in pressure inside the tank of 35.5 MPa at 20°C (calculated by Abel-Noble real gas EoS) is accepted for the consequence analysis in this QRA as an arbitrary value, but the consequence analysis for the tank rupture at SoC=100% (immediately after refuelling) is out of consideration in this example (making it less conservative).

It is also worth noting, that the tank rupture can be eliminated at the SoC below about 50%, as demonstrated in (Kashkarov *et al.*, 2021), for Type IV tanks of different volumes with HDPE liner (this limiting SoC value is lower for PA liner making it less inherently safe in this sense). It is assumed as well, that based on a car length (calculated average from "What are the average dimensions of a car in the UK?", 2021), a spacing between cars is 5 m and the average number of passengers per car of 1.55 ("Average car and van occupancy England 2002-2018 Statistic," 2021), the total number of cars trapped in the tunnel is 968 (both lanes), totalling 1500 people trapped in the tunnel.

Using the data available from (Bassan, 2016; LaFleur *et al.*, 2017; National Highway Traffic Safety Administration (NHTSA), 2015), the fire initiation probability was assessed as: $Frequency_{fire\ init.} = Frequency_{tunn.accident} \times Probability_{severe\ accident} \times Probability_{post-crash\ fire}$=3.1×10^{-1} accident/10^{6} vehicle-mile/year × 5.94×10^{-2} × 3.17×10^{-1}=5.84×10^{-3} fire/10^{6} vehicle-mile/year.

The TPRD failure probability is 5.03×10^{-1} for localised fire, as per (Saw *et al.*, 2016). The fire escalation probability value for the example of a tank with a fire-resistance rating of FRR=8 min (Makarov *et al.*, 2016) is 6.57×10^{-1} (Dadashzadeh *et al.*, 2018).

A probability of failure of emergency operations to extinguish a fire (which leads to tank rupture), i.e. Escalation Probability, EP, is assessed by using a probit function, Y (Landucci *et al.*, 2015, 2009). To avoid complications of integration, the EP was expressed using the error function (erf) following (Papoulis, 1965): $EP = \frac{1}{2}\left[1 + erf\ (\frac{Y-5}{\sqrt{2}})\right]$, where Y is the probit function previously used as the general equation in the probit analysis (Landucci *et al.*, 2015, 2009), (Finney, 1971) which assumes log-normal distribution. As established in the study (Dadashzadeh *et al.*, 2018), the probit function in a scenario of a fire brigade arrival at an accident involving a fire considering a 90% failure probability for 5 mins response time and 10% for 20 mins response time with a hydrogen-powered vehicle should be written as: $Y = 9.25 - 1.85 \times ln(FRR)$.

For example, for 36 L and 700 bar Type IV tank the FRR=8 min, as reported in (Makarov *et al.*, 2016; Molkov *et al.*, 2021), the use of above equations for EP and for probit function Y, allow calculation of EP as: Y=9.25-1.85×ln(8)=5.403, hence EP=1/2[1+ $erf\left(\frac{5.403-5}{\sqrt{2}}\right)$]=6.57×10^{-1}.

Tank rupture probability is calculated as: $Probability_{tank\ rupture} = Probability_{TPRD\ fail.} \times Escalation\ Probability \times Probability_{no\ leak}$.

The "no hydrogen leak" probability value of 9×10^{-1} was adopted from (LaFleur *et al.*, 2017). It originates from the analysis of tests with damaged hydrogen systems where the presence of hydrogen leaks was analysed. It was found that there were no leaks in 90% of cases. Thus, in 10% of cases systems were leaking and we assume that no tank rupture would happen if a leak happens from a tank as a result of the incident. In our case the tank rupture is considered in the study as a result of an accident that escalates to fire and fire affects the hydrogen tank. So, by bringing the probability of no hydrogen leak in the formulation, we obtain:

$Probability_{tank\ rupture}$=5.03×10^{-1} × 6.57×10^{-1} × 9×10^{-1} = 2.97×10^{-1}.

The tank rupture frequency is calculated as: $Frequency_{tank\ rupture} = Frequency_{fire\ init.} \times Probability_{tank\ rupture} \times Length_{tunnel}$=5.84×10^{-3} fire/10^{6} vehicle-mile/year × 2.97×10^{-1} × 2.89 mile = 5.013×10^{-3} rupture/vehicle/year for the tunnel under the consideration.

The risk of fatality per year is calculated as $Risk_{fatality}$=$Number\ of\ fatalities\ per\ rupture$ ×$Frequency_{\text{tank}\ rupture}$. By multiplying the obtained number of 22.84 fatalities per incident by the fatality cost of £1,336,800 (HSE, 1999), we obtain the cost of human life (due to fatalities) associated with tank rupture as £30,519,144 /accident in the considered tunnel. By variation of the tank FRR, it is possible to change $Frequency_{\text{tank}\ rupture}$ and, hence, affect the $Risk_{fatality}$ in terms of fatality/vehicle/year (see Figure 6-5a). By increasing the tank FRR (to "infinity" in the case of using explosion free in fire μLNB self-venting tank) and hence decreasing the tank rupture probability, it is possible to achieve the risk values in terms of cost per accident comparable and below of that for fossil-fuelled vehicles (see Figure 6-5b).

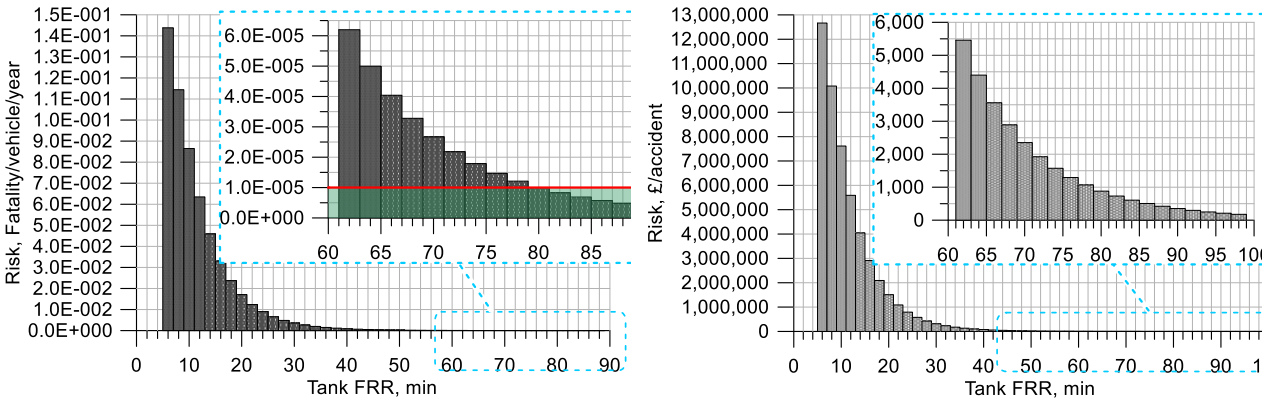

(a) (b)

Figure 6-5. (a) Risk (fatality/vehicle/year) dependence on hydrogen storage tank's FRR in a localised fire (tank SoC=59%); (b) Risk (£/accident) dependence on hydrogen storage tank's FRR in a localised fire (tank SoC=59%)

It is seen in Figure 6-5a that one of the examples of the hydrogen tank FRR=8 min gives $Risk$=1.7×10^{-2} fatality/vehicle/year, which is almost 3 orders of magnitude bigger than the acceptable level of 10^{-5} (LaChance, 2010; LaChance *et al.*, 2011) shown with a red line with a light green transparent filling under it. The increase of the tank FRR for a localised fire reduces the fatality rate progressively, until the risk becomes below the acceptable level at the FRR as long as 81 min, i.e. 1 hour 21 min (Figure 6-5b). The increase of tank FRR to 96 min, i.e. 1 hour 36 min, will provide the decrease of cost of an accident as low as £200/accident (Figure 6-5b). Hence, it is recommended for the achievement of an acceptable level of risk:

1. Increase the FRR, i.e. time to tank without TPRD rupture in a fire, of hydrogen onboard storage tank from several minutes to value (depends on the application) that provides acceptable level of risk.
2. Use explosion free in fire self-venting (TPRD-less) tanks (Molkov *et a*l., 2018) which have unlimited FRR.

6.2.2 QRA of hydrogen vehicle in a road tunnel: Varano tunnel (Italy)

As a second example of the QRA methodology application to road tunnels, an Italian tunnel was considered, i.e. the Varano tunnel. It is a curved bi-directional road tunnel, 1.2 km long, 10.5 m wide and 5.5 m high, with an almost uniform upward slope of 2%. The tunnel has a rectangular cross-section with two lanes. The annual average daily traffic (AADT) is more than 10,000 vehicles per day for each traffic direction, with a percentage of heavy-goods vehicles (HGV) slightly less than 5%. The speed limit for vehicles is 50 km/h.

The scenario under congested traffic is assumed as follows: an HGV collides at high speed into the last vehicle (an HPV) in a queue, at the tunnel centre (600 m from the exit), blocking both lanes of the tube. In each lane of the tube, 72 cars (carrying two persons per car, in total

72×2=144 persons) are assumed to queue up and stop, maintaining a minimum distance from the vehicle in front of about 2 m, up to the tunnel downstream portal, which is reached by the queue after about 10 min from the accident. People caught up in the traffic jam downstream of the HGV can be considered as being unable to leave the tunnel by car. From the middle of the tunnel length, the maximum distance to walk to reach exit B is 600 m. It is assumed that the vehicle has two onboard storage tanks, whereas only the rupture on the larger tank of 62.4 L, NWP=70 MPa (Yamashita *et al*., 2015) is considered. Considering the onboard hydrogen tank's state of charge (SoC) will normally not be 100% (immediately after fuelling), but rather 40% on average (Mattelaer, 2020) after driving before refuelling, the value of SoC=40% (giving tank pressure of 24.4 MPa at 20°C, as calculated using Abel-Noble real gas EoS) is selected for the consequence analysis.

The event tree analysis for the case study of the Varano tunnel is reported in Figure 6-6. For the calculation of the probability of different scenarios, an average tunnel accident rate of 0.46 per 10^6 vehicle-km is used as reported by ANAS (2009) for Italian tunnels, and an average fire rate of 5.6×10^{-3}per 10^6 vehicle-km as reported by PIARC (2017) for tunnels in Italy. The latter corresponds to a probability that an accident in tunnels results in a fire of 1.2%. For all the other branches of the event tree, the probability values are those available from literature, as detailed in the HyTunnel-CS deliverable D5.3 (2022).

Figure 6-6. Event tree for crash scenarios involving hydrogen vehicles (case of SoC=100%) in Varano road tunnel (case of localised fire).

The results of the analysis show that the most likely consequence includes scenarios with no release of hydrogen (3.6 events per year) or hydrogen release without ignition (0.36 events per year). When the hydrogen does ignite, it is most likely a jet fire from the hydrogen system (4.2×10^{-2} events per year) rather than from a TPRD (1.2×10^{-3} events per year for SoC=100% and 4.4×10^{-4} events per year for SoC=40%). If a hydrogen-air flammable cloud is accumulated under the ceiling, it is more unlikely that deflagration of the cloud occurs (5.8×10^{-4} events per year for SoC=99% and 2.2×10^{-4} events per year for SoC=40%).

In the presence of a localised fire, if the TPRD is not affected by a fire or engulfing fire, and fails to open, or is blocked from a fire during an incident, the catastrophic hydrogen tank rupture is the most likely scenario (6.8×10^{-4} events per year). For this worst-case tunnel scenario, the

overpressures along the tunnel at different distances from the tunnel centre, where an accident occurs, are calculated using the universal correlation for the blast wave decay after a hydrogen tank rupture in a tunnel fire (Molkov and Dery, 2020). The probability of fatality at different distances from the tunnel centre is predicted using the Probit function from LaChance *et al.* (2011). The individual risk is then calculated by multiplying the frequency of the tank rupture and the probability of fatality along the tunnel length (Figure 6-7).

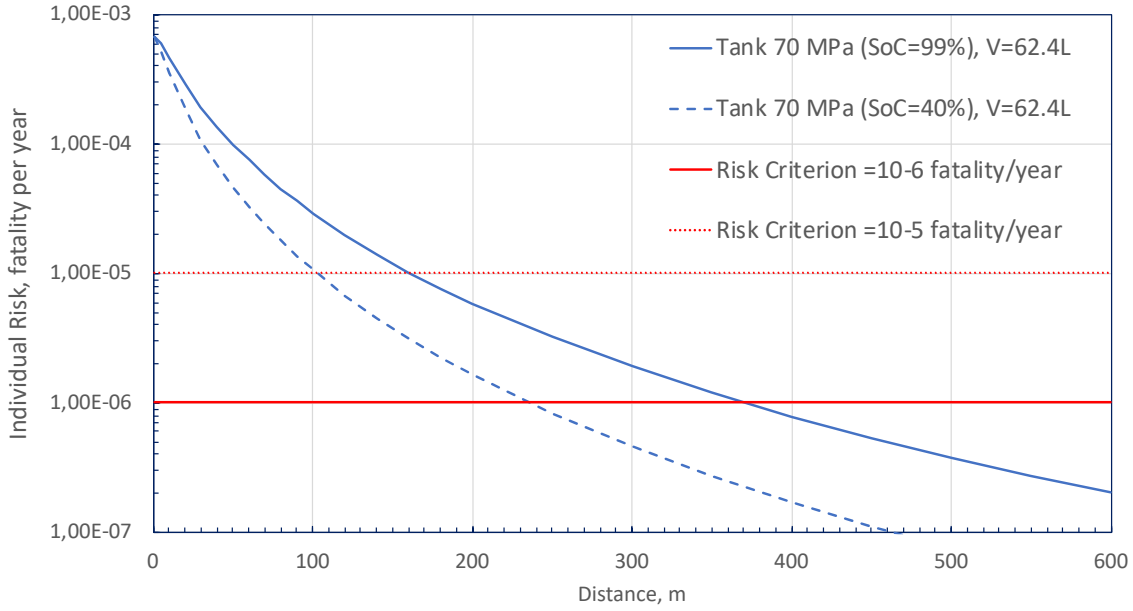

Figure 6-7. Individual risk vs. distance from the tunnel centre in the case of H_2 tank rupture (localised fire) (tank of 62.4 L: SoC=99% and SoC=40%)

The individual risk is in the range of 6.8×10^{-4} to 1.0×10^{-5} fatality per year up to a distance from the tunnel centre of 160 m for SoC=99% and of 100 m for SoC=40%.

Assuming a risk acceptance criterion of 10^{-6} fatality per year, a fatality hazard distance of 375 m and 240 m is evaluated for SoC=99% and SoC=40%, respectively. These distances correspond respectively to a queue of 52 and 33 cars for each lane, and assuming an occupancy of 2 people per car, respectively 103 and 66 fatalities.

On the other hand, using as risk acceptance criterion of 10^{-5} fatality per year, for firefighters, the hazard distances are 160 m and 100 m for SoC=99% and SoC=40%, respectively. Correspondingly, the number of cars in the queue for each lane is 22 and 14, and the fatalities 44 and 28, respectively.

These hazard distances are significantly higher than the no-harm distance calculated in the case of a hydrogen jet fire from TPRD of 15-25 m for SoC=40-100% (Molkov, 2012).

With respect to damage to the equipment and cars in the tunnel, the overpressure reached in the accident location is higher (657 kPa) than the threshold value of 200 kPa to crush cars up to 5 m from the tunnel centre (SoC=99%).

The probability of failure of the tunnel structure is evaluated at different distances from the tunnel centre using the Eisenberg model (American Institute of Chemical Engineers, 1998). The Eisenberg Probit provides as a result, a probability of tunnel failure of 100% up to a distance of 50 m and 30 m from the tunnel center for SoC=99% and SoC=40%, respectively, which

decreases to 50% probability of failure at a distance of 154 m and 98 m respectively for SoC=99% and SoC=40%.

In the case of hydrogen release and accumulation under the ceiling, four cases of hydrogen cloud formation in a tunnel cross-section were analysed for car and bus incidents, as shown in

Figure 6-8:

- Case 1: Uniform hydrogen concentration distributed over the full tunnel cross-section for the given hydrogen inventory;
- Case 2: Uniform hydrogen concentration distributed inside a layer of hydrogen-air mixture for the given hydrogen inventory;
- Case 3: Stratified layer of hydrogen-air mixture for the given hydrogen inventory; and
- Case 4: Stratified hydrogen-air mixture filling the whole tunnel cross-section for the given hydrogen inventory.

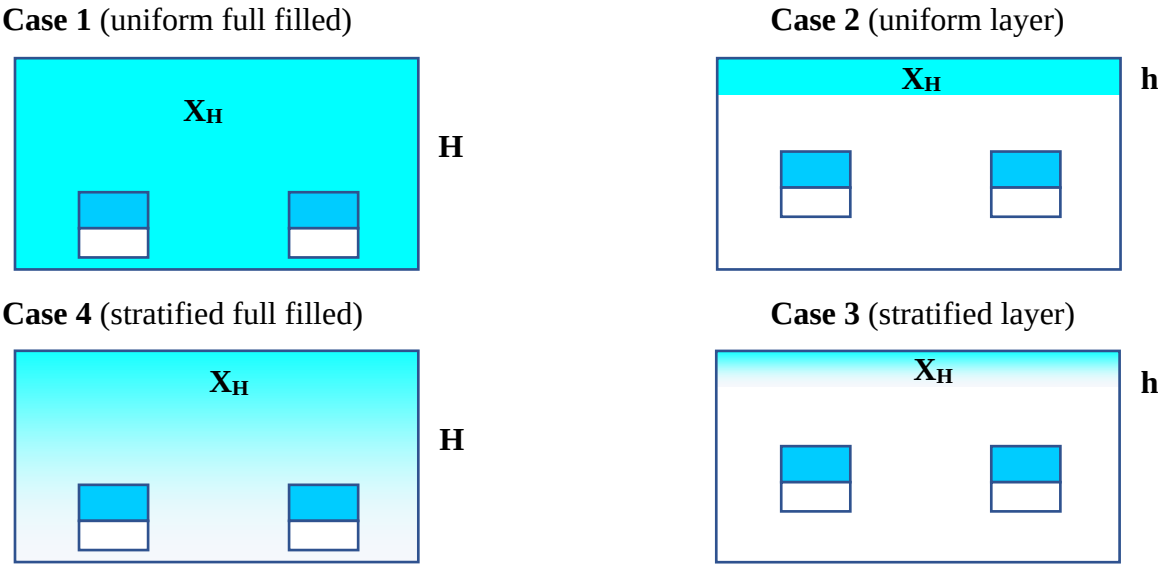

Figure 6-8. Hydrogen distribution profiles in a tunnel.

If a hydrogen cloud is ignited after a delay, a deflagration or DDT may occur. The evaluation of flame propagation and eventual DDT is performed by the method of flame propagation regime evaluation developed by KIT which is based on the so-called sigma-criterion for flame acceleration, lambda criterion and run-up distance criterion for detonability evaluation. A detailed description of the method is reported in Appendix A3.2.4.

Different amounts of hydrogen inventory from 2.48 kg for a car accident and to 41.64 kg for a bus accident could lead to different size of hydrogen-air flammable cloud. The traffic and hydrogen cloud characteristics considered in the model are reported in

Table 6-1 and

Table 6-2; as well as Table 6-3 and Table 6-4 for car accidents (I) and bus accidents (II), respectively.

Table 6-1. Traffic characterisation for car accidents (I)

Title	Value	Units
Cars in queue lane 1	125	-
Cars in queue lane 2	125	-
Car density	10000	vehicles/day
Car height	1.7	m
Car width	1.8	m
Car cross-sectional area	3.06	m2
Car length	6	m
Parking distance	2	m
Distance between cars (front to front)	8	m
Blockage ratio BR (single lane)	0.052987	-
Blockage ratio BR (double lane)	0.105974	-

Table 6-2. Hydrogen cloud characterisation for car accidents (I)

Title	Value	Units
Tank pressure	700	bar
Hydrogen inventory cars	62.4	litre
Mass of hydrogen	2.48	kg
Volume of hydrogen (STP conditions)	30.0	m^3

Table 6-3. Traffic characterisation for bus accidents (II)

Title	Value	Units
Buses in queue lane 1	1	-
Buses in queue lane 2	1	-
Bus height	3.1	m
Bus width	2.5	m
Bus cross-sectional area	7.75	m^2
Bus length	12	m
Parking distance	2	m
Distance between buses (front to front)	14	m
Blockage ratio BR (single lane)	0.1342	-
Blockage ratio BR (double lane)	0.2684	-

Table 6-4. Hydrogen cloud characterisation for bus accidents (II).

Title	Value	Units
Tank pressure	350	bar
Number of tanks	8	tanks
Hydrogen inventory buses	200	Litre/tank
Mass of hydrogen	41.64	kg
Volume of hydrogen (STP conditions)	503.5	m^3
TPRD vent size	5	mm

Table 6-5 shows the calculated release time for the car accident in a tunnel depending on TPRD orifice diameter from 1 mm to 5 mm in the event of an accident (speed of sound 1909 m/s).

Table 6-5. Calculated hydrogen release time for tank 70 MPa, 62.4 L.

TPRD orifice diameter, mm	**1**	**2**	**3**	**5**
Characteristic release time, t_{ch}, s	41.6	10.4	4.6	1.7
Total release time, *t*, s	166	42	18	6.7

Table 6-6 shows the calculated release time for the bus accident in a tunnel depending on TPRD orifice diameter from 1 mm to 5 mm. The difference from the previous Table *6-5* is the hydrogen tank volume and pressure (speed of sound 1614 m/s).

Table 6-6. Calculated hydrogen release time for tank 35 MPa, 200 L

TPRD orifice diameter, mm	**1**	**2**	**3**	**5**
Characteristic release time, t_{ch}, s	157.8	39.4	17.5	6.3
Total release time, *t*, s	631	158	70	25

The case of hydrogen car accident in a tunnel with tank of 70 MPa and TPRD=5 mm was numerically simulated using GASFLOW-MPI CFD code (Li *et al.*, 2019, 2021). A semiconfined layer of hydrogen-air mixture at the ceiling of the tunnel of about 1 m thickness is formed in 4 s (Figure 6-9a and Figure 6-9b, snapshots 1 s and 4 s) without any tunnel ventilation i.e. a still atmosphere, velocity of 0 m/s. (stagnant air gives a conservative case). Then, it develops along the ceiling at almost constant thickness of 1m with longitudinal velocity starting from 2 m/s and approaching the velocity of 0.3 m/s after 8 s (Figure 6-9c, snapshot 8 s). In parallel, the average hydrogen concentration reduces inversely proportional to the time. At time 16 s (Figure 6-9d), a layer of 25-m length will be formed in the tunnel with a maximum hydrogen concentration of 15-20% vol. at the ceiling (Li *et al.*, 2019, 2021).

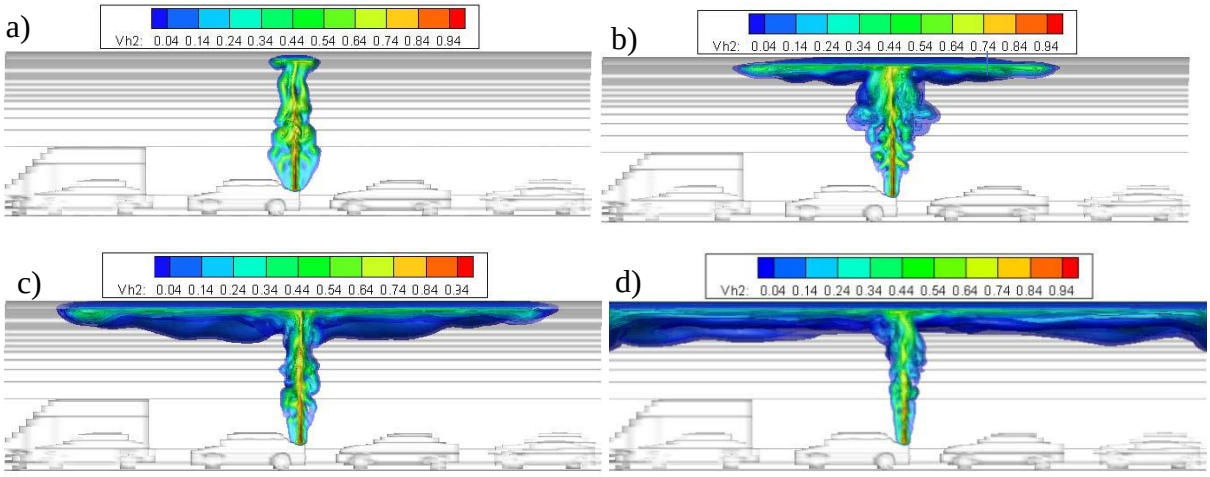

Figure 6-9. Hydrogen distribution profiles in a tunnel vs. time after release: a) 1 s; b) 4 s; c) 8s; d) 16 s

The model allows the evaluation of the possible flame propagation regimes of the hydrogen-air cloud formed by the release of 2.48 kg and 41.64 kg of hydrogen in the four defined cases of hydrogen release and distribution profile in the tunnel. Five levels of average hydrogen mole

fraction in the cloud (cases 1 and 2) and five levels of maximum hydrogen mole fraction at the top of the cloud (cases 3 and 4) from 10% to 30% vol. of hydrogen were analysed.

The results of the flame propagation and DDT modelling are summarised as follows:

- The two scenarios (**case 1 and case 4**) for fully filled tunnel cross-section with a hydrogen-air mixture are more likely for a very short release time. In both cases the length of the cloud is not sufficient for flame acceleration to the speed of sound and transition to detonation. The flame propagates comparatively slowly, with maximum combustion overpressure not higher than 0.1-0.2 MPa. Note that this was a preliminary simulation case that assumed a very large TPRD diameter and 0m/s tunnel air velocity, which may not be representative of reality.
- The two scenarios (**case 2 and case 3**) for formation of a layer of hydrogen-air mixture are more likely for relatively longer release time of the order of 10 s. In both cases the length of the cloud is much longer and can be enough for flame acceleration to the speed of sound and detonation only in the case of bus accident if hydrogen concentration of 20-30% vol. is assumed.
- For all car accidents, there is no scenario of hydrogen release with formation of detonable cloud. The flame propagates comparatively slowly with a maximum deflagration overpressure not higher than 0.1-0.2 MPa.
- Figure 6-9 shows that if the simulations of release are then performed, the realistic hydrogen concentration is likely to be lower than 15-20% vol. Thus, it makes the detonation scenario impossible even for the bus accident. An earlier ignition also prevents elongated cloud formation leading to detonation.
- Ventilation in a tunnel also facilitates the reduction of the maximum hydrogen concentration below 15% vol. and thus prevents the detonation for the considered car and bus incidents scenarios.

6.2.3 QRA of hydrogen train in a rail tunnel: the Severn rail tunnel (UK)

To illustrate the application of the proposed QRA methodology to rail tunnels, the Severn rail tunnel in the UK is analysed. Data for the UK rail network in the year 2018/19 reporting period (01/04/18-31/03/19) indicate that in this period there were 220,711 freight train movements. There were also 7,566,972 passenger trains nationally, giving a total of 7,787,683 trains on the UK rail network (Office of Rail and Road, 2019). The Severn rail tunnel is a double bore tunnel, 7.0 km long, 7.9 m wide and 6.1 m high. The tunnel has a horseshoe cross-section. The annual average daily traffic (AADT) is 72 trains per day for each traffic direction.

The scenario analysed considers a train accident at the tunnel entrance. It is assumed that the train has different onboard storage tanks, whereas only one tank of 160 L, NWP=35 MPa ruptures. The tank is considered to be equipped with a TPRD 5 mm-orifice size. The onboard hydrogen tanks may have different SoC, but for a conservative estimation only 99% (immediately after fuelling) is selected for the consequence analysis. Typical passenger occupancy is around 148 passengers per train. The train length is assumed to be three cars (64 m). The peak passenger load at rush hour is around 304 passengers (Office of Rail and Road, 2019).

Statistics from the International Union of Railways (UIC) is used for the analysis (UIC, 2021). In 2020 an average accident rate of 0.62 per 10^6 train-km is reported for a total number of 6122×10^6 train-km, but only 0.4% of the accidents occurred in tunnels, hence a tunnel accident rate of 2.3×10^{-3} per 10^6 train-km is calculated. The probability that an accident in tunnels results in a fire is 7%, i.e. 1 fire in 14 incidents in tunnels (UIC, 2021). For all the other branches the

probability values are those available from the literature as detailed in (HyTunnel-CS, D5.3, 2022).

The event tree for crash scenarios involving a hydrogen train in the Severn Tunnel (localised fire) is reported in *Figure 6-10*. The results of the analysis show that the most likely consequence includes scenarios with no release of hydrogen (7.7×10^{-4} events per year) or hydrogen release without ignition (1.2×10^{-4} events per year). When the hydrogen does ignite, it is most likely a jet fire from the hydrogen system (1.3×10^{-5} events per year) or a TPRD (6.3×10^{-6} events per year for SoC=99%) [LaFleur *et al.* (2017), Aarskog *et al.* (2020)]. In the presence of a localised fire, if the TPRD fails to open, the catastrophic hydrogen tank rupture is the most likely scenario (1.7×10^{-6} events per year).

For this scenario, the individual risk is then calculated by multiplying the frequency of the tank rupture and the probability of fatality along the tunnel length (Figure 6-11. Individual risk vs. distance in Severn Tunnel for the tank of 160 L at 35 MPa: SoC=99%). Risk numbers are relatively lower than those of road tunnels, due to the very low number of accidents that occur in rail tunnels with respect to road tunnels. The individual risk is in the range of 1.7×10^{-6} -1.0×10^{-6} fatality per year up to a distance from the tunnel portal of 12.5 m (SoC=99%) which is below the acceptance criterion of 10^{-5} fatality per year proposed by (EIHP2, 2003). On the contrary, assuming a risk criterion of 10^{-6} fatality per year a fatality hazard distance of 12.5 m is evaluated (SoC=99%). This hazard distance is lower than the no-harm distance calculated in the case of a hydrogen jet fire released from TPRD, i.e. 45 m for SoC=100% (Molkov, 2012). Assuming the train length is three cars, 64 m long, typical passenger occupancy is around 148 passengers per train, and at peak times the maximum passenger load is around 304 passengers (Lipscomb, 2021), the number of potential victims is 30 with a maximum of 59. Furthermore, if it is assumed that another train is traveling in the tunnel in the opposite lane, the number of fatalities could be double (60 with a maximum of 118). Regarding the probability of failure of the tunnel structure as a result of a catastrophic rupture of the hydrogen tank, it is estimated equal to 20% at the tunnel entrance.

Initiating Event										
Tunnel accident per million vehicle km	Does the accident cause a fire post crash?	Is H2 released from the system?	Is the fire estinguished on time?	Is H2 released from the TPRD?	Does the H2 ignite?	Is the H2 ignition delayed ?	Branch Frequency (per million vehicle km)	Event chain	Consequences	UK Rail Tunnel "Severn" Frequency (per year)
		0.9					2.09E-03	A	No H2 is released	7.70E-04
		no H2 released								
	0.930									
	no fire									
					0.853		1.98E-04	B	H2 is released but is not ignited until concentration dropped below LFL	7.30E-05
					no ignition					
		0.1								
		H2 released								
						0.667	2.28E-05	C	H2 is released and ignited immediately ->jet deflagration followed by jet fire	8.38E-06
						immediate				
					0.147					
					ignition					
						0.333	1.14E-05	D	H2 is released and has a delayed ignition-> deflagration of turbulent jet and possible deflagration of cloud under the ceiling (if created), flowed by jet fire	4.19E-06
0.0025						delayed				
Crash in tunnel										
			0.00				0.00E+00	E	No H2 is released	0.00E+00
			yes	no						
		0.9								
		no H2 released		0.030						
							4.73E-06	F	Catastrophic rupture of the H2 tank->blast wave, fireball and projectiles	1.74E-06
				TRPD failure to open						
			1.00							
			no							
					0.800		1.22E-04	G	H2 is released but is not ignited	4.50E-05
					no ignition					
				0.970						
				TRPD activation						
						0.667	2.04E-05	H	H2 is released by TPRD and ignited immediately ->turbulent jet deflagration followed by jet fire (if TPRD designed to exclude the flame blow-off)	7.50E-06
						immediate				
					0.200					
	0.070				ignition					
						0.333	1.02E-05	I	H2 is released by TPRD ignited with a delay -> possible turbulent jet deflagration and/or flammable cloud deflagration under the ceiling (if created) and DDT	3.74E-06
	fire					delayed				
						0.667	1.17E-05	j	H2 is released and ignited immediately ->jet deflagration followed by jet fire	4.29E-06
						immediate				
		0.1			1					
		H2 released			ignition					
						0.333	5.83E-06	K	H2 is released and has a delayed ignition-> deflagration of hydrogen jet that can be or not followed by deflagration of flammable cloud under the ceiling (depends on TPRD diameter and release location and orientation).	2.14E-06
						delayed				

Figure 6-10. Event tree for crash scenario involving a hydrogen train (SoC=100%) in Severn railway Tunnel (localised fire)

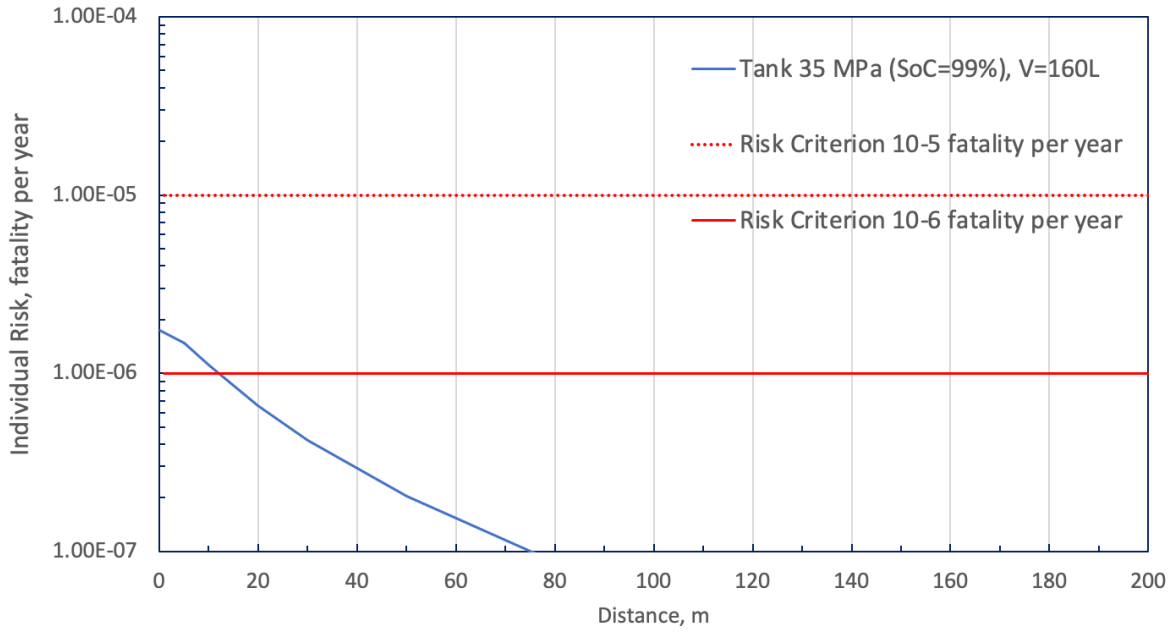

Figure 6-11. Individual risk vs. distance in Severn Tunnel for the tank of 160 L at 35 MPa: SoC=99%

In the event that hydrogen is released from the TPRD, but it is not immediately ignited, a cloud can form under the ceiling and if it is ignited with delay, a deflagration or DDT may occur (3.7×10^{-6} events per year).

The scenario of transition from deflagration to detonation in a narrow space between the train and tunnel was considered. The evaluation of flame propagation and eventual DDT is performed using the flame propagation regime evaluation method developed by KIT. A detailed description of the method is reported in Appendix A3.2.4.

Two UK rail tunnels (i.e. Severn and Channel) with a different cross-section area were analysed (*Table 6-7*). The hydrogen inventory of train and of single tank are shown in

Table 6-8.

Table 6-7. Dimensions of UK rail tunnels

	Tunnel Description	Cross-sectional Area, CSA (m^2)	Real Diameter, D (m)	Equivalent Diameter, D (m)
1	Severn tunnel, two rail	60.0	7.93	8.74
2	Channel tunnel single rail	53.5	7.6	8.25

Table 6-8. Initial hydrogen inventory, mass flow rate and discharge time for train

Vehicle	Total Vehicle Inventory (kg)	Single Tank Inventory (kg)	Initial mass flow rate (kg/s)	Discharge time (sec)	Cross-section area (m^2)
Train 1 (350 bar)	96.0	4.14	7.85	67	10.7
Train 2 (350 bar)	105.0	5.80	5.89	97	13.9

In the analysis the following four cases were considered for different hydrogen clouds (i.e. with uniform hydrogen concentration and linear hydrogen concentration gradient) in a tunnel cross section:

Case I:

- Single rail tunnel of two-tubes tunnel with a circular cross-section 64.3 m^2
- Equivalent diameter Deq=8.98 m
- Tunnel roughness equivalent to BR = 1% which is equal to 2.2 cm of roughness.
- Hydrogen inventory 5.8 kg due to the accident, then cloud formation with a late ignition.
- Uniform hydrogen-air mixture of 10 to 30%H_2 in air filled a layer of h=0.6 m thick above the train. The cloud is formed in a gap between the roof of the train and the ceiling (*Figure 6-12*a).

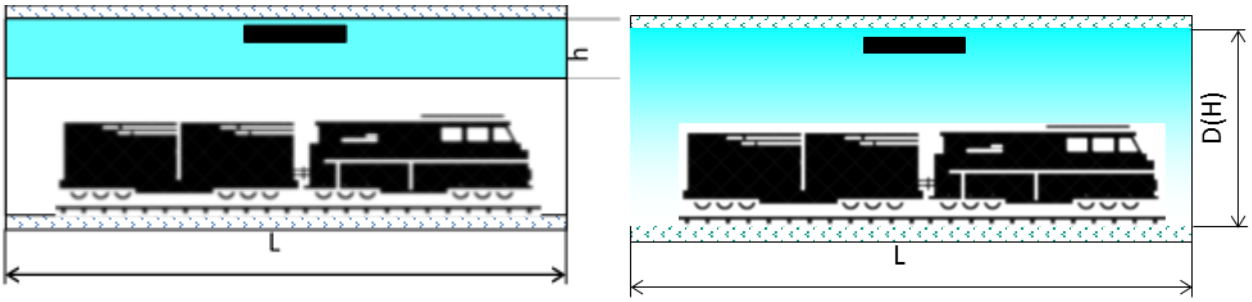

(a) (b)

Figure 6-12. Hydrogen cloud geometry: a layer of uniform hydrogen-air mixture (a); fully filled tunnel cross-section with a stratified hydrogen-air mixture (b).

Case II:

- Single rail tunnel of two-tubes tunnel with a circular cross-section 64.3 m^2
- Equivalent diameter Deq=8.98 m
- Tunnel blockage by the train is equivalent to BR = 40%.
- Hydrogen inventory 5.8 kg due to the accident, then cloud formation with a late ignition.
- Stratified hydrogen-air mixture filled the whole tunnel cross-section
- A linear hydrogen concentration gradient with maximum concentration 10, 15, 20, 25, 30% H_2 at the ceiling and 0% H_2 at the bottom of the tunnel is assumed (*Figure 6-12*b).

Case III:

- Single rail tunnel of two-tubes tunnel with a circular cross-section 53.5 m^2.

- Equivalent diameter Deq=8.25 m.
- Tunnel blockage by the train is equivalent to BR = 40%.
- Hydrogen inventory 10 kg due to the accident, then cloud formation with a late ignition.
- Stratified hydrogen-air mixture filled the whole tunnel cross-section.
- A linear hydrogen concentration gradient with maximum concentration 10, 15, 20, 25, 30% H_2 at the ceiling and 0% H_2 at the bottom of the tunnel is assumed (*Figure 6-12*b).

Case IV:

- Single rail tunnel of two-tubes tunnel with a circular cross-section 53.5 m^2.
- Equivalent diameter Deq=8.25 m.
- Tunnel blockage by the train is equivalent to BR = 40%.
- Hydrogen inventory 100 kg due to severe accident, then the cloud formation with a late ignition.
- A stratified hydrogen-air mixture filled the whole tunnel cross-section.
- A linear hydrogen concentration gradient with maximum concentration 10, 15, 20, 25, 30% H_2 at the ceiling and 0%H_2 at the bottom of the tunnel is assumed (*Figure 6-12* b).

In summary, the results show that:

- Independent of hydrogen inventory, for maximum hydrogen concentration of 10 and 11% H_2 the flame cannot accelerate to the speed of sound. It will propagate as a slow subsonic flame with a maximum combustion over-pressure 1-2 bar.
- Independent of maximum hydrogen concentration at the ceiling, for hydrogen inventories 5.8 and 10 kg only a slow subsonic flame with a maximum combustion over-pressure 1-2 bar may develop because the size of the cloud is too small.
- Only in the case **IV** for 100 kg of hydrogen inventory will the size of the cloud be sufficient for flame acceleration and detonation onset at maximum hydrogen concentration above 15%. Then, it needs the ventilation to keep the hydrogen concentration below 15% to prevent detonation.

6.2.4 QRA of hydrogen vehicles in an underground car park

The risk of a typical underground car park in Denmark is assessed as follows. Many different variants of such car parks exist with various sizes and car capacities (Nørregaard *et al.*, 2022). Larger car parks have several decks for parking cars.

The case from the road tunnel scenario is applied in the following, with some adaptations to a scenario where hydrogen cars are parking in an underground parking. While accident scenarios involve severe collisions in road tunnels, the situation in a car park is different due to the very low speeds of the vehicles in such an infrastructure. Also, only personal cars and smaller vans are expected to park in an ordinary car park. Nevertheless, vehicles still may self-ignite due to technical defects or may be ignited due to arson.

Fires in car parks are not very frequent and the vast majority are only involving a few cars (up to 7) (Tohir and Spearpoint, 2014). There have been very big car park fires reported involving

many cars (e.g. Liverpool, Stavanger airport). The dynamics of these very big and complex fire scenarios have not yet been analysed, with regards to the behavior and potential safety risks for hydrogen vehicles. Due to the great complexity of the involved scenarios for such big car park fires, in this QRA only single and multiple (1-7) burning cars are included in the ETA.

The fire incident statistics used for the case study are based on the approach made by (Li and Spearpoint, 2007) and refined by (Tohir and Spearpoint, 2014). The prediction of the fire frequency of a vehicle per year in a car park (2.76×10^{-6} $year^{-1}$ for the period from 1995–2012) is based on national fire statistics in New Zealand. The vehicle exchange rate of a large parking facility is calculated and scaled by an estimated total amount of public parking booths of 200,000 in New Zealand. They determined the frequency *f* as fires per vehicle visit using a car park and estimated the probability of a vehicle catching fire during a visit to car park buildings in New Zealand as 1.71×10^{-7}. In order to calculate the fire incidents, the following equation was developed by the authors:

$$F = f \cdot R \cdot \frac{A}{P}$$

f = 1.71×10^{-7} *vehicle fire frequency per vehicle visit*
R = annual usage ratio or turnover ratio
A = total floor area [m^2]
P = efficiency of parking (assumed 29 m^2 /space)
F = vehicle fire frequency per year

The vehicle fire frequency per year F is the Fire frequency per year depending on the cars per year using the respective car park. The calculated frequency assumes that cars mostly ignite within the first 20 min after arrival and by that, the number of arrivals and not the duration of parking is the determining parameter for vehicle fires.

The following event tree provides the results of a case study for the underground Danish car park Prismet in the town Århus (*Figure 6-13*). It has an area of 2144 m^2 and 58 parking slots giving a parking efficiency P = 37 m^2/car, which is close to the value found by Spearpoint (2007) reporting 29 m^2/car. It is also in line with the general tendency that car parks are cost-benefit optimised. Assuming a scenario with longer term parking of the cars as it could be typical for a company car park, each slot is thought of being used by 583 different cars during a year. This results in 33841 cars using this car park during a year and the corresponding vehicle fire frequency F is 0.006 fires per year.

ETA for FCEV in undergroud car parking

smaller car park without sprinklers	Danish example	area [m2]	capacity cars	efficiency P	turn over R	cars per year	F [year-1]
	P-kælder under prismet Århus	2144	58	37	583	33841	0,0058

Initiating Event

Fires per 33841 cars per year in car park	Fire spreads to neighboring cars	Is the fire extinguished in time?	Is H2 released from the TPRD?	Does the H2 ignite?	Is the H2 ignition delayed ?	Frequency	Event chain	Consequences
		0,48				3,94E-04	E	No H2 is released
		yes	no					
	0,142							
	2 to 7 cars on fire				0,333	8,99E-06	I*	H2 from 1 - 7 cars is released by TPRD ignited with a delay -> possible turbulent jet deflagration and/or flammable cloud deflagration under the ceiling (if created) and DDT
				0,08	delayed			
				ignition	0,667	1,80E-05	H*	H2 from 1 -7 cars is released by TPRD and ignited immediately ->turbulent jet deflagration followed by jet fire (if TPRD designed to exclude the flame blow-off)
			0,79		immediate			
			TPRD activation of a single car out of 7 cars					
				0,92	yes	3,11E-04	G*	H2 from 1 - 7 cars is released but is not ignited
		0,52		no ignition				
		no						
0,006								
Fires			0,21			8,97E-05	F*	Catastrophic rupture of 1 - 7 H2 tanks->blast wave, fireball and projectiles
			TPRD failure to open of a single car out of seven cars					
			OR gate --> sum of P(1) for 7 cars = 0.03 *7					
		0,48				2,38E-03	E	No H2 is released
		yes	no					
	0,858							
	1 car on fire				0,333	6,67E-05	I	H2 is released by TPRD ignited with a delay -> possible turbulent jet deflagration and/or flammable cloud deflagration under the ceiling (if created) and DDT
				0,08	delayed			
				ignition	0,667	1,34E-04	H	H2 is released by TPRD and ignited immediately ->turbulent jet deflagration followed by jet fire (if TPRD designed to exclude the flame blow-off)
			0,97		immediate			
			TPRD activation					
				0,92		2,30E-03	G	H2 is released but is not ignited
		0,52		no ignition				
		no						
			0,03			7,75E-05	F	Catastrophic rupture of the H2 tank->blast wave, fireball and projectiles
			TPRD failure to open					
							K **)	H2 is released by activated TPRD's in far areas of car park because of heat convectionand (100 C limit). This possibly cause a delayed ignition-> deflagration of hydrogen jet that can be or not followed by deflagration of flammable cloud under the ceiling (depends on TPRD diameter and release location and orientation).

) remark: combinations of the event chains I, H*, G* and F* are likely to occure during a fire involving 3 to 7 cars

**) the typical carpark fires involve only a few cars. There are though reported very large carpark fires involving many more cars. This sceanrio is not modelled in this Event tree It possibly could add scenario K as a consequence.

Figure 6-13. Event tree for fires involving hydrogen vehicles in a car park

It was found that the most severe scenarios of catastrophic tank rupture (F/F*) and flammable cloud deflagration under ceiling /DDT (I/I*) are predicted with a frequency in the range 0.9×10^{-4} to 0.9×10^{-5} per year, which is a rather high occurrence and potentially above the localised individual risk acceptance criteria of 1×10^{-5} or 1×10^{-6} lethality per year. Usually, the number of people in a carpark is very low during an incident, due to immediate evacuation. To date, fire statistics report no lethality. Only in very few cases have people been harmed and a very low number of emergency personnel have been injured/lethally affected.

The scenarios of potential catastrophic rupture and deflagration need more detailed consideration as these may develop in a very short time, leaving very little time for safe egress of people from the car park. It should also be assessed in more detail whether the consequences of such explosions and the resulting blast waves will impact the structural integrity of the car parks, *etc*.

6.2.5 Recommendations from QRA on tunnels and underground parking fires

The risks with the largest consequences are shown to be scenarios leading to deflagration of a hydrogen flammable cloud (which could be eliminated by proper TPRD design) and tank rupture in a fire (which could be eliminated by using self-venting tanks, as previously described). The former scenario, i.e. deflagration, DDT or detonation, could happen when a TPRD of comparatively large diameter opens due to malfunction (i.e. TPRD activation without demand), or due to flame blow-off during a release from the TPRD, and the vessel's hydrogen is released into a tunnel or underground parking facility creating a flammable cloud that is ignited. The latter scenario could happen when the same TPRD does not activate in case of a thermal exposure (i.e. TPRD failure of activation on demand). In that case, the thermal exposure may lead to a catastrophic tank rupture followed by consequences such as blast waves, fireballs and projectiles. The initiating event could be a strong heat source like a vehicle fire of the hydrogen vehicle itself, another vehicle in close proximity to the hydrogen vehicle, or any external fire source, e.g. spill and ignition of combustible substances like gasoline or diesel.

Naturally, the common measures to prevent tunnel incidents and underground parking fires are crucial for the incident likelihood of all vehicles and the frequency of posterior starting fires[3]. Posterior fire here means fires that start at the posterior section/back of the car. Reducing the number and likelihood of posterior fires is thus a direct measure to reduce the likelihood of having an external fire source close to a hydrogen vehicle's pressure vessel[4]. Some of the common safety measures in any tunnel are, e.g. speed limits, sufficient separation distance between vehicles, proper traffic regulation, queue control, and others. Consequently, tunnels with one-directional traffic in each tube should be considered safer than bidirectional traffic tunnels.

Inherently safer vehicles designed to the state-of-the-art technology that is well- maintained alongside improvement of mentioned measures in underground transportation infrastructure, would provide better traffic safety for all vehicles and thus is the cornerstone of the safety provision of hydrogen vehicles. The worst-case incident scenario in a tunnel is assumed to be a collision of a heavy-duty vehicle at high speed into the last vehicle in a queue, followed by a fire

[3] Accident scenarios involve severe collisions in road tunnels and literature provide a 2% likelihood of posterior fire ignition (Otxoterena *et al*, 2020).
[4] The situation that a collision is directly leading to tank rupture is assumed here of negligible risk as these vessels have a very high strength and are built-in within the safety cell of a vehicle. This may though not be fully the case in certain traffic accidents involving heavy goods vehicles. Both are recommended to be investigated further in the future.

and hydrogen storage tank rupture. This 'new' typical for hydrogen storage tank hazard should be addressed to exclude incidents that could affect the public acceptance of the technology.

Whilst accident scenarios could involve severe collisions in road tunnels, the situation in underground parking is normally quite different, due to the very low speeds of the vehicles in such infrastructure. Also, only cars and small vans are expected to use ordinary underground parking. Nevertheless, vehicles may still self-ignite due to technical defects, or be ignited by an arsonist, *etc*. Fires in car parks are not very frequent and the vast majority are extinguished within a short time. The mitigation systems that are required for underground parking vary from country to country, depending on the size of the carpark. Mitigation measures are well established and include, e.g. fire compartments, fire ventilation, water sprinklers, *etc*. The existing European Regulations are rather old and may not sufficiently cope with the development of modern cars which tend to be more lightweight but with larger dimensions, whilst the parking spaces remain un-adapted accordingly. The vehicles have a certain distance to the neighbouring vehicles and only the burning vehicle's heat radiation is impinging the potential hydrogen vehicles body, while the pressure vessel is shielded due to the vehicle body unless the fire of a spill of combustible liquid is involved. It may be realistic to assume that only in the case where fire spreads to the hydrogen vehicle after a certain duration, the hydrogen tank could be exposed to a strong enough thermal impact. Here the reduction of distance between vehicles may be an important factor and may increase the likelihood of fire spread from car to car.

As previously mentioned, most car park fires involve only very few cars burning simultaneously, but there have been some very big car park fires involving many cars, e.g. Liverpool and Stavanger airport. The dynamics of these very big and complex fire scenarios have not yet been analysed thoroughly. These big fires may potentially simultaneously and remotely activate the TPRDs of several vehicles, resulting in a flammable hydrogen-air mixture/layer/cloud being created. In addition, the pressure vessels of several HPVs could be impacted by these large fires and with failure of activation on demand of the TPRDs, more than one tank may burst, resulting in an additional severe scenario to these very large car park fires.

The performed QRA shows that the likelihood of deflagration/DDT/detonation of large flammable cloud and tank rupture scenarios are closely linked with the designed parameters and failure rate on demand for the installed TPRDs. It has been established that a localised fire may more often than not, lead to a TPRD failure on demand compared with a fully engulfing vessel fire.

The regulated fire test protocol (GTR#13, R134) has two phases, where in the first phase a localised fire is simulated that does not directly expose the TPRD for 10 minutes. In the second phase, a fully engulfing vessel fire is established. For both phases of the fire test procedure, a vessel is directly impinged by the propane flames from a burner. This may be quite different from the real situation of a vehicle fire scenario described above. Some authors, therefore, have suggested testing the fire-resistance rating of pressure vessels and TPRD activation using additional shielding and a car mock-up. This is likely to provide much better input to a QRA analysis and the data needed for performance-based hydrogen safety engineering. It is therefore recommended to review the current practice, aiming to develop more refined fire tests for pressure vessels built into road vehicles.[5] It is expected that a pressure vessel should withstand any fire intensity and thus the design of the fire test burner and its specific heat release rate, HRR/A, should satisfy this important safety requirement.

[5] This may especially apply to vehicles such as cars with enclosed shielded pressure vessels. trucks and buses often have a pressure vessel on the roof and may be directly impacted by flames.

The reliability of the TPRDs is not reported sufficiently. There are only very limited literature data available in the FireCOMP risk assessment study (Saw *et al*., 2016) and the SANDIA publication (Erhart *et al*., 2019). These data are also not based on reliability measurements, but expert judgements comparing the TPRD with the reliability of a bursting disc. To add to this, TPRD technology can vary significantly. Consequently, any development in pressure vessel technology that may improve/assist TPRD activation in a localised fire should be investigated, e.g. UU's self-venting TPRD-less LNB storage tank design. This type of microleak-no-burst (μLNB) tank represents, by itself, distributed over the whole tank surface "TPRD". Other important recommendations include the reduction of the TPRD release diameter and its proper location and direction of release (design should be done for tank-TPRD system as a whole). The CFD studies have provided evidence that with TPRD diameters of fractions of 1 mm, there is likely to be no flammable cloud accumulation under the underground parking ceiling, and thus tunnels with higher ceiling heights. HyTunnel-CS developed and validated a model of thermal behaviour of an arbitrary tank-TPRD system in an engulfing fire that excludes its rupture (Molkov *et al*., 2021b). It must be stressed that the last is valid for engulfing fires only. It is recommended that at least generic data for different types of hydrogen storage tank-TPRD systems used in different hydrogen-powered vehicles should be published.

7. Other key HyTunnel-CS recommendations

7.1 Deliverable D6.10: Recommendations to the update of relevant RCS

A separate report (HyTunnel-CS, D6.10, 2022) is available with regards to recommendations to the update of relevant Regulations, Codes and Standards (RCS). The report also draws on the HyTunnel-CS studies that fed into this deliverable.

7.2 Deliverable D5.4: Harmonised recommendations for response and intervention strategies for first responders

The development of first responders' intervention strategies and tactics are not the primary objectives within the scope of this report. It is, however, covered separately in a deliverable prepared by partners led by the International Fire Academy (HyTunnel-CS, D5.4, 2022) using the conclusions and recommendations of this pre-normative research project.

8. References

(NB: the references listed here are for the main body of the report. Appendices will have their own respective list of references at the end of each appendix)

Aarskog F.G., Hansen O.R., Strømgren T., Ulleberg Ø., (2020). Concept risk assessment of a hydrogen driven high speed passenger ferry. IJHE 45, 1359-1372

American Institute of Chemical Engineers, 1998. Guidelines for evaluating the characteristics of vapor cloud explosions, flash fires, and BLEVEs, Center for Chemical Process Safety.

Amorim, D.L.N.F., Proenca, S.P.B., Florez-Lopez, J., Simplified modeling of cracking in concrete: Application in tunnel linings, Engineering Structures 70, 2014, pp. 23-35.

ANAS. *Linee Guida per la Progettazione Della Sicurezza nelle Gallerie Stradali Secondo la Normativa Vigente. Circolare* n.179431/2009.
https://www.stradeanas.it/sites/default/files/pdf/Linee_guida_sicurezza_gallerie_2009.pdf

ANSI/ ASHRAE Standard 62-1989, Ventilation for Acceptable Indoor Air Quality.

Arnau O., Molins C. (2011). Experimental and analytical study of the structural response of segmental tunnel linings based on an in situ loading test. Part 2: Numerical simulation. Tunnelling and Underground Space Technology, 2011, 26, pp. 778–788.

Arnau O., Molins C. (2012), Three-dimensional structural response of segmental tunnel linings, Engineering Structures, v.44, pp. 210-221.

Asadi I., Shafigh P., Abu Hassan, Bin Z. F., and Mahyuddin N. B. (2018). Thermal conductivity of concrete – A review. Journal of Building Engineering, 20, 81–93. https://doi.org/10.1016/j.jobe.2018.07.002

Average car and van occupancy England 2002-2018 Statistic. Statista. URL https://www.statista.com/statistics/314719/average-car-and-van-occupancy-in-england/ (accessed 10.12.21).

Baker W.E., Cox P.A., Kulesz J.J., Strehlow R.A. and Westine P.S. (1983), Explosion Hazards and Evaluation, Elsevier.

Ballesteros-Tajadura R., Santolaria-Morros C. & Blanco-Marigorta E. (2006). Influence of the slope in the ventilation semi-transversal system of an urban tunnel. Tunnelling and Underground Space Technology, 21(1), pp.21–28.

Bassan S. (2016). Overview of traffic safety aspects and design in road tunnels. IATSS Res. 40, 35–46.

Bernard-Michel G. and Houssin-Agbomson D., (2017) Comparison of helium and hydrogen releases in $1m^3$ and $2m^3$ two vents enclosures: Concentration measurements at different flow rates and for two diameters of injection nozzle, International Journal of Hydrogen Energy 42, 7542-7550.

Bontempi F., Malerba P.G., The role of softening in the numerical analysis of RC framed structures Structural Engineering & Mechanics 5(6), November 1997, DOI: 10.12989/sem.1997.5.6.785

Brennan S., Makarov D., Molkov V. (2011). Dynamics of flammable hydrogen-air mixture formation in an enclosure with a single vent. In D. Bradley, G. Makhviladze, & V. Molkov (Eds.), Proceedings of the Sixth Int. Seminar on Fire and Explosion Hazards, 11-16 April 2010, University of Leeds, pp. 493-503.

BS 7346-7:2013, BSI Standards Publication. Components for smoke and heat control systems– Part 7: Code of practice on functional recommendations and calculation methods for smoke and heat control systems for covered car parks. BSI Group, 31 August 2013.

Casey N. (2020). Fire incident data for Australian road tunnels, Fire Safety Journal 111, 102909.

Cavalaro S.H.P., Blom C.B.M., Walraven J.C., Aguado A. (2011), Structural analysis of contact deficiencies in segmented lining, Tunnelling and Underground Space Technology, v.26(6), 734-749.

Cirrone D., Makarov D., Molkov V. (2019), Cryogenic Hydrogen Jets: Calculation of Hazard Distances. International Conference on Hydrogen Safety, 24th-26th September 2019, Adelaide, Australia. Paper ID191.

Colombo C., Martinelli M., Di Prisco M. (2015) A design approach for tunnels exposed to blast and fire, Structural Concrete, v.16(2), pp. 262-272.

Crosti C., Olmati P. and Gentili F. (2012). Structural Response of Bridges to Fire After Explosion, Proceedings of the 6th International Conference on Bridge Maintenance, Safety and Management (IABMAS 2012), pp. 2017-2023, Stresa, Lake Maggiore, Italy, 8–12 July 2012.

Dadashzadeh M., Kashkarov S., Makarov D., Molkov V., (2018). Risk assessment methodology for onboard hydrogen storage. Int. J. Hydrogen Energy 43, 6462–6475. https://doi.org/10.1016/j.ijhydene.2018.01.195.

De Cesare V., Bontempi F., Van Wingerden K., Chillè F., Petrini F. (2010). Response against explosion loads, in electronic proceedings of Handling Exceptions in Structural Engineering: Structural Systems, Accidental Scenarios, Design Complexity Rome, July 8 and 9, 2010.

Deeny S.M., Stratford T., Dhakal R.P., Moss P.J., Buchanan A.H. (2008), Spalling of Concrete: Implications for structural performance in fire, Australasian Conference on Mechanics of Structure and Materials (ACMSM20), Toowoomba, Queensland, December 2008.

Directive 2004/54/EC Minimum Safety Requirements for Tunnels in the Trans-European Road Network.

DCLG Department for Communities and Local Government Publications London (UK) (2010), BD2552, 'Fire spread in car parks' Report, December 2010.

Du T., Yang D., Ding Y., (2018). Driving force for preventing smoke back-layering in downhill tunnel fires using forced longitudinal ventilation, Tunnelling and Underground Space Technology 79, 76–82.

e-Laboratory, The European Educational platform for Fuel cells and Hydrogen (https://fch2edu.eu/home/e-laboratory/, accessed 15 June 2021)

EIHP2 (2003), European Integrated Hydrogen Project – Phase II: Hydrogen Applications -Risk Acceptance Criteria and Risk Assessment Methodology, (http://www.eihp.org/public/Reports/Final_Report/Sub-Task_Reports/ST5.2/EHEC%20paper_final.pdf, accessed 28 July 2022)

EN1990. (2002). Eurocode 0 - Basis of structural design. Brussels, Belgium: *Comité Européen de Normalisation*.

Fan C.G., Li X.Y., Mu Y., Guo F.Y., Ji J., (2017). Smoke movement characteristics under stack effect in a mine laneway fire, Applied Thermal Engineering 110, 70–79.

Ehrhart B. D., Brooks D.M., Muna A.B. and LaFleur C.B., (2019). Risk Assessment of Hydrogen Fuel Cell Electric Vehicles in Tunnels. Fire Technology.

Ekoto I.W., Houf W.G., Ruggles A.J., Creitz W.L., Li J.X., (2012). Large-scale hydrogen jet flame radiant fraction measurements and modelling, Proceedings of the International Pipeline Conference, Calgary, Canada, September 24-28.

Ekoto I.W., Ruggles A.J., Creitz W.L., Li J.X., (2014). Updated jet flame radiation modelling with buoyancy corrections, Int. J. Hydrog. Energy, 39, 20570-20577.

FCH 2 JU (2021). Safety planning and management in EU hydrogen and fuel cells projects - guidance document. URL https://www.fch.europa.eu/ (accessed 26 October 2021).

Friedrich A., Grune J., Jordan T., Kotchourko A., Kotchourko N., Kuznetsov M., Sempert K., Stern G. (2007), Experimental study of hydrogen-air deflagrations in flat layer, Intl. Conf. on Hydrogen Safety, 11 – 13 September 2007, San Sebastian, Spain.

Giannissi S.G., Tolias I.C., Ebne Abbasi H., Makarov D., Grune, J., Sempert, K. (2021). Modelling of ventilated hydrogen dispersion in presence of co-flow and counter-flow, In 9th Int. Conf. on Hydrogen Safety, Edinburgh, UK, September 21-24 (online).

Grune J., Sempert K., Kuznetsov M., Jordan T. (2021). Hydrogen jet structure in presence of forced CO-, counter-and cross-flow ventilation, In 9th Int. Conf. on Hydrogen Safety, Edinburgh, UK, September 21-24 (online)

Hankinson G., and Lowesmith B.J. (2012), A consideration of methods of determining the radiative characteristics of jet fires, *Combust. Flame*, vol. 159, nº 3, p. 1165-1177, mars 2012, doi: 10.1016/j.combustflame.2011.09.004.

Hertz K.D. (2003), Limits of spalling of fire-exposed concrete, Fire Safety Journal 38, 103–116.

Hertz K. D., & Sørensen L. S. (2005). Test method for spalling of fire exposed concrete. Fire Safety Journal, 40(5), 466–476. https://doi.org/10.1016/j.firesaf.2005.04.001.

Hertz K.D. (2018): Design of Fire-Resistant Structures, ICE Publishing, 2019

HSE, Risk management: Expert guidance - Cost Benefit Analysis (CBA) checklist [https://www.hse.gov.uk/managing/theory/alarpcheck.htm]. Health Safety Executive (accessed 07 April 2022).

HSE, 2006. Response spectra for explosion resistant design and assessment. Research Report RR484, Prepared by Atkins MSL Engineering Limited for the Health & Safety Executive, 2006.

https://www.hse.gov.uk/managing/theory/alarpcheck.htm#footnotes (accessed 10 July 2021).

HyIndoor project (2014), Deliverable D5.1 "Widely accepted guidelines on Fuel Cell indoor installation and use" (https://www.researchgate.net/profile/Simon-Jallais/publication/302692394_Work_Package_5_Widely_accepted_guidelines_on_Fuel_Cell_indoor_installation_and_use_-_Hyindoor_-_Pre-normative_research_on_safe_indoor_use_of_fuel_cells_and_hydrogen_systems/links/5731fa2008ae9ace840475be/Work-Package-5-Widely-accepted-guidelines-on-Fuel-Cell-indoor-installation-and-use-Hyindoor-Pre-normative-research-on-safe-indoor-use-of-fuel-cells-and-hydrogen-systems.pdf, accessed 15 June 2021).

HyResponse (2015) D2.1. Description of selected FCH systems and infrastructure, relevant safety features and concepts.

HySafe, “Internal project on investigating the use of hydrogen vehicles in road tunnels, Deliverable D111, (Section 1.1), 15 April 2009” by European Network of Excellence HySafe (NoE HySafe).

HyTunnel-CS D1.1 (2019). Report on assessment of effectiveness of conventional safety measures in underground transportation systems and similar confined spaces.

HyTunnel-CS D1.2 (2019). Report on hydrogen hazards and risks in tunnels and similar confined spaces.

HyTunnel-CS D1.3 (2019). Selection and Prioritisation of Accident Scenarios

HyTunnel-CS D2.2. (2020). Intermediate Report on Analytical, Numerical and Experimental Studies.

HyTunnel-CS D2.3. (2022). Final report on analytical, numerical and experimental studies on hydrogen dispersion in tunnels, including innovative prevention and mitigation strategies.

HyTunnel-CS D3.1 (2020). Detailed Research Programme on Hydrogen fires in Confined Structures.

HyTunnel-CS D3.3 (2022). Final report on Experimental, Analytical and Numerical Studies on Thermal and pressure effects of hydrogen jet fires and structure integrity.

HyTunnel-CS D4.3 (2022). Final Report on Analytical, Numerical and Experimental Studies on Explosions, including Innovative Prevention and Mitigation Strategies.

HyTunnel-CS D4.4 (2022). Final Report on Blowdown Model, HSE jet fire and Scaled-tunnel Explosion Experiments: Results of the deferred experimental programme and associated activities.

HyTunnel-CS D5.3 (2022). Report on QRA methodology for tunnels and similar confined spaces.

HyTunnel-CS D5.4 (2022). Harmonised recommendations for response and intervention strategies for first responders

HyTunnel-CS D6.10 (2022). Recommendations to the update of relevant RCS.

IEA (2017). Energy Technology Perspectives 2017: Catalysing Energy Technology Transformations. https://iea.blob.core.windows.net/assets/a6587f9f-e56c-4b1d-96e4-5a4da78f12fa/Energy_Technology_Perspectives_2017-PDF.pdf

INERIS (2005a) Transport of Dangerous Goods Through Road Tunnels: Quantitative Risk Assessment Model (v. 3.60 and v. 3.61) - Reference Manual. Research Report N° 20504, 1 August 2005.

INERIS (2005b) Transport of Dangerous Goods Through Road Tunnels: Quantitative Risk Assessment Model (v. 3.60 and v. 3.61) - User’s Guide. Research Report N° 20504, 1 December 2005.

Ingason H., Li Y. Z. and Lönnermark A. (2015) Tunnel Fire Dynamics. New York, NY: Springer New York. doi: 10.1007/978-1-4939-2199-7.

International Organization for Standardization. (2015) ISO 13344:2015 Estimation of lethal toxic potency of fire effluents.

International Organization for Standardization. (2020). ISO 19880-1:2020 Gaseous hydrogen — Fuelling stations — Part 1: General requirements.

International Organization for Standardization. (1999). ISO 834-1:1999 Fire-resistance tests - Elements of building construction — Part 1: General requirements.

IStructE (2002), Design recommendations for multi-storey and underground car parks, The Institution of Structural Engineers.

Ji J., Wan H., Li K., Han J., Sun J., (2015). A numerical study on upstream maximum temperature in inclined urban road tunnel fires. International Journal of Heat and Mass Transfer 88, 516–526.

Kashkarov S., Li Z., Molkov V., (2020). Blast wave from a hydrogen tank rupture in a fire in the open: Hazard distance nomograms. Int. J. Hydrog. Energy 45, 2429–2446. https://doi.org/10.1016/j.ijhydene.2019.11.084

Koutsourakis, N. Tolias, I.C., Giannissi, S.G., Venetsanos, A.G. (2021). Numerical study of the effects of tunnel inclination and ventilation on the dispersion of hydrogen released from a car, In 9th Int. Conf. on Hydrogen Safety, Edinburgh, UK, September 21-24 (online).

Krarti M. & Ayari A., (2001). Ventilation for enclosed parking garages. ASHRAE J, vol. 43, 52-57.

Lach A., Gaathaug A.V., Vågsæther K. (2020), Pressure peaking phenomena: Unignited hydrogen releases in confined spaces – Large-scale experiments. International Journal of Hydrogen Energy 2020; Volume 45 (56) s. 32702-32712 USN

Lach A., Gaathaug, A.V. (2021a), Experimental work on hydrogen safety during accidental hydrogen releases in underground parking scenario. https://doi.org/10.23642/usn.14405903

Lach A., Gaathaug A.V. (2021b), Effect of Mechanical Ventilation on Accidental Hydrogen Releases – Large scale Experiments. *Energies* 2021; Volume 14(11), 3008; https://doi.org/10.3390/en14113008. Same paper also presented as part of Proceedings of 9th International Conference on Hydrogen safety (ICHS2021), pp.1000-1011.

Lach A., Gaathaug A.V. (2021c), Large scale experiments and model validation of Pressure Peaking Phenomena-ignited hydrogen releases, International Journal of Hydrogen Energy, Volume 46, Issue 11, 2021, Pages 8317-8328, ISSN 0360-3199, https://doi.org/10.1016/j.ijhydene.2020.12.015

Lach A.W., Gaathaug A.V. and Vågsæther K., Thermal effects from downwards hydrogen impinging jet flame – experimental results from high-pressure releases in a carpark, submitted to the 10th International Seminar on Fire and Explosion Hazards, 2022.

LaChance J.L. (2010), Progress in Risk Assessment Methodologies for Emerging Hydrogen Applications. In: Sixth international short course and advanced research workshop “Progress in hydrogen safety e regulations, codes, and standards”, 25-29 January 2010, Belfast, Northern Ireland, UK.

LaChance J., Tchouvelev A., Engebo A., (2011). Development of uniform harm criteria for use in quantitative risk analysis of the hydrogen infrastructure. Int. J. Hydrog. Energy 36, 2381-2388.

LaFleur C., Bran-Anleu G., Muna A. B., Ehrhart B.D., Blaylock M., Houf W.G., (2017). Hydrogen Fuel Cell Electric Vehicle Tunnel Safety Study, SANDIA Report SAND2017-11157.

Lipscomb, M., Private communication (2022).

Li Y., Spearpoint M., (2007). Analysis of vehicle fire statistics in New Zealand parking buildings, Fire Technology, 43(2), pp. 93–106.

Li Y., Xiao J., Zhang H., Breitung W., Travis J., Kuznetsov M., Jordan T., (2019). Analysis of transient hydrogen release, dispersion and explosion in a tunnel with fuel cell vehicles using all-speed CFD code GASFLOW-MPI. Proc. of the 8th International Conference on Hydrogen Safety (ICHS 8th) September 24-26, 2019, Adelaide (Australia), paper ID: #169, p. 1-12

Li Y., Xiao J., Zhang H., Breitung W., Travis J., Kuznetsov M., Jordan T, (2021). Numerical analysis of hydrogen release, dispersion and combustion in a tunnel with fuel cell vehicles using all-speed CFD code GASFLOW-MPI. Int. J. Hydrog. Energy 46, 12474-12486.

Makarov D., Kim Y., Kashkarov S., Molkov V., (2016). Thermal protection and fire resistance of high-pressure hydrogen storage, in: Eight International Seminar on Fire and Explosion Hazards (ISFEH8). Hefei, China.

Makarov D., Hooker P., Kuznetsov M., Molkov V. (2018) Deflagrations of localised homogeneous and inhomogeneous hydrogen-air mixtures in enclosures, Int. J. Hydrogen Energy, V.43, pp.9848-9869. https://doi.org/10.1016/j.ijhydene.2018.03.159.

Makarov D., Shentsov V., Kuznetsov M., Molkov V. (2018) "Pressure peaking phenomenon: Model validation against unignited release and jet fire experiments," Int. J. Hydrog. Energy, vol. 43, no. 19, pp. 9454–9469, https://doi.org/10.1016/j.ijhydene.2018.03.162.

Makarov D., Cirrone D., Shentsov V., Kashkarov S., Molkov V., Xu Z., Kuznetsov M., Venetsanos A., Giannissi S., Tolias I., Vågsæther K., Gaathaug A., Pursell M., Rattigan W., Markert F., Giuliani L., Sørensen L., Bernad A., Sanz Millán M., Kummer U., Brauner C., Russo P., van den Berg J., de Jong F., Van Esbroeck T., Van De Veire M., Bouix D., Bernard-Michel G., Kudriakov S., Studer E., Ferero D., Grune J., Stern G., (2021). Overview of first outcomes of PNR project HyTunnel-CS, in: International Conference on Hydrogen Safety (ICHS2021) "Safe Hydrogen for Net Zero. Edinburgh, UK.

Makarov D., Shentsov V., Kuznetsov M., Molkov V., (2021b). Hydrogen Tank Rupture in Fire in the Open Atmosphere: Hazard Distance Defined by Fireball. Hydrogen 2, 134–146. https://doi.org/10.3390/hydrogen2010008

Mannan S. (2005), Lee's Loss Prevention in the Process Industries.

Markert F. and Giuliani L. (2019) 'Hydrogen fueled car fire spread to adjacent vehicles in car parks', in International Conference on Hydrogen Safety, p. 12. Available at: https://hysafe.info/ichs2019/conference-papers-and-presentations/

Mattelaer V., 2020. Private communication, in: Toyota Europe.

Mcnamee R. J., & Jansson R. (2015). Fire Spalling of Concrete : Theoretical and Experimental Studies Fire Spalling of Concrete Theoretical and Experimental Studies. October 2013.

Mindeguia J.-C., Pimienta P., Carre H., & La Borderue C. (2009). Experimental study on the Contribution of Pore Vapour Pressure to the Thermal Instability Risk of Concrete. 1st International Workshop of Concrete Spalling Due to Fire Exposure, Leipzig.

Mogi T., Horiguchi S., 2009. Experimental study on the hazards of high-pressure hydrogen jet diffusion flames. Journal of Loss Prevention in the Processes Industries 22, 45–51.

Molkov V. (1996) Venting gaseous deflagrations, D.Sc. thesis, 1996.

Molkov V. (2012) Fundamentals of Hydrogen Safety Engineering. bookboon.com, free download online book: https://bookboon.com/en/fundamentals-of-hydrogen-safety-engineering-i-ebook; https://bookboon.com/en/fundamentals-of-hydrogen-safety-engineering-ii-ebook.

Molkov V. and Saffers J.-B. (2013), Hydrogen jet flames, 2013. International Journal of Hydrogen Energy, 38, 19, 8141–8158. https://doi.org/10.1016/j.ijhydene.2012.08.106

Molkov V., Makarov D., Kashkarov S. (2018) Composite Pressure Vessel for Hydrogen Storage. PCT International Application P119851PC00, WO 2018/149772 A1.

Molkov V. and Dery W., (2020). The blast wave decay correlation for hydrogen tank rupture in a tunnel fire, *Int. J. Hydrog. Energy*, vol. 45, no. 55, pp. 31289–31302, Nov. 2020, doi: 10.1016/j.ijhydene.2020.08.062.

Molkov V., Cirrone D., Shentsov V., Dery W., Kim W., Makarov D. (2021a). Dynamics of blast wave and fireball after hydrogen tank rupture in a fire in the open atmosphere. International Journal of Hydrogen Energy, 46:4644-4665. https://doi.org/10.1016/j.ijhydene.2020.10.211

Molkov V., Dadashzadeh M., Kashkarov S., Makarov D. (2021b) Performance of hydrogen storage tank with TPRD in an engulfing fire. International Journal of Hydrogen Energy.

Molkov V., Makarov D., Kashkarov S., European Patent Application No 18706224.5 "Composite Vessel for Hydrogen Storage", 2019.

Moodie K. and Rattigan W. (2021). HyTunnel: Basis of Safe Vessel Design & Safe Operation of Overall System.

Mukai S., Suzuki J., Mitsuishi H., Oyakawa K. & Watanabe S. (2005). CFD simulation of diffusion of hydrogen leakage caused by fuel cell vehicle accident in tunnel, underground parking lot and multi-story parking garage. In 19th Int. Technical Conf. on the Enhanced Safety of Vehicles (ESV), Washington D.C., June 6–9.

Musto M., Rotondo G., (2014). Numerical comparison of performance between traditional and alternative jet fans in tiled tunnel in emergency ventilation, Tunnelling and Underground Space Technology 42. 52–58.

National Highway Traffic Safety Administration (NHTSA), (2015). Traffic safety facts 2015: a compilation of motor vehicle crash data from the fatality analysis reporting system and the general estimates system.

Nørregaard K., Roed L. V., Skov S. M., (2022). *Analyse af brandsikkerhed i garageanlæg, oplag af litium-ion batterier og batterier til solcelleanlæg i bygninger*. Copenhagen, Denmark. Available at: https://bpst.dk/sites/default/files/2022-02/Analyse af brandsikkerhed i garageanlæg - Ved batterioplag og BESS 02_2022_01_14.pdf.

Office of Rail and Road (ORR), Passenger Rail Usage 2019-20 Q1, Published 3 October 2019, Passenger Rail Usage 2019-20 Q1 (orr.gov.uk) (accessed 10 July 2022)

Okamoto K., Watanabe N., Hagimoto Y., Chigira T., Masano R., Miura H., Ochiai S., Satoh H., Tamura Y., Hayano K., Maeda Y., Suzuki J. (2009) Burning behaviour of sedan passenger cars. Fire Safety Journal, V.44, pp.301–310. https://doi.org/10.1016/j.firesaf.2008.07.001

Otxoterena P., Björnstig U. and Lindkvist M. (2020) 'Post-collision fires in road vehicles between 2002 and 2015', Fire and Materials, 44(6), pp. 767–775. doi: 10.1002/fam.2862.

Park J., Yoo Y., Kim W. (2021), Analysis of effect of hydrogen jet fire on tunnel structure, Journal of Korean Tunnelling and Underground Space Association, 30 November 2021. 535-547, https://doi.org/10.9711/KTAJ.2021.23.6.535

Phan, L. T. (2008). Pore pressure and explosive spalling in concrete. Materials and Structures, 41, 1623–1632.

PIARC, (2008). Risk analysis for road tunnels, report 2008R02 of Technical Committee C3.3 Road tunnel operation.

PIARC, (2017). Tunnels Manual 2017R35EN Chapter 4.

Rijkswaterstaat & Efectis Nederland. (2020). Efectis-R0695:2020 - Fire testing procedure for concrete tunnel linings and other tunnel components. 46. http://efectis.com/wp-content/uploads/2016/07/RWSProcedureFireProtectionforTunnels.pdf

Road Tunnel Association (RTA), (2019). UK & Eire Road Tunnel Directory.

Rouilloux G., Znojek B., Klink G., Wadivkar O., Plastics. The Future Automakers and Chemical Companies, (2012). Plastics. The Future for Automakers and Chemical Companies (kearney.com)

Sautter P., Schäfer F., Dobeschinsky H. (2007), Feasibility Study concerning High-Speed-Railway-Lines in Norway, Conference in Lillestrøm, 5 November 2007.

Sauzedde F., Martin M., Forero D. and Studer E. (2021), Experimental devices of 2021 CEA tests HYTUNNEL-CS, 2021.

Saw J.L., Flauw Y., Demeestere E.M., Naudet V., Blanc-Vannet P., Hollifield K., (2016). The EU FireComp Project and risk assessment of hydrogen composite storage applications using bow-tie analysis. In: Hazards 26, Edinburgh UK.

Schefer R.W., Houf W.G., Williams T.C., Bourne B., Colton J. (2007) Characterization of high-pressure, underexpanded hydrogen-jet flames. Int. J. Hydrogen Energy 32, 2081–2093. https://doi.org/10.1016/j.ijhydene.2006.08.037

Schefer R.W., Houf W.G., Williams T.C. (2008), Investigation of small-scale unintended releases of hydrogen: momentum-dominated regime, Int. J. H_2 Energy 33, 2008, 6373-6384.

Schleich J., Cajot L., Pierre M., Brasseur M., Franssen J., Kruppa J., Joyeux D., Twilt L., Oerle J. V., Aurtenetxe G., (1999) Development of design rules for steel structures subjected to natural fires in closed car parks.

Seike M., Kawabata N., Hasegawa M. & Tanaka H. (2019). Heat release rate and thermal fume behavior estimation of fuel cell vehicles in tunnel fires. International Journal of Hydrogen Energy, 44(48), pp.26597–26608.

Shebeko Yu. N., Tsarichenko S.G., Yeremenko O. Y., Keller V.D., Trunev A.V. (1990) Combustion of lean hydrogen-air mixtures in an atomized water stream. Combustion Explosion and Shock Waves. Vol. 26(4), pp. 426-428.
https://link.springer.com/article/10.1007/BF00745082

Shentsov V., Makarov D., Molkov V. (2021). Effect of TPRD diameter and direction of release on hydrogen dispersion in underground parking, at the International Conference on Hydrogen Safety, Edinburgh, UK. Paper ID88.

Simulia (2011), Simulia Corporation, ABAQUS v6.11 Documentation, Dassault Systèmes, RI, USA, 2011.

Sorelli L., Toutlemonde, F. (2005). On the design of steel fiber reinforced concrete tunnel lining segments. In: 11th Intl. Conf. on Fracture, 2005.

Sørensen L.S. (2019). Concrete types – proposals. Note, Department of Civil Engineering, Technical University of Denmark, September 2019.

Sørensen L.S. (2021) Spalling tests Exposure of concrete walls with gas flame. Subtask 3.4.3 Fire effect on structure integrity and concrete spalling. Presentation on 6th HyTunnel-CS Project meeting held on 15-17 September 2021.

Spoelstra M.B., (2021) Institute for Safety *Hydrogen cars in parking garages - Part 1*. Kemperbergerweg 783, Arnhem - Netherlands

Svensson S., Van de Veire M. Experimental Study of Gas Cooling During Firefighting Operations. *Fire Technology* **55,** 285–305 (2019). https://doi.org/10.1007/s10694-018-0790-3.

Takeno K., Okabayashi K., Kouchi A., Nonaka T., Hashiguchi K., Chitose K. Dispersion and explosion field tests for 40 MPa pressurized hydrogen 2007;32:2144–53.

Tohir M. Z. M. and Spearpoint M. (2013) 'Distribution analysis of the fire severity characteristics of single passenger road vehicles using heat release rate data', 2(1), p. 1. doi: 10.1186/2193-0414-2-5.

Tohir M., Spearpoint M., (2014). Development of Fire Scenarios for Car Parking Buildings using Risk Analysis, Fire Safety Science 11, 944–957. doi: 10.3801/IAFSS.FSS.11-944.

Tuovinen H., Holmstedt G., Bengtson S., (1996). Sensitivity Calculations of Tunnel Fires Using CFD, Fire Technology 32(2), 99-119.

UIC, (2021). Safety Report 2021. https://safetydb.uic.org/IMG/pdf/uic-safety-public-report_2021.pdf

Venetsanos A., Giannissi S., Tolias I., Vågsæther K., Gaathaug A., Pursell M., Rattigan W., Markert F., Giuliani L., Sørensen L., Bernad A., Sanz Millán M., Kummer U., Brauner C., Russo P., van den Berg J., de Jong F., Van Esbroeck T., Van De Veire M., Bouix D., Bernard-Michel G., Kudriakov S., Studer E., Ferero D., Grune J., Stern G., (2021a). Overview of first outcomes of PNR project HyTunnel-CS, in: International Conference on Hydrogen Safety (ICHS2021) "Safe Hydrogen for Net Zero. Edinburgh, UK.

Vivanni L. (2021): Numerical modelling of the response of a tunnel concrete slab to hydrogen fire, MSc report, Civil Engineering Department, Technical University of Denmark.

What are the Average Dimensions of a Car in the UK? [WWW Document], (2021). URL https://www.nimblefins.co.uk/cheap-car-insurance/average-car-dimensions (accessed 10.12.21).

Winkler A., Edvardsen C. & Kasper T. (2014), Examples of bridge, tunnel lining and foundation design with steel fibre reinforced concrete, in proc. of FRC 2014, Joint ACI-fib International Workshop Fibre Reinforced Concrete.

Winkler B., Hofstetter G., Lehar H. (2004). Application of a constitutive model for concrete to the analysis of a precast segmental tunnel lining. International Journal for Numerical and Analytical Methods in Geomechanics, 28, pp. 797–819.

Woodburn P.J., Britter R.E. (1996). CFD Simulations of a Tunnel Fire - Part II, Fire Safety Journal 26, 63-90.

Yamashita A., Kondo M., Goto S., Ogami N., (2015). Development of High-Pressure Hydrogen Storage System for the Toyota "Mirai." SAE Tech. Pap., SAE International. https://doi.org/10.4271/2015-01-1169.or Development of High-Pressure Hydrogen Storage System for the Toyota "Mirai" (sae.org)

Yanez J., Kuznetsov M.., Souto-Iglesias A (2015). An analysis of the hydrogen explosion in the Fukushima-Daiichi accident. International Journal of Hydrogen Energy, 40(25): 8261-8280.

Zaineb T. Experimental and numerical study of concrete exposed to rapid fire. Masters Thesis, August 2020. Department of Civil Engineering, Technical University of Denmark.

Zalosh N., & Wayandt R. (2005). Hydrogen Fuel Tank Fire Exposure Burst Test. *SAE Paper Number 2005-01-1886*.

Zhao S., Li Y.Z., Kumm M., Ingason H. & Liu F. (2019). Re-direction of smoke flow in inclined tunnel fires. Tunnelling and Underground Space Technology, 86, pp.113–127.

Appendices

Appendix 1. Harm criteria

To assess hazards and associated risks resulting from hydrogen vehicles in tunnels and similar confined spaces there is a need for harm and damage criteria. These criteria are related to harm to people, damage to property, structures and environment. In incidents involving hydrogen vehicles in tunnels, the environmental damage may be reduced to potential polluting materials, which are collected by the appropriate sewer systems within a tunnel, smoke emissions that can be dispersed into the environment at the tunnel exits or tackled by ventilation systems. The largest safety concerns in tunnel incidents are those related to life safety, including increased probability of fatalities due to space confinement in case of severe incidents such as high-pressure hydrogen storage tank rupture in a fire. The property loss, i.e. demolition and damage to vehicles and tunnel equipment and structures, are concerns as well. These safety concerns are related to the "new" hazard of high-pressure blast waves propagating throughout the tunnel with little decay and fireball/combustion products moving at high velocity on long distances producing harmful thermal effects and potential asphyxiation due to burning out of oxygen.

A1.1 Tenability and harm criteria for humans in case of tunnel fire scenarios

People in a tunnel may be exposed to different hazards during a fire (HyTunnel-CS, D1.2, 2019). Parts of the text below and tables of harm and tenability criteria are taken from this deliverable. Tenability in this context is the ability of humans to perform cognitive and motor-skill functions at an acceptable level when exposed to a fire environment. Therefore, a tenability limit is the limit at which a human being is rendered physically incapacitated or is killed as a consequence of exposure to one or more factors such as temperature, heat flux, toxicity or smoke obscuration generated by a fire.

In cases of fire, the main exposures are high temperature, radiative and convective heat fluxes, toxic smoke and other combustion products. An important issue is reduced visibility due to dense smoke generation. To enable safe egress, a certain tenability level or acceptance criteria need to be evaluated (ISO/TR 13571-2, 2016). The standard is to ensure safe egress in the early stages of any fire, supporting persons' individual egress and not the rescue by the fire brigades. It should be noted that the tank rupture with harmful and destructive blast waves reduces the efficiency of evacuation strategies if the tank rupture occurs. The following tenability conditions are typically considered for incidents with fossil-fuel vehicles fires:

- Loss of visibility.
- Thermal effects: hyperthermia of the human body, skin burns, burns in the lungs.
- Toxic effects.

In the case of hydrogen-powered vehicles the considerations of "new" hazards, such as consequences of a hydrogen storage tank rupture in a fire, must be considered.

The visibilities are calculated using the optical density of smoke based on Lambert Beers law. The standard (ISO/TR 13571-2, 2016) uses the equations of safe egress that links visibility to walking speed. Such speeds have been experimentally measured and may be calculated using

the equations by Nelson and Mowrer that also allow predicting the speeds of crowds. In situations of good visibility (≥10 m), the movement speed may be 0.5 m/s, while less visibility reduces the movement speed by 50%. Here an acceptance criterion may be formulated that relates the time to evacuate, such as required time to safe egress (RSET), with the available time (ASET) until the visibility is reaching the defined threshold value. Comparison of the ratio ASET/ RSET being less or greater than 1 provides the acceptance of any scenario. The use of explosion free in a fire self-venting storage tank would exclude catastrophic consequences of tank rupture and the recommendations of ISO/TR 13571-2 (2016) can adhere. The potential of tank rupture would require the update of requirements to evacuation. For example, the issue of people staying in a vehicle with closed windows should be investigated and addressed. Indeed, the vehicle could protect people from serious injuries by a blast wave due to protection by a vehicle body and from asphyxiation and thermal attack by fireball due to the availability of air within a car.

The ISO standard identifies several necessary models to predict the thermal effects, such as exposure models predicting temperature impacts on persons being dressed normally or being almost naked. The relative humidity in such scenarios should be less than 10%. The impact on persons can be calculated by dose models using the thermal model Fractional Effective Dose (FED) equation given in the standard. Exposure to heat radiation e.g. from hydrogen fires may result in first, second or third-degree burns. It is often conservatively assumed that direct contact with jet flames results in fatality (LaChance *et al*., 2011).

The surrounding air may be heated up significantly, causing harm to people in the fire vicinity. Exposure to high-temperature air may also lead to difficulty of breathing and respiratory tract burns (HyResponse, 2015). Table A1-1 presents the effects of high-temperature air on people.

Table A1-1. Effect of air temperature on people (HyResponse, 2015).

Temperature, °C	**Physiological response**
70	No fatal issues in a closed space except the uncomfortable situation
115	The threshold for pain (exposure longer than 5 minutes)
127	Difficulty breathing
149	Breathing via mouth is difficult, temperature limit for escape
150	Skin burns occur in less than 5 minutes
160	Rapid, unbearable pain with dry skin
182	Irreversible injuries in 30 seconds
203	Respiratory system tolerance time is less than 4 minutes with wet skin
309	Third-degree burns for 20 seconds exposure, causes burns to larynx after a few minutes, escape is not possible

The associated effects due to heat radiation on unprotected people are widely reported, e.g. LaChance *et al*. (2011). Values are shown in

Table A1-2. A radiative heat flux level of 1.6 kW/m^2 is identified as a no-harm criterion. It should be reminded that a sunny day provides basic heat radiation of about 1.2 kW/m^2.

Table A1-2. Example effects of radiative heat flux on people (LaChance et al., 2011)

Thermal radiation intensity, kW/m^2	Effects on people
1.6	No harm for long exposures; safe for the general public and the stationary personnel
4-5	Pain for 20 s exposure; first-degree burn
9.5	Second-degree burn after 20 s.
12.5-15	First-degree burn after 10s, 1% lethality in 1 min
25	Significant injury in 10 s; 100 % lethality in 1 min
35-37.5	1% lethality in 10 s [6]

Operators not wearing protective clothing should not be exposed to radiative heat flux above 1.5 kW/m^2 (Heus and Denhartog, 2017). This value agrees with the acceptable radiative heat flux indicated by Pleß and Seliger (2009) for firefighters for a long exposure (see Table A1-3). However, both sources report a limit slightly lower than the no-harm level of 1.6 kW/m^2 reported by LaChance *et al*. (2011). Firefighters responding to an incident will be equipped with thermal protective clothing and equipment. Therefore, they can withstand higher levels of thermal radiation. Heus and Denhartog (2017) reported that firefighters wearing protective clothing (EN469) can perform emergency operations for approximately 3 min when exposed to heat fluxes up to 4.6 kW/m^2, which agrees with the intensity indicated as tolerable for emergency personnel (HyResponse, 2015). Refinery industry API 521 standard (2014) allows 4.7 kW/m2 for people who may be exposed to radiation from flares that activate in an emergency (but wearing flame proof overalls). Citing Koinig (1999), Pleß and Seliger (2009) provided values in Table A1-3 on acceptable heat radiation for firefighters. However, it should be noted that these are indicative thresholds.

Table A1-3. Acceptable heat radiation for firefighters

Heat radiation kW/m^2	Effect on firefighters
1.5	Bearable for a long time.
4.5	Bearable with normal protective turn-out coats.
8.0	Need cooled protective coats.

The harm level is a function of both thermal radiation intensity and exposure duration; thus, it is usually expressed in terms of thermal dose (TD).

The toxic impact is calculated based on a categorisation of the gases into asphyxiating gases such as CO, HCN and irritating gases such as HCl, HBr. Threshold values for these gases are shown in Table A1-4. Conditions like low oxygen concentration causing hypoxia or high carbon dioxide causing hyperventilation are also recognised. There may be other effects as well such as clogging of the respiratory tracts due to soot, *etc*. The toxicity of gas composition is calculated using the Fractional Effective Dose, FED. The FED is defined in ISO 13344:2015 as a “ratio of the exposure dose for an asphyxiant toxicant to that exposure

[6] QRAs assume 100% fatality for heat flux 35-37.5 kW/m^2

dose of the asphyxiant expected to produce a specified effect on an exposed subject of average susceptibility". This subject is, in other words, a healthy male adult.

Table A1-4. Threshold values examples for incapacitation and lethal effects of toxic impacts during a fire taken from (Ingason et al., 2015, p. 394)

Species	**Exposure 5 min**		**Exposure 30 min**	
	Incapacitation	*Lethal*	*Incapacitation*	*Lethal*
CO [ppm]	6000-8000	12000-16000	1400-170	2500-4000
HCN [ppm]	150-200	250-400	90-120	170-230
O_2 [%]	10-13	<5	<12	6-7
CO_2 [%]	1-8	>10	6-7	>9

Exposure to more than one toxic gas could lead to incapacitation at lower concentration that impacts the evacuation and may lead to lethality. The fractional effective dose can be calculated with the type of equations shown below. The additive effects of several gases present are summed to provide the total dose. Such doses are used as acceptance criteria as shown in Table A1-5. It may be seen that the recommended Swedish acceptance criteria for tunnels are close or identical to those of the building requirements:

$$F_{IN,n} = \left(F_{I_{CO},n} + F_{I_{CN}}\right) V_{CO_2,n} + F_{I_{O_2},n},$$

where $F_{IN,n}$ is the fraction of incapacitating dose calculated on the respective doses for carbon monoxide ($F_{I_{CO},n}$) and hydrogen cyanide ($F_{I_{CN}}$) as well as low oxygen concentration ($F_{I_{O_2},n}$). Volume V_{CO2} is the carbon dioxide volume in the room that leads to more frequent respiration.

The partial incapacitation fractions $F_{I,n}$ are calculated e.g. by the following type of expressions given by Ingason *et al*. (2015) exemplified for the carbon monoxide fractional incapacitation dose:

$$F_{I_{CO},n} = \frac{3.317*10^{-5}[CO]^{1.036}\, RMV(t_n - t_{n-1})}{I},$$

where $F_{I_{CO},n}$ is the CO fractional incapacitation dose, [CO] is the CO concentration in ppm at time step t_n in min, RMV is the breathing rate (typically 25 L/min for light activity), I is the indicator for incapacitation; the blood COHb (carboxyhaemoglobin) value for incapacitation is equal to 30% for light activity. The individual fractions are summed to obtain the fractional effective dose for incapacitation $F_I(t=t_N)$ after a certain exposure time t_N:

$$FI(t = t_N) = \sum_{n=2}^{N} F_{IN,n}. \qquad (4.3)$$

In terms of acceptance criteria for tunnel fires in Sweden, the EU project UPTUN, an analysis of different aspects was performed and the values given in Table A1-5 were suggested (Ingason, 2005)- under the column heading EU UPTUN. Within another Swedish project aiming at developing a proposal for a Swedish performance-based design guide for fire safety in road tunnels different acceptance criteria were also discussed (Gehandler *et al*., 2013). These are also included in Table A1-5 under the column heading SE-FKR-BV. The Swedish Transport Administration (Trafikverket) has published advice related to technical requirements for road and rail tunnels in Sweden (TRV, 2011). These are presented under the column heading SE-TRVR in Table A1-5. For comparison also, values to be used for

performance-based (analytical) design of buildings in Sweden (BBRAD 1) (BFS, 2011) are included in Table A1-5 under the column heading SE-BBRAD.

In the EU UPTUN report (Ingason, 2005), specific acceptance criteria were also given for the fire and rescue services:

• Gas temperature ≤ 100 °C

• Radiation ≤ 5 KW/m2

• Toxic gases: no limitation due to breathing apparatus (BA)

• Visibility: No limitation due to infra-red cameras

Table A1-5. Acceptance criteria for tunnel fires in Sweden (Ingason et al., 2015)

Parameter	EU UPTUN	SE-FKR-BV	SE-TRVR	SE-BBRAD
Visibility [m]	>= 10	-	10 (unknown place) 5 (known place)	10 (space >100 m^2) 5 (space < 100 m^2)
Smoke layer height [m]	-	-	1.6 + H*0.1	1.6 +H_{room}*0.1
Gas temperature [^oC]	<= 60	< 80	<80	<80
Radiation [kW/m^2]	<= 2	<2.5	<2.5 < 10 (short time)	<= 2.5
Toxic gas	FI_{tot} < 1	5% CO_2 <2000 ppm CO 15 % O_2 (max 1 min) or FI_{tot} 0.3 (min. CO, CO_2, O_2 HCN)	-	5% CO_2 <2000 ppm CO < 15% O_2

References

API Standard 521 (2014). Pressure-relieving and Depressuring Systems. 6th Ed.

BFS (2011) *Boverkets allmänna råd om analytisk dimensionering av byggnaders brandskydd. Boverkets Författningsamling*, BFS 2011:27 BBRAD 1 (in Swedish)

Gehandler J., Ingason H., Lönnermark A., Frantzich H., Strömgren M. (2013) Performance-based requirements and recommendations for fire safety in road tunnels (FKR-BV12). SP Technical Research Institute of Sweden.

Heus, R. and Denhartog, E.A. (2017), Maximum allowable exposure to different heat radiation levels in three types of heat protective clothing, Ind Health. 2017 Dec 7;55(6):529-536. doi: 10.2486/indhealth.2017-0137.

HyResponse (2015) D2.1. Description of selected FCH systems and infrastructure, relevant safety features and concepts.

Ingason H (ed) (2005) TG2.2– Target criteria. UPTUN Report WP2– task Group 2.

ISO 13344:2015 Estimation of the lethal toxic potency of fire effluents.

ISO/TR 13571-2 (2016) Life-threatening components of fire — Part 2: Methodology and examples of tenability assessment

LaChance J., Tchouvelev A., Engebo A., (2011). Development of uniform harm criteria for use in quantitative risk analysis of the hydrogen infrastructure. Int. J. Hydrog. Energy 36, 2381-2388.

TRV (2011) TRVR Tunnel 11: *Trafikverkets tekniska råd Tunnel. Trafikverket, TRV publ nr*

2011:088 (in Swedish)

A1.2 Damage criteria for structures and equipment

Structures and equipment will be affected by exposure to radiant heat flux emitted by hydrogen combustion.

Table A1-6 shows the damage criteria according to the radiant heat flux level reported in HyResponse (2015). An exposure of 30 minutes to a radiant heat flux of 4 kW/m^2 would be sufficient to cause the breakage of glass. Domino effects may be present for levels of 8 kW/m^2.

Table A1-6. Effect of radiant heat flux on structures, equipment and environment (HyResponse, 2015)

Radiant heat flux, kW/m^2	**Effects on structures, materials, equipment and environment**
4	Glass breakage (30 min exposure)
5	Significant windows breakage
8-12	Radiation intensity threshold capable to cause domino effects
10	Heating structures; temperature and pressure increase in LH2/GH2 storage
10-12	Ignition of vegetation
10 or 20	Ignition of fuel, oil (120 s or 40 s, respectively)
12.5-15	Piloted ignition of wood; melting of plastics (>30 min exposure)
16	Failure of structures (except concrete) in prolonged exposures
18-20	Cable insulation degradation (>30 min exposure)
20	Intensity, which concrete structures can withstand for several hours
25-32	Unpiloted ignition of wood; steel deformation (>30 min exposure)
35-37.5	Equipment and structural damage, including storage tanks (>30 min)
100	Steel structure collapse (>30 min exposure)
200	Concrete structures failure (in several dozen minutes)

The overpressure hazards associated with hydrogen explosions may severely damage the structure or equipment of a tunnel or confined space. Overpressure above 15 kPa may already cause a collapse of unreinforced concrete walls. The overpressure thresholds for structures and equipment along with associated damage is shown in

Table A1-7.

Table A1-7. Effects of overpressure on structures and equipment (LaChance et al., 2011)

Overpressure, kPa	**Description of damage**
1	Threshold for glass breakage
15-20	Collapse of unreinforced concrete or cinderblock walls
20-30	Collapse of industrial steel frame structure
35-40	Displacement of pipe bridge, breakage of piping
70	Total destruction of buildings, heavy machinery damaged
50-100	Displacement of cylindrical storage tank, failure of pipes

The effect of overpressure on structures and equipment depends on the combined effect with the impulse of a pressure wave. Table A1-8 shows the damage associated to the levels of overpressure and impulse as reported in HyResponse (2015).

Table A1-8. Combined effect of overpressure and impulse on the level of damage (HyResponse, 2015)

Overpressure peak, kPa	**Impulse, kPa·s**	**Description of damage**
3.6	0.10	Border of minor structural damages
14.6	0.30	Threshold for moderate structural damages: failure of some load-bearing elements
34.5	0.52	Threshold for partial destruction: 50-75% of walls destroyed
70.1	0.77	Total destruction of buildings

A1.2.1 Evaluation of harm using probit functions

The harm to humans and structure may be described by the harm criteria presented above. They can also be assessed using Probit functions. These relate a harmful dose to the probability of harm effects, e.g. lethality. The dose is a concentration times duration of exposure, but the concentrations may be replaced by heat radiation flux, pressure load, *etc*. The harm criteria in these evaluations maybe the 1% percentile that the exposure to a certain dose may lead to a 1% fatality. This may be used to calculate hazard distances, i.e. the distance from the source, e.g. a fire, to a distance where the exposure is providing a fatality of less than 1% of humans. Other harm criteria definitions may be possible. The general equation of a Probit function is:

$$Pr = a + b \times ln(L),$$

where a and b are constants and L is the load (dose) related to the studied effect. This is to be seen as a linearisation of the lethality density distribution of dose – lethality effects on a population, as known from toxicological assessments (the dose where 50% of the rats will die).

The specific functions used by the QRAM tool to evaluate lethality and injuries are based on relevant literature data reported by INERIS (2005a).

A list of typical Probit relations is as follows (see also HyTunnel-CS D1.2, 2019):

- *Thermal effect from fires and BLEVEs:*

  $$Pr = -14.9 + 2.56 \times \ln\left(q^{\frac{4}{3}} \times t\right),$$

where *t* is a time of exposure (s), *q* is the thermal radiation flux (kW/m²).

- *Overpressure direct effects from VCEs:*
  $Pr = -77.1 + 6.91 \times \ln(p°)$,
  where $p°$ is the peak overpressure (Pa).
- *Thermal effect from fires and BLEVEs:*
  $Pr = -39.83 + 3.0186 \times \ln(q^{4/3} \times t)$ for first-degree burns,
  $Pr = -43.14 + 3.0186 \times \ln(q^{4/3} \times t)$ for second-degree burns,
  where *t* is a time of exposure (s), *q* is the thermal radiation flux (kW/m²).
- *Overpressure effects from VCEs:*
  $Pr = -15.6 + 1.93\ln(p°)$ for eardrum rupture,
  $Pr = -27.1 + 4.26\ln(J)$ for injury from missiles (glass),
  $Pr = -39.1 + 4.45\ln(J)$ for injury from whole body translation,
  where $p°$ is the peak overpressure (Pa) and *J* the impulse (Pa s).

Besides physiological consequences, structural and environmental consequences can also be evaluated by means of specific tools reported by INERIS (2005a).

References

HyResponse (2015) D2.1. Description of selected FCH systems and infrastructure, relevant safety features and concepts.

INERIS (2005a) Transport of Dangerous Goods Through Road Tunnels: Quantitative Risk Assessment Model (v. 3.60-3.61) - Reference Manual. Research Report 20504, August 2005.

Appendix 2. Information on existing Regulations, Codes and Standards (RCS)

A report on critical analysis of RCS for tunnels and similar confined spaces (HyTunnel-CS, D1.4, 2019) overviewed current relevant regulations, codes or standards (RCS). It was concluded that no guidance is available for evaluating the appropriateness of conventional mitigation technologies, safety management and first responder intervention strategies in case of an incident with a hydrogen-powered vehicle or transport in tunnels or similar confined spaces. This is the reasoning for pre-normative research in the HyTunnel-CS project.

Hydrogen is considered as a flammable gas with regards to production, transport, storage and use. National RCS for hydrogen in general are the same as for all flammable gases.

National safety requirements for tunnels and confined spaces often go beyond the minimum requirements of the EU legislation. Only generic and not hydrogen specific aspects are taken into consideration, e.g. escape routes, sprinklers, ventilation, *etc*. The risk assessment methodology also only has generic requirements and does not account for specific hazards characteristic for hydrogen, e.g. the pressure peaking phenomenon and high-consequences event of hydrogen storage tank rupture in a fire. Hydrogen-powered vehicles are mostly not yet integrated into risk analysis. HyTunnel-CS addressed this issue.

There are no RCS for hydrogen transport in relation to confined spaces. There are no specific requirements for HPVs in national RCS for tunnels and similar confined spaces. The only mentioned exceptions are examples of airports and the Channel Tunnel.

In most countries local regulations may affect the technical design of hydrogen vehicles and confined spaces and may differ from place to place. Different RCS may apply based on the type of confined space. These do not take into consideration the fuels of the vehicles that may be parked there. The absence of hydrogen related RCS resulted in no admission policies for HPVs in underground parking. The HyTunnel-CS partners hope that these recommendations will underpin inherently safer design of hydrogen vehicles and they will be considered as safe or safer compared to fossil fuel vehicles, e.g. when the various measures and improvements identified are included in future regulations.

For certification and operation of underground infrastructure with regards to hydrogen transport and HPVs, the following RCS are most important.

ADR

The Agreement on the International Carriage of Dangerous Goods by Road (ADR) was concluded under the auspices of the United Nations Economic Commission for Europe (UN ECE).

The most important article is the second, which states that, apart from some extremely dangerous goods, other dangerous goods may be carried internationally in road vehicles provided that the following conditions are met:

- the conditions set out in Annex A of ADR for the goods concerned, in particular with regard to their packaging and labelling; and
- the conditions set out in Annex B, in particular, with regards to the construction, equipment and functioning of the vehicle carrying the goods concerned.

Annexes A and B have been regularly amended and updated since the entry into force of ADR.

The structure of ADR is in line with that of the United Nations Recommendations on the Transport of Dangerous Goods, Model Regulations, the International Maritime Dangerous Goods Code (of the International Maritime Organization), the Technical Instructions for the Safe Transport of Dangerous Goods by Air (of the International Civil Aviation Organization) and the Regulations concerning the International Carriage of Dangerous Goods by Rail (of the Intergovernmental Organization for International Carriage by Rail).

RID

The international rail transport of dangerous goods is regulated by the RID (*Règlement concernant le transport international ferroviaire des marchandises dangereuses*). The RID describes exactly what dangerous goods are, how they are classified, how to recognise them, the requirements for packaging, tanks and vehicles, the transport conditions, as well as the obligations of all parties involved. Every two years, this convention is updated to reflect the latest scientific and technological developments related to the transport of dangerous goods.

ATEX

The ATEX directive consists of two EU directives that describe which equipment and workspace are permitted in an environment with an explosive atmosphere. European harmonised standards for the ATEX directive are produced by the European Standardisation Organisations:

- CEN: CEN/TC 305 - Potentially explosive atmospheres - Explosion prevention and protection; and
- CENELEC: CLC/TC 31 - Electrical apparatus for potentially explosive atmospheres.

UN ECE GTR#13

The United Nations Economic Commission for Europe Global Technical Regulation Number 13 on Hydrogen and Fuel Cell Vehicles.

It is the defining document regulating minimum safety requirements for hydrogen vehicles, and in particular, FCEVs. GTR#13 has been formally adopted and will serve as the basis for the national regulatory standards for FCEV safety. The GTR#13 defines safety requirements for these vehicles, including specifications on the allowable hydrogen levels in vehicle enclosures during in-use and post-crash conditions and on the allowable hydrogen emissions levels in vehicle exhaust during certain modes of normal operation, fire test protocol, *etc*.

EUROCODES

The EN Eurocodes are developed under the guidance and co-ordination of CEN Technical Committee 250 (CEN/TC250) "Structural Eurocodes".

The EN Eurocodes are a set of European Standards which provide common rules for the design of buildings and other construction works to check their strength, stability and fire resistance. There are no parts devoted to the design of tunnels, as the Eurocodes do not explicitly include all underground structures.

For more detailed information, please see HyTunnel-CS deliverable D1.4 (2019).

HyTunnel-CS Deliverable D6.10 (2022) “Recommendations for RCS”, includes new recommendations based on the analytical, numerical and experimental studies performed in this project. The recommendations for RCS are made for specific RCS and technical committees of standard development organisations (SDOs) working in certain areas. HyTunnel-CS D6.10 also contains a more complete list of relevance to the HyTunnel-CS project RCS.

Appendix 3. Hydrogen safety engineering models and tools

This appendix includes a brief description of models and tools, including references to their detailed description, for hydrogen safety engineering of systems, e.g. vehicles that can be useful for assessment of hazards and associated risks in underground traffic infrastructure. The models and tools allow assessment of hazards, incident consequences and could facilitate the development of prevention and mitigation strategies and innovative engineering solutions. They are built of the accumulated knowledge in hydrogen safety and results of experimental, numerical and theoretical studies, including within the HyTunnel-CS project.

A3.1 Tools for assessment of unignited hydrogen releases and jet fires

A3.1.1 The similarity law for concentration decay in momentum-dominated jets

Releases from pressurised hydrogen storage and equipment will be in the momentum-dominated regime. Hydrogen concentration in buoyancy-controlled jets decays faster (Molkov, 2012) compared to momentum-dominated jets correlations which could be taken as a conservative estimate. The semi-empirical correlation for gaseous jet decay along the centre-line of a free, unobstructed **subsonic** jet was proposed by Chen and Rody (1980):

$$\frac{C_{ax}}{C_N} = 5.4 \cdot \sqrt{\frac{\rho_N}{\rho_S}} \frac{D}{x}, \quad (1)$$

where x is the axial distance from the nozzle to the point of interest where the mass fraction decays to C_{ax} (m); D is the real nozzle exit diameter (m); C_{ax} is a mass fraction of hydrogen in air at axial distance x; C_N is hydrogen mass fraction in the nozzle ($C_N = 1.0$ for pure hydrogen release); ρ_N is the density in the orifice (kg/m^3); ρ_S is the ambient air density (kg/m^3).

The correlation was extended and thoroughly validated for under-expanded sonic and supersonic hydrogen jets for storage pressures up to 40 MPa, storage temperature as low as 80 K and range of ratios of axial distance to diameter in the range x/D=4-28,580 (Molkov, 2012). To apply the original correlation to under-expanded jets from high-pressure hydrogen storage the hydrogen density in the release orifice ρ_N should be found beforehand, for details please see (Molkov, 2012).

The similarity law is available as a free access online tool of the e-Laboratory of Hydrogen Safety (https://elab.hysafer.ulster.ac.uk/) developed as a part of a wider e-Laboratory within the NET-Tools project (https://www.h2fc-net.eu/).

A simple safety strategy may be based on the minimisation of release opening to provide hydrogen concentration decay below the lower flammability limit (LFL) before the jet reaches the enclosure ceiling. Once hydrogen concentration under the ceiling is below the LFL, i.e. 4% vol. hydrogen in air, then formation and build-up of flammable hydrogen-air cloud can be avoided to prevent possible ignition followed by deflagration with pressure and thermal effects that would be harmful to people and destructive for structures.

The similarity law may serve as a tool for the above safety strategy realisation. The distance along the jet axis to the location where hydrogen mass fraction reaches the specified value is directly proportional to the release diameter and can be calculated as:

$$x = \frac{5.4 \times D}{C_{ax}} \cdot \sqrt{\frac{\rho_N}{\rho_S}}, \quad (2)$$

where x is the distance between the release orifice, e.g. TPRD location, and the ceiling (m); and $C_{ax} = 0.00288$ is the hydrogen mass fraction corresponding to the hydrogen LFL (4% vol.).

More details on use of the Similarity Law, typical errors in the interpretation of this law for concentration decay in hydrogen jets, as well as engineering nomogram for its realisation and justification of the safety strategy to avoid flammable mixture accumulation under ceilings are available in Molkov (2012).

References

- Chen C, Rody W. (1980) Vertical turbulent buoyant jets – a review of experimental data. Oxford: Pergamon Press.
- Molkov, V. (2012) Fundamentals of Hydrogen Safety Engineering. www.bookboon.com, free download online e-books, Part I and Part II. https://bookboon.com/en/fundamentals-of-hydrogen-safety-engineering-i-ebook; https://bookboon.com/en/fundamentals-of-hydrogen-safety-engineering-ii-ebook.

A3.1.3 Model of storage tank blowdown (Helmholtz free energy-based EoS)

The DISCHA integral engineering standalone tool was extended to account for tank wall heat transfer effects. The tool was validated against an experiment involving He release from gaseous storage at 700 bar (KIT tests) and H_2 boil-off release from LH2 storage (LLNL tests). Details on the performed model extension and validation can be found in (HyTunnel-CS, D4.4, 2022). Future development work will consist in extending DISCHA for tank-to-tank transfer simulations.

A3.1.4 Model of non-adiabatic compressed gaseous hydrogen tank blowdown

The model for non-adiabatic tank blowdown is a sub-model of a wider tank-TPRD system model able to describe thermal performance of a tank in an engulfing fire (see Appendix A3.3.2). The full description of the model including its validation can be found in (Molkov *et al*., 2021b).

A3.1.5 The pressure peaking phenomena model

The detailed description of the pressure peaking phenomenon model for both ignited and unignited releases is given in (Makarov *et al*., 2018). The tool is freely accessible online as a part of the e-Laboratory of Hydrogen Safety (https://elab.hysafer.ulster.ac.uk/).

A3.1.6 Design of TPRD to avoid jet flame blow-off

A TPRD should be designed to sustain hydrogen flame during the blowdown and prevent its blow-off to eliminate the hazards associated with hydrogen accumulation and follow-up deflagration/ DDT/detonation. The decrease of TPRD diameter below 1 mm, which is needed to prevent demolition of a garage structure by the pressure peaking phenomenon, will result in flame blow-off when the pressure in the tank will drop during blowdown as shown in Figure A3-1 (Mogi and Horiguchi, 2009).

The solution to prevent flame blow-off at TPRD diameters below 1 mm could be a transition to larger diameter of exit from TPRD sufficient to sustain the flame at all storage pressures, e.g. 2 mm. The increase of exit diameter compared to the minimum diameter of TPRD, that defines the mass flow rate, would result in somewhat longer flame from TPRD but would mitigate the pressure peaking phenomenon.

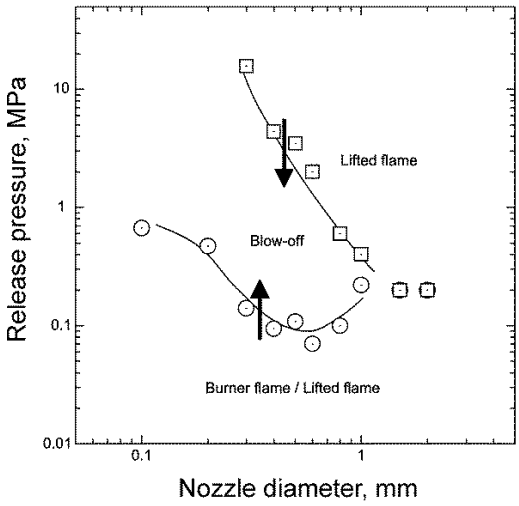

Figure A3-1. Hydrogen jet flame blow-off region (Mogi and Horiguchi, 2009)

A3.1.7 Hydrogen flame length correlation and three jet fire hazard distances

The dimensionless hydrogen flame length correlation (Molkov and Saffers, 2013) is valid for laminar and turbulent flames, buoyancy-controlled fire plumes and momentum-dominated jet fires, expanded (subsonic and sonic) and under-expanded (sonic and supersonic) hydrogen jet fires. The tool is freely available online as a part of the e-Laboratory of Hydrogen Safety and allows calculation of a flame length and three hazard distances (fatality, injury and no-harm) for free jets (https://elab.hysafer.ulster.ac.uk/).

A3.1.8 Experiments on the effect of cross-flow ventilation on hydrogen dispersion

Experimental results from the project can be used to validate models to allow them to be used for design and safety studies. The figure below (HyTunnel-CS, D2.3, 2022) shows the contour plots of hydrogen volume fraction at a converged steady state (0.132 s). The total length of the hydrogen jet by simulation is shorter than that of experimental result. For the simulation performed by partner NCSRD, a high hydrogen concentration region can be observed under the hydrogen jet (downstream of ventilation), where, however, a low hydrogen concentration (but longer jet) is seen in the experiment.

The conclusions drawn from the work is that cross-flow ventilation produces strong turbulence and effective mixing. The turbulence generated by the fan is found to be the most significant factor. The dimensions of both 4% and 10% by volume of hydrogen clouds are reduced by the ventilation airflow in a cross- direction, leading to a smaller flammable cloud. Cross-flow ventilation is the most effective way to reduce the flammable length by, for example, more than 50% in some cases of airflow velocity of 3.5 m/s.

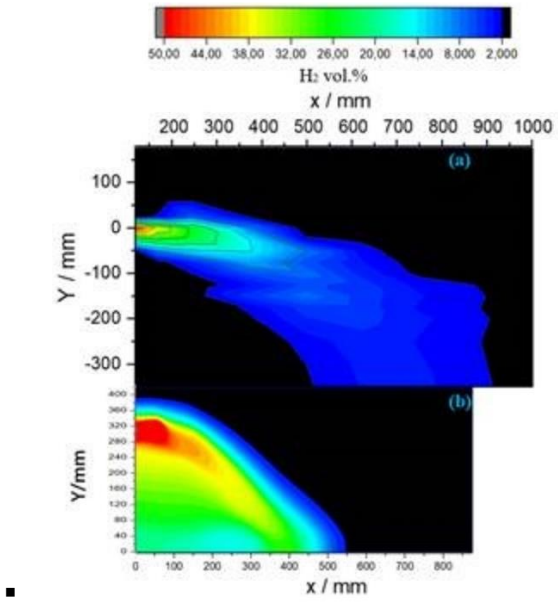

Figure A3-2. Hydrogen concentration (molar fraction) contour plots in cross-section cutting through the centre of the jet with 5 m/s cross-flow ventilation: (a) experiment; (b) simulation.

Appendix 3.2 Tools for assessment of deflagrations, DDT and detonations

A3.2.1 Upper limit of hydrogen inventory in closed space without ventilation

A thermodynamic model (Makarov *et al.*, 2018) was developed to allow the estimation of the maximum possible inventory of hydrogen that can be released in a large, closed space like warehouse and, if ignited and combusted, will not destroy a structure that can withstand an overpressure of the order of 10 kPa typical for civil structures. The incident scenario presumes that the released hydrogen fills the large enclosure only partially forming a localised hydrogen-air mixture. The overpressure was calculated based on the assumption of complete hydrogen-air mixture combustion and fully sealed enclosure (no vents). The tool based on the model is available at the e-Laboratory of Hydrogen Safety (https://elab.hysafer.ulster.ac.uk/). The tool can be used in two ways:

1. Calculation of maximum hydrogen inventory, for which combustion in a given enclosure volume will not lead to overpressure above the specified limit. For example, to prevent overpressure above 10 kPa, which is considered as a limit for integrity of civil structures, the hydrogen mass can be calculated as $m_{H2} < 2.61 \cdot 10^{-4} V$, where m_{H_2} is the maximum mass of hydrogen (kg) that will not destroy a closed structure of volume V (m^3) if the mixture burns inside.

2. Calculation of the enclosure volume required to prevent pressure build up above a specified limit in the case of accidental release and combustion of a given hydrogen inventory. In the case of 10 kPa overpressure limit, the enclosure volume should be equal or above $V > m_{H2}/2.61 \cdot 10^{-4}$, where V is enclosure volume (m^3) and m_{H_2} is mass of released hydrogen (kg).

Note that the thermodynamic equilibrium model presumes uniform pressure distribution across the whole enclosure during deflagration. Localised pressure damage may still occur if higher hydrogen concentrations are formed locally and transition to detonation occurs in an area of high congestion (Friedrich *et al.*, 2007).

References

- Makarov, D., Hooker, P., Kuznetsov, M., Molkov, V. (2018) Deflagrations of localised homogeneous and inhomogeneous hydrogen-air mixtures in enclosures, International Journal of Hydrogen Energy, 43:9848-9869, https://doi.org/10.1016/j.ijhydene.2018.03.159.
- Friedrich, A., Grune, J., Jordan, T., Kotchourko, A., Kotchourko, N., Kuznetsov, M., Sempert, K., Stern, G. (2007) Experimental study of hydrogen-air deflagrations in flat layer, Intl. Conf. on Hydrogen Safety, 11 – 13 September 2007, San Sebastian, Spain.

A3.2.2 Correlation for deflagration from a spurious hydrogen release

The delayed ignition of a highly turbulent under-expanded hydrogen jet causes a deflagration, which can harm people and damage civil structures. The developed correlation for hydrogen safety engineering predicts the maximum overpressure generated by delayed ignition of a hydrogen jet at an arbitrary location for known storage pressure and release diameter. The correlation is applicable to free jets in the open atmosphere and in the confined spaces with dimensions comparable to the jet axial distance to LFL. Description of the correlation is available in (HyTunnel-CS, D4.3, 2022).

Nomenclature

Table A3-1 reports the nomenclature of parameters used in the correlation.

Table A3-1. Nomenclature for correlation on pressure load from delayed ignition of a turbulent jet

Parameter	**Symbol**	**Unit**
Nozzle diameter	d	m
Ambient pressure	P_0	Pa
Storage pressure	P_s	Pa
Distance between the centre of the fast-burning mixture in the jet (25-35% by volume) and the target location	R_w	m
Ambient temperature	T_0	K
Target coordinates	(x_t, y_t, z_t)	m
Overpressure	ΔP_t	Pa

Model description

The similitude analysis has been applied to build a correlation. The dimensionless overpressure generated by delayed ignition of hydrogen jets at an arbitrary location, $\frac{\Delta P_{exp}}{P_0}$, is correlated to the dimensionless parameter composed of the product of the ratio of the dimensionless storage pressure, $\sqrt{\frac{P_s}{P_0}}$, and the square of the ratio of the jet release diameter to the distance between the centre of the fast burning mixture in the jet (25-35% of hydrogen by volume in air) and the target location, $\left(\frac{d}{R_w}\right)^2$. The correlation can be used to estimate the pressure at a target location:

$$\frac{\Delta P_{exp}}{P_0} = 5000 \cdot \left[\left(\frac{P_s}{P_0}\right)^{0.5} \cdot \left(\frac{d}{R_w}\right)^2\right]^{0.95} .$$

The distance between the centre of the fast-burning part (25-35%) of the flammable cloud and the pressure sensor (in experiment) or "target" (person or structure) location in calculation of hazard is defined as R_w, and is calculated as:

$$R_w = \sqrt{(x_{30\%} - x_t)^2 + (y_{30\%} - y_t)^2 + (z_{30\%} - z_t)^2}.$$

The location in the jet with concentration equal to 30% by volume of hydrogen in air can be calculated using the similarity law (see Appendix A3.1.1).

Validity range

The correlation is built using experiments with hydrogen storage pressures in the range 0.5-65 MPa, storage temperatures 80-300 K, jet release diameters 0.5-52.5 mm. Maximum distance of the target from the release source in experiments was 50 m. The correlation is valid for free jets, thus in absence of obstacles and impingement up to the axial distance where the jet decays to LFL and thus combustion is not possible.

Input and output values: example of application

Let us consider a hydrogen tank having a storage pressure of P_s=35 MPa and nozzle diameter of d=2 mm. Hydrogen is stored at ambient temperature. The release is horizontal and originates at the location (0, 1, 0). The location of the target is (x_t, y_t, z_t)=(2, 1, 2). Ambient temperature and pressure are 288 K and 101325 Pa. The calculation steps are as follows:

1. The similarity law (see A3.1.1) is used to calculate the location in the jet with hydrogen concentration equal to 30%:

$$x_{30\%} = 5.4 \sqrt{\frac{\rho_N}{\rho_S}} D \frac{C_N}{C_{30\%}} = 1.3\ m$$

2. The distance between the fast-burning cloud and the target location is calculated:

$$R_w = \sqrt{(x_{30\%} - x_t)^2 + (y_{30\%} - y_t)^2 + (z_{30\%} - z_t)^2} = 2.1\ m$$

3. The maximum pressure at the target location is finally assessed:

$$\Delta P_t = P_0 \cdot 5000 \cdot \left[\left(\frac{P_S}{P_0} \right)^{0.5} \cdot \left(\frac{d}{R_w} \right)^2 \right]^{0.95} = 14.5\ kPa$$

The developed correlation may be used to estimate the hazard distances corresponding to defined harm criteria for people. In this example, a "no-harm" overpressure of 1.35 kPa is considered, according to the harm criteria proposed in (Baker *et al.*, 1983). An "injury" and "fatality" thresholds are taken as 16.5 kPa and 100 kPa respectively (Mannan, 2005):

$R_{no\_harm} = 7.4\ m$; $R_{Injury} = 2.0\ m$; $R_{Fatality} = 0.8\ m$.

The maximum hazard distance by overpressure from the release source will be reached along the jet axis (thermal hazards should be assessed at the same location to finally decide on the hazard distance) and can be calculated as:

$$x_{no\_harm} = x_{30\%} + R_w = 8.7\ m\ .$$

The distances from the release source for the "injury" and "fatality" limit can be calculated similarly as 3.3 and 2.1 m respectively.

References

- Baker, W.E., Cox, P.A., Kulesz, J.J., Strehlow, R.A., Westine, P.S. (1983), Explosion Hazards and Evaluation, Elsevier.
- Mannan, S. (2005), Lee's Loss Prevention in the Process Industries.

A3.2.3 Venting of non-uniform hydrogen-air deflagrations

Realistic releases of hydrogen in confined spaces most often lead to formation of highly non-uniform, stratified hydrogen-air mixtures. Venting remains the most cost-effective deflagration mitigation technique. It was demonstrated that vented deflagrations of stratified hydrogen-air mixture may lead to significantly higher overpressure compared to the leaner uniform hydrogen-air composition with the same hydrogen inventory (HyIndoor, 2014) creating a need for a specially adopted vent sizing methodology for mitigation of localised hydrogen-air mixture deflagrations.

The vent sizing correlation for localised mixture deflagration in an enclosure was first developed theoretically (Molkov, 1996) and later validated against experiments performed in the European pre-normative research project HyIndoor and described in detail in (Makarov *et al*., 2018). The vent sizing correlation to mitigate non-uniform hydrogen-air deflagrations is implemented in the e-Laboratory of Hydrogen Safety (https://elab.hysafer.ulster.ac.uk/) as a free access hydrogen safety engineering tool. The tool can be used in two ways:

1. Calculation of vent area to reduce deflagration pressure of localised hydrogen-air mixture to a given level.

2. Calculation of overpressure for specified localised mixture and a vent of known size.

References

- HyIndoor project (2014), Deliverable D5.1 "Widely accepted guidelines on Fuel Cell indoor installation and use" (https://www.researchgate.net/profile/Simon-Jallais/publication/302692394_Work_Package_5_Widely_accepted_guidelines_on_Fuel_Cell_indoor_installation_and_use_-_Hyindoor_-_Pre-normative_research_on_safe_indoor_use_of_fuel_cells_and_hydrogen_systems/links/5731fa2008ae9ace840475be/Work-Package-5-Widely-accepted-guidelines-on-Fuel-Cell-indoor-installation-and-use-Hyindoor-Pre-normative-research-on-safe-indoor-use-of-fuel-cells-and-hydrogen-systems.pdf, accessed 15 June 2021)
- Makarov, D., Hooker, P., Kuznetsov, M., Molkov, V. (2018) Deflagrations of localised homogeneous and inhomogeneous hydrogen-air mixtures in enclosures, International Journal of Hydrogen Energy, V. 43, pp.9848-9869, DOI: https://doi.org/10.1016/j.ijhydene.2018.03.159.
- Molkov V. (1996) Venting of gaseous deflagrations, DSc thesis, All-Russian Institute for Fire Protection (VNIIPO).

A3.2.4 Correlation for DDT in horizontal and vertical systems

The developed criteria for hydrogen detonation at KIT are introduced in Section 4.1.4.4 "Flame acceleration and transition to detonation". The relevant correlations are described here.

1. The first required condition is the mixture of hydrogen with air should be within the flammability limits of 4–75% by volume of hydrogen in air. Then, being ignited, the mixture can burn in different regimes depending on ignition source, geometry (channel,

layer, or a sequence of rooms), scale or dimensions, confinement degree, mixture reactivity and its uniformity or stratification.

2. Potentially, only a flammable mixture in which flame propagation reaches the speed of sound is able to detonate. The major criterion for flame acceleration to the speed of sound is that the expansion ratio of the mixture σ should exceed the critical expansion ratio σ* (Dorofeev *et al*., 2001):

$$\sigma > \sigma^*. \tag{1}$$

For hydrogen–air mixtures inside an enclosed channel σ*=3.75 at ambient pressure and temperature. In general, it depends on the scale but not for the tunnel dimensions because the critical Peclet number $Pe = D/\delta >> 100$ for tunnels (the ratio of tunnel equivalent diameter D to the laminar flame thickness of the mixture δ).

3. For partially confined envelope of hydrogen–air mixture such as a layer of the mixture at the ceiling of the tunnel, the critical expansion ratio depends on the opening degree, mixture uniformity and blockage ratio as the ratio of blocked area to the total cross-sectional area (Kuznetsov *et al*., 2011; Grune *et al*., 2013; Kuznetsov *et al*., 2015):

$$\sigma^* = \sigma_0^* \left(1 + K \cdot s/h\right), \tag{2}$$

where σ_0*=3.75 is the critical expansion ratio for uniform hydrogen-air mixture fully occupying the tunnel cross-section; K = 0.175 is the constant depending on the blockage ratio BR = $\Sigma A_i/A$, A is the tunnel cross-section, A_i is the total visible blockage by cars, buses, trucks, ventilators and other supporting equipment inside the tunnel; the spacing s can be a distance between cars in one lane. Equation (2) is also valid for a layer of stratified hydrogen-air mixture; h is the layer thickness. It is valid for relatively small gradients (less than 30% H_2/m) in an assumption that the process of flame propagation is governed by the highest hydrogen concentration at the ceiling.

4. The DDT criterion is based on the ratio of characteristic tunnel dimension (for instance, an equivalent diameter $D = \sqrt{4A/\pi}$ to the detonation cell size, D/λ. The ratio D/λ should exceed the critical value N* dependent on geometry, mixture reactivity, uniformity of the mixture (Moen *et al*., 1981; Teodorczyk *et al*., 1988; Dorofeev *et al*. 2000):

$$\frac{L}{\lambda} > N^*, \tag{3}$$

where L is the characteristic size for tunnel cross-section; λ is the detonation cell size as a measure of detonability for hydrogen-air mixture; N* is the critical value for detonation onset (DDT) or detonation propagation dependent on geometry of the system.

5. Critical conditions for uniform or stratified semi-confined layer of hydrogen-air mixture are given in terms of the ratio h/λ, where h is the layer thickness (Kuznetsov *et al*., 2011; Grune *et al*., 2013; Kuznetsov *et al*., 2015):

$$h/\lambda = 13.5. \tag{4}$$

For a stratified layer of hydrogen-air mixture, if the hydrogen concentration gradient is not larger than 60% H_2/m, the critical condition for a detonation onset is the same (see Eq. 4) as for uniform hydrogen composition of the same hydrogen concentration as the maximum concentration of the stratified composition.

6. All aforementioned criteria for flame acceleration and DDT (Eqs. 1-4) require the satisfaction of so called "run-up distance (RUD) criterion":

$$X\text{s} < L, \tag{5}$$

where L is a characteristic length of hydrogen – air cloud along the tunnel (Veser *et al*., 2002; Kuznetsov *et al*., 2005; Ciccarelli *et al*., 2008). If the cloud dimension L is longer than the run-up distance Xs to the speed of sound then the detonation may occur. Without the satisfaction of the run-up-distance criterion (Eq. 5) the FA and DDT conditions might be over-conservative and the maximum combustion pressure will be over-predicted.

7. The run-up distance to detonation depends on mixture reactivity and the level of turbulence. Both factors can promote flame acceleration and shorten the run-up distance Xs. Considering an empty tunnel as a smooth channel, according to (Kuznetsov *et al*., 2005), the run-up distance to detonation is proportional to the detonation cell size

$$X\text{s} = 550\ \lambda. \tag{6}$$

Equation (6) is valid for very large channels similar to a tunnel with $D > 20\lambda$. For relatively narrow channels with $10\lambda < D < 20\lambda$ the run-up-distance Xs is proportional to the tube diameter D for roughness Δ=5 mm typical for an empty tunnel without obstacles:

$$X\text{s} = (12\text{-}14)D\ (\Delta\text{=}5\text{ mm}). \tag{7}$$

In presence of blocked cars, trucks and trains within the range of BR = 0.3–0.75 inside a tunnel there is a relationship for run-up distance to supersonic flame (Veser *et al*., 2002):

$$X_S = \frac{a_p D\cdot(1-BR)}{(1+1.5\cdot BR)\cdot 10 S_L(\sigma-1)}, \tag{8}$$

as a function of blockage ratio BR, tunnel diameter D, expansion ratio σ, laminar flame velocity S_L, and the speed of sound in combustion products a_p. The next equation fills the gap between the rough channel (BR~0) and a rough channel with BR<0.1 involving a boundary layer theory Eqs. (6-7) (Kuznetsov *et al*., 2005, Ciccarelli *et al*., 2008)

$$X_S = D\frac{\gamma}{C}\left[\frac{1}{\kappa}\ln\left(\gamma\frac{D}{h}\right)+K\right], \tag{9}$$

where κ, K, and C are the physical constant from turbulent boundary layer theory κ=0.4, K=5.5, and C=0.2; D/h can be expressed through the blockage ratio; $\delta=\nu/S_L$ is the laminar flame thickness; v is the kinematic viscosity; η and m are two incognita derived from experimental data (Kuznetsov *et al*., 2005). Main combustion properties in Eqs. 2, 3, 4, 6, 8-9 can be calculated using thermodynamic tools STANJAN (Reynolds, 1986), Cantera (Goodwin, 2001) and CELL_H2 program (Gavrikov *et al*., 2000) for detonation cell size evaluation.

Now, the conditions Eqs. (1–4) can only be satisfied if the conditions for run-up distance (Eq. 5) is also satisfied. If the length of hydrogen-air cloud in a tunnel is too short, then only slow subsonic deflagration will occur with a maximum combustion pressure of 1-3 bar.

References

- Ciccarelli, G., Dorofeev, S., Flame acceleration and transition to detonation in ducts, Progress in Energy and Combustion Science, Volume 34, Issue 4, 2008, Pages 499-550.
- Dorofeev S.B., Kuznetsov M.S., Alekseev V.I., Efimenko A.A., Breitung W. Evaluation of limits for effective flame acceleration in hydrogen mixtures. Journal of Loss Prevention in the Process Industries, 2001, Vol 14/6, pp. 583-589.
- Gavrikov, A.I., Efimenko, A.A., Dorofeev, S.B, A model for detonation cell size prediction from chemical kinetics, *Combustion and Flame*, Volume 120, Issues 1–2, 2000, Pages 19-33.
- Goodwin, D.G., Cantera User's Guide, Cal. Inst. of Techn., Pasadena, CA, November, 2001.
- Grune, J., Sempert, K., Haberstroh, H., Kuznetsov, M., Jordan, T., Experimental Investigation of Hydrogen-Air Deflagrations and Detonations in Semi-Confined Flat Layers, *Journal of Loss Prevention in the Process Industries*, Volume 26, Issue 2, March 2013, Pages 317-323.
- Grune, J., Sempert, K., Kuznetsov, M., Jordan, T., Experimental investigation of fast flame propagation in stratified hydrogen–air mixtures in semi-confined flat layers, *Journal of Loss Prevention in the Process Industries*, Volume 26, Issue 6, November 2013b, Pages 1442-1451.
- Dorofeev S.B., Sidorov V. P., Kuznetsov M. S., Matsukov I. D., Alekseev V. I. Effect of scale on the onset of detonations. *Shock Waves*, 2000, v. 10, pp. 137-149.
- Kuznetsov M., Alekseev V., Matsukov I., Dorofeev S. DDT in a Smooth Tube filled with Hydrogen-Oxygen Mixtures. *Shock Waves*, vol. 14, No 3, pp 205 - 215 (2005).
- Kuznetsov, M., Grune, J., Friedrich, A., Sempert, K., Breitung, W. and Jordan,T., Hydrogen-Air Deflagrations and Detonations in a Semi-Confined Flat Layer, In: Fire and Explosion Hazards, Proceedings of the Sixth International Seminar (Edited by Bradley, D., Makhviladze, G., and Molkov V.), 2011, pp 125-136.
- Kuznetsov, M., Yanez, J., Grune, J., Friedrich, A., Jordan, T., Hydrogen Combustion in a Flat Semi-Confined Layer with Respect to the Fukushima Daiichi Accident, *Nuclear Engineering and Design*, Volume 286, May 2015, Pages 36-48.
- Landau, L.D., and Lifshiz, E. M., Hydrodynamics, Edition 3, Nauka, Moscow, 1986.
- Moen, I. O., Donato, M., Knystautas, R., Lee, J. H. S. (1981) The influence of confinement on the propagation of detonations near the detonability limit. *Symp. (Int.) Combust., 18th*, pp. 1615-23.
- Teodorczyk, A., Lee, J.H., Knystautas, R. (1988) Propagation mechanism of quasi-detonations. *22nd Symposium (Int.) on Combustion.* The Combustion Institute, Pittsburgh, pp 1723–1731.
- Reynolds, W.C., The Element Potential Method for Chemical Equilibrium Analysis: Implementation in the Interactive Program STANJAN Version 3, Dept. of Mechanical Engineering, Stanford University, Palo Alto, California, January 1986.
- Rudy, W., Kuznetsov, M., Porowski, R., Teodorczyk, A., Grune, J., Sempert, K., Critical conditions of hydrogen–air detonation in partially confined geometry. *Proceedings of the Combustion Institute*, Volume 34, Issue 2, 2013, Pages 1965-1972.

- Veser, A., Breitung, W., Dorofeev, S.B., Run-up distances to supersonic flames in obstacle-laden tubes, *J. Phys. IV France*, 12, No 7, 2002, pp333-340**.**

A3.3 Prevention and consequences of hydrogen tank rupture in tunnel fire

A3.3.1 Model to design a tank-TPRD system that excludes rupture in engulfing fire

The model for the prevention of rupture of high-pressure hydrogen storage equipped by TPRD is described in detail in (Molkov *et al*, 2021b).

Reference:

Molkov V., Dadashzadeh M., Kashkarov S., Makarov, D. (2021b) Performance of hydrogen storage tank with TPRD in an engulfing fire. International Journal of Hydrogen Energy.

A3.3.2 Dimensionless correlation for blast wave decay in a tunnel

The correlation for blast wave decay after a hydrogen tank rupture in a tunnel fire (Molkov and Dery, 2020) can be used for the assessment of hazard distances of an arbitrary tank rupture in a tunnel of any cross-sectional area, aspect ratio and length.

Reference:

Molkov V., Dery W., (2020). The blast wave decay correlation for hydrogen tank rupture in a tunnel fire, *Int. J. Hydrog. Energy*, vol. 45, no. 55, pp. 31289–31302, Nov. 2020, doi: 10.1016/j.ijhydene.2020.08.062.

Appendix 4. HSE scaling technique for tunnel hydrogen releases

HSE designed an experimental programme to assess, on a reduced scale, the consequences of releases in tunnels that represent "worst-case" scenarios, specifically blowdown releases following activation of TPRDs in a fire and the catastrophic failure of a single vessel, also in a fire, assuming the entire content of the cylinders (cars/buses/trains) is released. The releases are undertaken both without and with scale vehicles models being present in the tunnel, with both unignited and ignited releases being undertaken. Hydrogen concentrations are measured together with overpressures and flame speeds, supported by high-speed video recordings. In designing the experimental programme, HSE was required to consider typical releases from cars, buses and trains in actual tunnels and to scale these to the HSE test tunnel as follows:

A4.1 Blowdown releases

The objective of the scaled experiment is to match the concentration of hydrogen in the downstream flow and the proportion of the tunnel over which the flow is distributed. Scaling of the release scenarios therefore follows the scaling principles outlined in *Scaling rules for reduced-scale field releases of hydrogen fluoride* (Hall and Walker, 1997). Thus, the scaled volume released is the cube of the ratio of the length scales, where the length scale is the representative tunnel diameter. In respect of the time scales for a release, the scaling parameter is dimensionless time (UT/L) which must have the same values at full and model scales. Thus, it also scales as the square root of the length scale ratio. Thus, given the scaled volume (mass) release and the same tank initial pressure the diameter of the nozzle for the scaled release can be calculated to match the scaled volume (mass) flowrate versus the scaled time tank blowdown curve for the full-scale release.

The appropriate scaling relationships between the tunnel airflow *U*, the hydrogen volume or mass flow rate *V* and the tunnel scaling factor *H* (ratio of full-scale tunnel diameter D to HSE tunnel diameter D_{HSE} for a *steady* release experiment in a model tunnel is: $U \propto H^{\frac{1}{2}}$ and $V \propto H^{\frac{5}{2}}$. If U and V are chosen in this way, then the concentration in the flow developing around the source will be the same and the relationship between the buoyancy head associated with the release and the dynamic head of the flow will be the same. This means there will be a similar tendency for the gas to be blown down stream or flow backwards at high level. If the timescale of the blow down process is reasonably long compared with the characteristic time scale for the tunnel flow past the source U/H then this quasi-steady scaling will give reasonable results.

In summary for a blowdown release at any rate.

Volume flow rate should be scaled as H^5/2

Tunnel velocity should be scaled as H^1/2

Total inventory should scale as H^3

This implies the total duration (or time to 50% flow) scales as H^1/2

A4.2 Short duration momentum-driven releases

In this case the inventory is released within a duration that is very short compared with the time scale of flow past the source. The structure of momentum-driven flow will not be greatly

affected by tunnel flow. Consequently, the resulting cloud will simply be convected downstream. In this case the most appropriate scaling for the total inventory would be as the cube of length scale.

A4.3 Scaling and incident scenarios assessed

The short duration momentum driven (catastrophic) releases have been undertaken using a 700 bar bespoke designed vessel with a capacity of between 5 to 18 litres, its contents being released through a 100 mm diameter double bursting disc unit at an initial rate exceeding 200 kg/s. The initial shock wave developed an overpressure of 55 bar with an initial velocity of about 2.3 km/s and ignition took place at the contact surface. Examination of the ignition mechanism is being studied as part of the test programme, including delayed ignition.

Four scaled releases (blowdowns) have been undertaken, characterised by the quantity released and the time scale of the releases. These will represent TPRD blowdowns from a representative car, bus and two trains as would occur in a typical full-sized tunnel. The actual representations have been derived following a study of the various accident scenarios. These have been scaled as described in the following sections using the method described by Hall and Walker (1997).

Based upon the accident scenario analysis carried out in (HyTunnel-CS, D1.3, 2019), we undertook a test programme for which the following assumptions were applicable:

1. In the case of normal TPRD operation in a fire, it was assumed that the total inventory was released through the TPRDs. All TPRDs opened at roughly the same time.
2. In the case of a spurious TPRD operation it was assumed that at least one tank was involved.
3. Only one tank failed catastrophically in a fire due to single TPRD malfunction.
4. A tunnel cross-sectional area was represented by a circle of the equivalent area.

The hydrogen inventories carried by the three different types of vehicle, based on (HyTunnel-CS, D1.3, 2019), are as follows:

1. **CAR:** Five makes specified, all operating at 700 bar. Tank capacity varies between 115 and 156 litres, usually made up from two tanks, each of similar capacity. Average capacity 135 litres, containing a mass of 5.4 kg hydrogen. Vent lines specified as between 2–4 mm diameter, although 4.2 mm diameter seems to be used in some cases. Vent line is downwards from underneath the vehicle at 135 degrees backward. The TPRD diameter is quoted as 2.0 mm, with one TPRD per tank.

2. **BUS:** Three makes specified, all operating at 350 bar. They use four and nine tanks, roof mounted, each with a capacity of 74 to 220 litres. Assume a representative worst case of 210 litres per tank on a four-tank pack each containing 4.97 kg each of hydrogen, giving a total capacity of about 40 kg. Vent line is upwards from top of vehicle. The TPRD diameter is 3.3 mm and there are two fitted to each cylinder, giving a total of eight. Other buses may have a slightly larger capacity with either 11 or 12 TPRDs fitted. Recently Wrightbus have introduced a series of single decker buses with a hydrogen capacity of between 35-50 kg. In view of which we have used a 40 kg capacity (say five tanks) with ten TPRDs fitted as the basis for our modelling.

TRAIN: Only one make specified, this being the 'Coradia iLint', manufactured by Alstom. They refer to a two-carriage unit each with 96 kg of hydrogen operating at 350 bar. Each unit has 24 cylinders each with a capacity of 175 litres containing 4.14 kg of hydrogen. Assume that only one carriage is involved in the fire. Each cylinder has two TPRDs, each with a diameter of 3.3 mm. This train is now in series production for use in Germany.

A three-carriage unit is also under consideration by Alstom for the UK market, known as "Breeze". This will have a mass of hydrogen of 417 kg at 350 bar pressure, contained in 72 cylinders each with a capacity of 245 litres. Each cylinder contains 5.8 kg of hydrogen and there are 36 cylinders in both the lead and trailing cars. Assume that only one car is involved in the fire, consequently the total inventory per car will be 209 kg. The tanks are arranged in cassettes, comprising nine tanks each. There are four cassettes per car, contained in a unit behind the cab. There are two cassettes on either side of the storage bay, assumed separated by a partition. Each cylinder has two TPRDs, hence each cassette has 18 TPRDs of 3.3 mm diameter. We assume that for modelling purposes only two cassettes (one side) would be involved in a fire. The inventory involved in a fire is therefore 105 kg with 36 TPRDs able to vent the inventory.

HSE Buxton test tunnel:

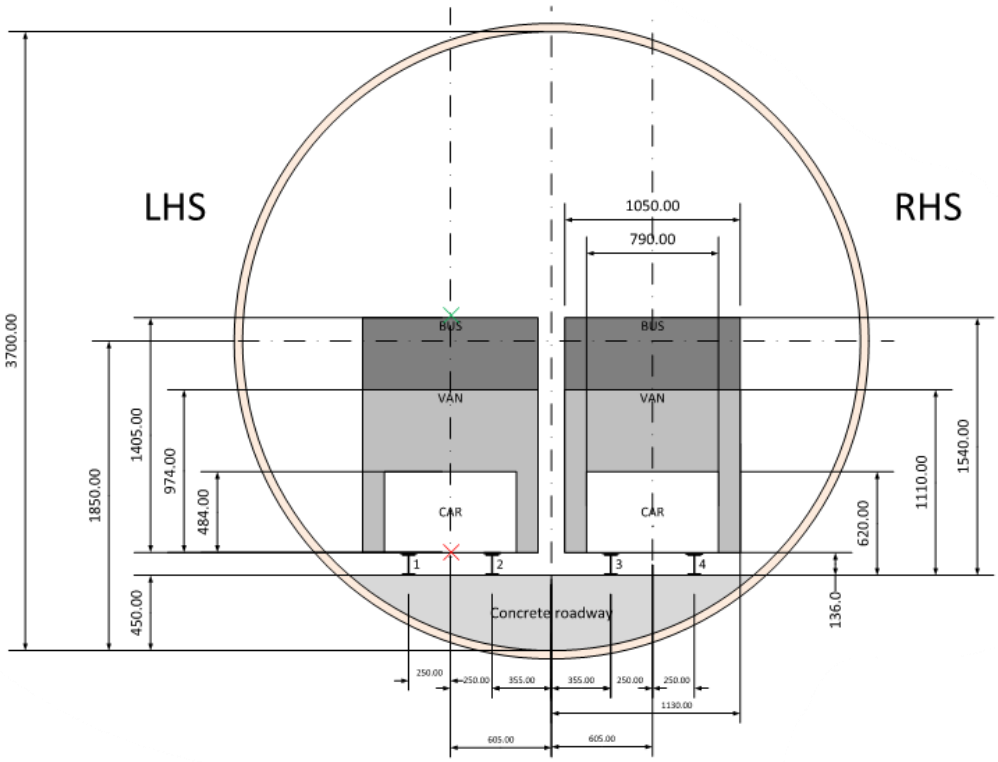

Figure A4-1. Engineering drawing of the HSE test tunnel

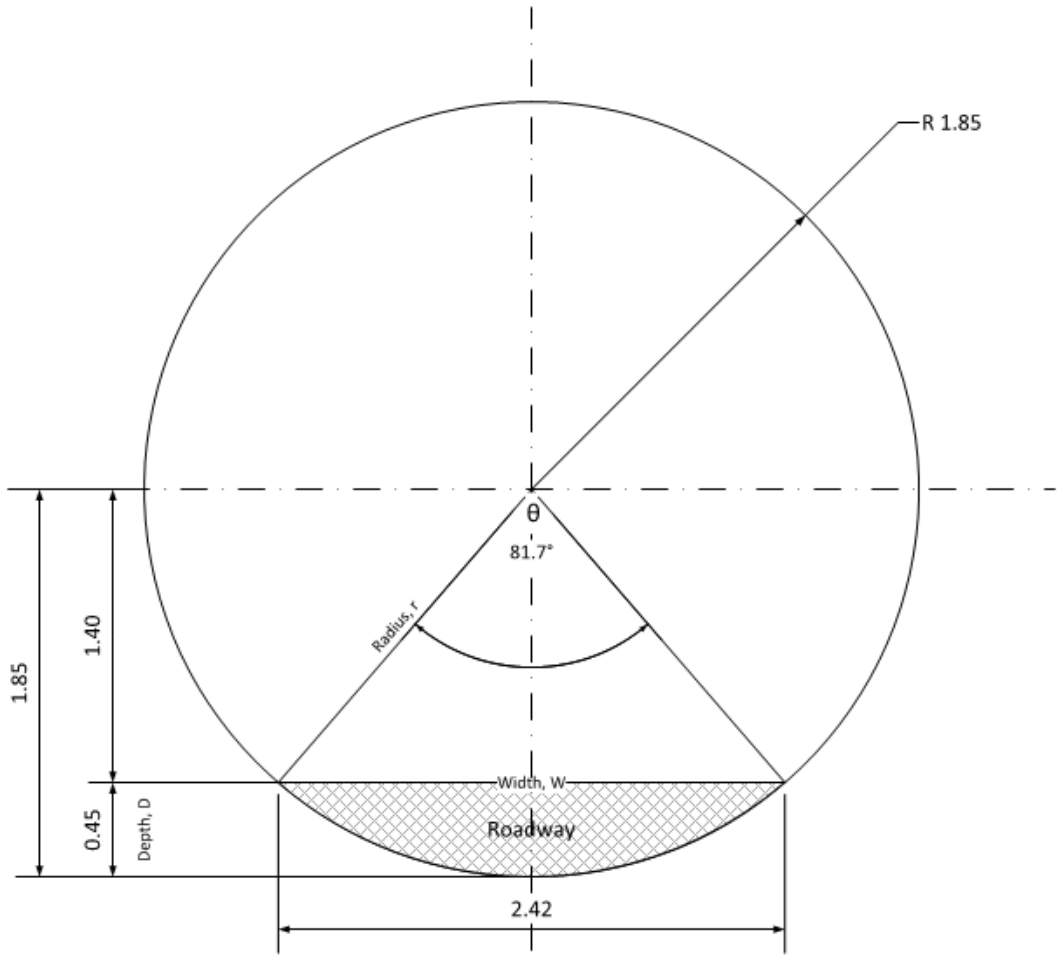

Figure A4-2. Simplified schematic of the cross section of the HSE test tunnel

- Length = 70m.
- Radius = 1.85 m.
- Depth of ballast = 0.45 m.
- Area of segment containing ballast = 0.745 m^2.
- Circular area of tunnel (no ballast) = 10.75 m^2.
- Area through which vehicles travel = 10.005 m^2.
- Equivalent diameter D_{HSE} = 3.57 m.

- Scaling factor (H) for tunnel diameter is D/D_{HSE}
- Scaling factor for mass of hydrogen stored is H^3
- Scaling factor for the mass flow rate is $H^{5/2}$.
- Scaling factor for the discharge time is: $H^{1/2}$.
- Scaling factor for the airflow in the tunnel is: $H^{1/2}$.

Based on the foregoing average scaling factors for the various tunnel types (All tunnels, Double bore only) can be obtained, then used to establish the scaled inventories for a car, bus, and train in the relevant tunnels for both continuous and catastrophic releases as shown in Table A4-1.

Table A4-1. Scaled hydrogen inventories for cars. buses and trains

		Total Inventory	Single Tank Inventory	Average scaling Factor	Scaled Total Inventory	Scaled Inventory Single Tank
CAR 700 bar	All Tunnels	5.4 kg	2.7 kg	2.13	0.56 kg	0.28 kg
CAR 700 bar	Double bore only	5.4 kg	2.7 kg	2.275	0.46 kg	0,23 kg
BUS 350 bar	All Tunnels	40.0 kg	4.97 kg	2.13	4,14 kg	0.51 kg
BUS 350 bar	Double bore only	40.0 kg	4.97 kg	2.275	3.40 kg	0.42 kg
TRAIN 350 bar	All Tunnels	96.0 kg 105.0 kg	4.14 kg 5.80 kg	2.513	6.05 kg 6.62 kg	0.26 kg 0.37 kg
TRAIN 350 bar	Double bore only	96.0 kg 105.0 kg	4.14kg 5.80kg	2.665	5.07 kg 5.54 kg	0.22 kg 0.31 kg

Note: (Values shown in red are those used for the actual modelling exercise).

Using a commercially available fixed volume off-the-shelf 53 litre tank (Maximum working Pressure, MWP=800 bar) or a combination of these, requires the desired inventory to be contained in them but at the relevant pressure. Consequently, the required pressures, scaled vessel inventories, capacities, orifice diameters and initial mass flow rates can be calculated using the suite of programmes given in the e-Laboratory of Hydrogen Safety: https://elab.hysafer.ulster.ac.uk/. We therefore obtain the scaled values using 1 or 3 vessels shown in Table A4-2.

We therefore obtain the relevant scaled values for the car, bus and two trains in a double bore tunnel only when using either one or three 53 litre vessels in combination, as shown in Table A4-2. Note that the first four rows show the tank volumes for the actual operating pressures (700 or 350 bar). The final four rows in bold show the pressures required when the volumes are fixed at either 53, 159 litres or 11 litres in the case of a single tank.

Table A4-2. Correlation of proposed hydrogen to actual tank inventories

	Total Inventory (kg)	**Pressure (bar)**	**Tank Volume (litres)**	**Single Tank Inventory (kg)**	**Pressure (bar)**	**Tank Volume (litres)**
CAR	0.46	700	12	0.23	700	6
BUS	3.40	350	145	0.42	350/700	18/11
TRAIN 1	5.07	350	215	0.22	350/700	10/5
TRAIN 2	5.54	350	251	0.31	350/700	13/8
CAR	**0.46**	**118**	**53**	**0.23**	**300**	**11**
BUS	**3.40**	**310**	**159**	**0.42**	**700**	**11**
TRAIN 1	**5.07**	**510**	**159**	**0.22**	**290**	**11**
TRAIN 2	**5.54**	**580**	**159**	**0.31**	**450**	**11**

Calculation of orifice sizes for the total inventory contained on a car, bus and train, from the literature typical TPRD orifice sizes are 2.0 mm and 3.3 mm diameter, in addition a car has two tanks, buses four to twelve (assume five) tanks, and trains eighteen or twenty-four tanks. In a fire it is assumed that the total inventories are discharged with all TPRDs open at the same time. The equivalent orifice sizes are shown in Table A4-3.

Table A4-3. Equivalent orifice sizes for full-sized releases

Orifice Dia. (mm) Single TPRD	**Car: Two TPRDs Equivalent diameter**	**Bus: 10 TPRDs Equivalent diameter**	**Train: 48/36 TPRDs Equivalent diameter**
2.0 mm	2.83 mm	-	-
3.3 mm	-	10.44 mm	22.86/19.80 mm

Using the above equivalent diameters, the initial mass flow rates, and discharge times (to choke point) are obtained for the actual full-size inventories using the actual storage pressures (700 or 350 bar) as shown in Table A4-4.

Table A4-4. Initial mass flow rates and discharge times for full size and for scaled inventories

	^^**Total inventory (kg)**	**Initial mass flow rates (kg/s)**	**Discharge times (sec)**	^^**Scaled total inventory (kg)**	**Scaled initial mass flow rates (kg/s)**	^**Scaled discharge times (sec)**	***Scaled orifice diam. used (mm)**
CAR 700 bar	5.4 (135 l)	0.215	168	0.46 (12 l)	0.0275	120 (111)	1.0
BUS 350 bar	40.0 (1700 l)	1.638	134	3.40 (145 l)	0.21	86 (89)	3.8
TRAIN 1 350 bar	96.0 (4050 l)	7.85	67	5.07 (215 l)	0.677	41 (41)	6.7
TRAIN 2 350 bar	105.0 (4450 l)	5.89	97	5.55 (235 l)	0.508	60 (60)	5.8

**These are the orifice diameters needed to give the correct scaled initial mass flow rates.*

^*The values in brackets are those obtained from scaling the values shown in column three.*

^^*Numbers in brackets are the volumes in litres required for the inventory at the pressures shown at the start of each row.*

NB: The approach is equally valid for other orifice sizes than those used here.

If using standard 53 litre size cylinders, then we can model the foregoing using different pressures but fixed volumes (multiples of 53 litres) to give the same initial mass flow rates as shown in Table A4-5, giving nozzle diameters appropriate to the different pressures.

As an example, the jet from a car cylinder at 700 bar pressure with an orifice diameter of 1.0 mm is the equivalent of releasing at 118 bar through a 2.2 mm diameter nozzle, given the same initial mass flow rates. This is because the fully expanded jets in both cases have an initial fully expanded diameter of 16.8 mm at atmospheric pressure and thereafter, they both behave in the same manner, namely as a free turbulent jet, for which the decay characteristics are well documented in the literature.

Table A4-5. Scaled orifice size for experimental release

	Scaled total inventory (kg)	Scaled initial mass flow rates (kg/s)	Discharge times (s)	Scaled orifice diameters used (mm)
CAR 118 bar	0.46 (53)	0.0275	70	2.2
BUS 310 bar	3.40 (159)	0.21	83	4.0
TRAIN 1 510 bar	5.07 (159)	0.677	46	5.7
TRAIN 2 580 bar	5.55 (159)	0.508	69	4.7

If we use the operating pressures 700/350 bar and use the cylinder volumes containing the required inventories for the catastrophic releases, then from the Brode equation: $E=(P_2-P_1)V/(\mu-1)$, where P_2-P_1 is the pressure increase, V is the vessel volume, and μ is the specific heat ratio; we can calculate the mechanical energy (E) contained in the respective volumes and hence by way of an illustration the TNT equivalence for each release scenario as shown in the first four rows of Table A4-6. We can then calculate the required volumes for the cylinder to give the same energy equivalence when operating at a fixed pressure of 700 bar, as shown in bold in the last four rows of Table A4-6.

Table A4-6. Scaled volumes to give same energy equivalence

	Single Tank Inventory (kg)	Pressure (bar)	Tank Volume (litres)	Mechanical energy (kJ)	TNT-equivalent (kg)
CAR	0.23	700	6	1024	0.22
BUS	0.42	350	18	1536	0.33
TRAIN 1	0.22	350	10	853	0.19
TRAIN 2	0.31	350	13	1110	0.23
CAR	**0.23**	**700**	**6**	**1024**	**0.22**
BUS	**0.42**	**700**	**9**	**1536**	**0.33**
TRAIN 1	**0.22**	**700**	**5**	**853**	**0.19**
TRAIN 2	**0.31**	**700**	**7**	**1110**	**0.23**

NB: 700 bar is the operating pressure for cars; and 350 bar for the bus and trains.

The values in bold are the intended base test parameters. The test vessel has a volume of 18 litres which can be reduced to the required volumes with inserts.

A4.4 Scaling of airflow in the HSE tunnel

HyTunnel-CS D1.1 (2019) makes recommendations for maximum required ventilation velocity in actual tunnels. This is deemed to be 3.5 m/s based on physiological and fire-fighting needs. HyTunnel-CS D1.3 (2019) has therefore recommended a range of actual tunnel ventilation velocities for study of 1, 2, 3.5 and 5 m/s. These values correspond to actual full-scale tunnel velocities and, according to the scaling rules which are being adopted, should be modified in line with the HSE tunnel being studied. Applying the velocity scaling factor given previously gives the reduced velocities shown in Table A4-7.

Table A4-7. Scaled ventilation velocities in HSE tunnel

Actual tunnel ventilation velocity (m/s)	HSE ventilation velocity (m/s)	
	Scale factor 2.275	Scale factor 2.665
1	0.66	0.61
2	1.33	1.22
3.5	2.32	2.14
5	3.31	3.06

References

Hall, D.J. and Walker, S., 1997. Scaling rules for reduced-scale field releases of hydrogen fluoride. *Journal of hazardous materials*, *54*(1-2), pp.89-111.